To the Graduate Council:

I am submitting herewith a dissertation written by Zhenping Li entitled "Photo- and Electroproduction Of Baryon Resonance In A Potential Quark Model." I have examined the final copy of this dissertation for form and content and recommend that it be accepted in partial fulfillment of the requirements for the degree of Doctor of Philosophy, with a major in Physics.

M W Guidry

M.W. Guidry, Major Professor

We have read this dissertation
and recommend its acceptance

Frank Close

Accepted for the Council:

Associate Vice Chancellor
and Dean of The Graduate School

PHOTO- AND ELECTROPRODUCTION OF BARYON RESONANCES IN A POTENTIAL QUARK MODEL

A Dissertation
Presented for the
Doctor of Philosophy
Degree
The University of Tennessee

Zhenping Li
May, 1991

This dissertation

is dedicated

to

my family,

Huiying and Mengmeng

ACKNOWLEDGEMENTS

First of all, I would like to thank my adviser – Prof. W.M. Guidry for his encouragement and useful advice. I also want to thank Prof. F. E. Close, who not only directed me into this field, but also taught me the art of research.

I am grateful to many people for very useful discussions, specially to Dr. N. Isgur and Dr. J. Weinstein.

Finally, I want to thank my wife Huiying for her support, patience and kindness.

ABSTRACT

The theories on photo- and electroproduction of baryon resonances in the nonrelativistic constituent quark model (NCQM) are reviewed. The electromagnetic interaction for a three-body system is discussed, with particular emphasis on the relativistic corrections and the role of binding potential, which have been neglected in previous calculations. The transition amplitudes are calculated consistently to $O(v^2/c^2)$ in the constituent quark model using the chromodynamics of Isgur and Karl. We find that the successes of the nonrelativistic quark model are preserved and some problems are removed. For the first time both spectroscopy and transitions receive a unified treatment within the framework of a potential quark model.

Table Of Contents

List of Figures

List of Tables

CHAPTER 1

Introduction

The concept of quarks was first introduced 27 years ago by Gell-Mann (Gell-Mann, 1964) and Zweig (Zweig, 1964) in their investigation of hadron spectroscopy. The quark model was highly successful in the sixties; in particular, it gave a systematic classifications of mesons, baryons and their excited resonance states according to $SU(6)\otimes O(3)$ symmetry, and good descriptions of their static properties and decays. Later, the successes of quark-parton phenomenology in deep inelastic lepton-hadron scattering and e^+e^- collision led to the idea of color and eventually to quantum chromodynamics (QCD).

QCD is a non-Abelian gauge theory, in which colored quarks interact by means of massless colored gauge bosons called gluons. The three quark colors are regarded as the basis of the color symmetry group $SU(3)_c$. Because of the renormalization of non-Abelian gauge theories, QCD exhibits an effective interaction strength that is small at short distance and becomes large as distance increases. This property of QCD, which is known as *asymptotic freedom*, divides QCD into perturbative and non-perturbative regions.

The mathematical techniques of perturbation theory, so successful in quantum electrodynamics (QED), can be applied with success to short-distance (very high energy) phenomena where QCD is perturbative. But non-perturbative QCD is not well understood, and no rigorous theoretical demonstration of the confinement property of QCD has yet been given, although it is widely believed that this is one of the basic features of QCD. There has been much progress in studying some of the hadronic properties in lattice QCD, but it is practically impossible to accommodate such a large amount of data in lattice QCD at present. Phenomenological models, such as the nonrelativistic constituent quark model (NCQM) (Close 1979) still play a major role in helping us to understand the nature of hadrons and the quark–quark interaction in the non-perturbative region. Of course, the NCQM is a simple model and lacks a comprehensive theoretical foundation in QCD, but it does exhibit many basic features of QCD. Attempts have been made to place the NCQM on a firmer ground, by means of models such as the flux tube model (Isgur and Paton 1983).

The basic feature of the NCQM is that the quark and gluon fields in a hadron state are treated as a finite number of constituent quarks (a meson as $q\bar{q}$ configuration and a baryon as three quarks) interacting by a two–body potential in a Shrödinger equation. The quark–quark interaction in the NCQM is divided into a long-range and short-range potential: the long-range potential represents the effect of confinement and is treated as linear or harmonic oscillator, while De Rujula, Georgi and Glashow (De Rujula *et al*, 1975) attribute the short-range potential to the one-gluon exchange interaction, which corresponds to the Coulomb potential in the nonrelativistic limit. The important spin-dependent mass splittings arise from the hyperfine interactions, i.e, the $O(v^2/c^2)$ Breit–Fermi generalization of the one-gluon exchange.

Although the näive quark model classification of the hadron spectroscopy has long been appreciated, it failed to give a quantitative description of the hadronic energy spectrum. Furthermore, the velocity of the constituent quarks within a hadron is not small for the light quarks u, d and s. Numerical calculations using the basic parameters of the model show that $v/c \simeq 1$, which implies that relativistic effects are significant in the model. This happens in spite of the fact that the constituent quark masses are much larger than the current quark masses of u, d and s. The work by Isgur and Karl (Isgur and Karl 1978, 1979) has shown systematically that one has to include relativistic effects in the binding potential for the light quark sector in order to give a quantitative description of the energy spectrum; this is particularly true of the hyperfine interaction, which is associated with higher-order relativistic effects in the Breit–Fermi interaction and which generates the $\Delta - N$ mass difference. These relativistic effects further induce $SU(6)\otimes O(3)$ configuration mixings, which will be discussed in detail in chapter 2. Relativistic effects on the wavefunction will also affect the NCQM prediction of dynamical processes, since the transition probabilities are very sensitive to the wavefunction. It will be crucial to test whether the model can simultaneously describe the energy spectrum and the transitions between the resonance states when relativistic effects are consistently included.

The photoexcitations of a nucleon into its resonance states could provide important information in this regard. The photon interaction is a clean probe in that it couples to the spin and flavour of the constituents and reveals the correlation among the flavours and spin inside the target. A photon has spin 1, so the helicity amplitudes where the photon and target spin are parallel (net helicity $\frac{3}{2}$) or antiparallel (net helicity $\frac{1}{2}$) give rich structure. Furthermore, since the photon is a mixture of isospin zero and one, proton and neutron targets give independent information.

By exciting nucleon resonances in various helicity states from proton and neutron targets, one can form ratios or linear combinations of amplitudes where specific features of confinement, common to all amplitudes, factor out. The information that remains probes the electromagnetic interaction of the quarks more directly, revealing their spin–flavour correlations. Knowledge of these correlations can give insights into the configuration mixing, predicted by QCD. This is not simply a rerun of old ground. Given the interest in gluonic degree of freedom and the possible existence of hybrid baryons (i.e, a $gqqq$ state) in the mass range accessible to the new machines, it is important to have the best understanding of the "conventional" baryons. Photoexcitations of the low-lying hybrid states contain some rather interesting selection rules (Barnes and Close, 1983), so electromagnetic interactions may allow these states to be isolated from qqq resonance states.

Such a program had its genesis with the early work of Copley, Karl and Obryk (Copley *et al*, 1969), and Feynman, Kisslinger and Ravndal (Feynman *et al*, 1971), who gave the first clear evidence of an underlying $SU(6) \otimes O(3)$ structure in the baryon spectrum. The standard nonrelativistic transition operator

$$H_{\text{em}} = \sum_{i=1}^{3} H_i;\ H_i \equiv -\frac{e_i}{2m_i}(\mathbf{p}_i \cdot \mathbf{A}(r_i) + \mathbf{A}(r_i) \cdot \mathbf{p}_i) - \mu_i \boldsymbol{\sigma}_i \cdot \mathbf{B}(r_i) \tag{1-1}$$

was used in their investigation, where quark i at position r_i has mass, charge, and magnetic moment m_i, e_i, μ_i; $\mathbf{A}(r_i)$ and $\mathbf{B}(r_i)$ are electromagnetic fields that will be discussed in more detail in chapter 3. Matrix elements of Eq. (1-1) have been found to be in remarkable agreement with data. Based on this model, Close and Gilman (Close and Gilman 1972) predicted a rapid change with q^2 of the helicity structure of the resonances $F_{15}(1688)$ and $D_{13}(1520)$ in electroproduction. This is our point of departure: given the fact that relativistic effects are important in hadron spectroscopy, the nonrelativistic transition operator (1-1) is not a priori justified, and relativistic corrections to Eq. (1-1) should be fully studied in order to give a consistent theoretical prediction. There have been some limited investigations of the phenomenological consequences of the spin–orbit interaction (Kubota and Ohta 1976);

$$H_{\text{SO}} = \frac{1}{2m}(2\mu - \frac{e}{2m})\, \boldsymbol{\sigma} \cdot \mathbf{p} \times \mathbf{E}. \tag{1-2}$$

However, as discussed by many authors (Close and Osborn 1970, Close and Copley 1970, Brodsky and Primack 1969), one can no longer write $H = \sum H_i$ at this order; to separate the internal motion from the motion of the center of mass in a many-particle system, there should be a "nonadditive" term that is associated with a Wigner rotation of the quark spins transformed from the frame of the recoiling quark to the center of mass frame. This term has been shown to be essential for satisfying the low energy theorem (Itzykson and Zuber, 1980) and the Drell–Hearn–Gerasimov (DHG) sum rule (Drell and Hearn, 1966), (Gerasimov, 1965). Furthermore, Le. Yaouanc *et al* (Le. Yaouanc *et al*, 1988) have argued that the binding potential may also play an explicit role in the electromagnetic transition operator. The question is how to incorporate all these effects into the transition operator and at the same time satisfy the DHG sum rule and low energy theorem; this will be addressed in chapter 4.

In chapter 5 we will show how the phenomenological successes of the binding potential and the electromagnetic transition operator separately combine "constructively", improving the overall fit to data. Perhaps most important, this is the first attempt to study photoproduction and electroproduction consistently in a quark model that gives a good description of hadron spectroscopy. The extension of photoproduction to electroproduction will be discussed in chapter 6, where relativistic effects in the binding potential change the behavior of the radial wavefunction and improve the overall fit to data. Finally, conclusions will be given in chapter 7.

Part of the work described here has been published in Close and Li 1990 and Li and Close 1990.

CHAPTER 2

Baryon Spectroscopy

In this section, we will concentrate on the baryons made up of light quarks u, d and s. These quarks have spin one-half, u and d form a nonstrange isospin doublet, and s is a strange isospin singlet. Therefore, the spin and flavour wavefunction should have $SU(6)$ symmetry. The fundamental representation of $SU(6)$ is formed by nonrelativistic Pauli spinors

$$u\uparrow,\ u\downarrow,\ d\uparrow,\ d\downarrow,\ s\uparrow,\ s\downarrow\,. \tag{2-1}$$

The total wavefunction of a baryon system should include four parts: a spatial wavefunction ψ that should have an $O(3)$ orbital angular momentum symmetry, a flavour wavefunction ϕ and a spin wavefunction χ that together form an $SU(6)$ symmetry, and finally a color wavefunction that should be a color singlet under $SU(3)$ symmetry and antisymmetric under exchange of the three quarks. We will first establish $SU(6)$ representations in section 2.1, then the spatial wavefunction for a three-body system in section 2.2, and finally the total $SU(6)\otimes O(3)$ wavefunction for a baryon system in section 2.3. Finally, we will introduce Isgur and Karl's potential model in section 2.5. We will concentrate only on the nonstrange baryons that are relevant to our calculations.

2.1 $SU(6)$ Wavefunctions.

To build $SU(6)$ wavefunctions for a three-quark system, one uses the representations of the permutation group S_3. Generally, there are four representations of S_3: a totally symmetric basis e^s, a totally antisymmetric vector e^a, and two mixed-symmetry vectors e^λ and e^ρ that are defined as

$$P_{12}\begin{pmatrix} e^\lambda \\ e^\rho \end{pmatrix} = \begin{pmatrix} 1 & 0 \\ 0 & -1 \end{pmatrix} \begin{pmatrix} e^\lambda \\ e^\rho \end{pmatrix} \tag{2-2}$$

and

$$P_{13}\begin{pmatrix} e^\lambda \\ e^\rho \end{pmatrix} = \begin{pmatrix} -\frac{1}{2} & -\frac{\sqrt{3}}{2} \\ -\frac{\sqrt{3}}{2} & \frac{1}{2} \end{pmatrix} \begin{pmatrix} e^\lambda \\ e^\rho \end{pmatrix}, \tag{2-3}$$

where P_{12} and P_{13} are the permutation operators that cause the exchange $1 \leftrightarrow 2$ and $1 \leftrightarrow 3$. Other operators of S_3 can be written as a product of these two operators.

To contruct an $SU(6)$ wavefunction one has to combine the spin ($SU(2)$) and flavour ($SU(3)$) degrees of freedom in the $SU(6)$ representation. The combination of two degrees of freedom corresponding to S_3 representations forms new S_3 representations. Let e_1 and e_2 denote two independent S_3 representations; then coupled representations e_3 are given by

$$e_3^s = e_1^s\, e_2^s,\ \ e_1^a\, e_2^a,\ \ \frac{1}{\sqrt{2}}\left(e_1^\lambda e_2^\lambda + e_1^\rho e_2^\rho\right), \tag{2-4}$$

$$e_3^\lambda = -e_1^a\, e_2^\rho,\ -e_1^\rho e_2^a,\ \frac{1}{\sqrt{2}}\left(e_1^\rho e_2^\rho - e_1^\lambda e_2^\lambda\right), \tag{2-5}$$

$$e_3^\rho = e_1^a e_2^\lambda,\ e_2^\lambda e_1^a,\ \frac{1}{\sqrt{2}}\left(e_1^\lambda e_2^\rho + e_1^\rho e_2^\lambda\right), \tag{2-6}$$

and

$$e_3^a = e_1^s e_2^a,\ e_1^a e_2^s,\ \frac{1}{\sqrt{2}}\left(e_1^\rho e_2^\lambda - e_1^\lambda e_2^\rho\right). \tag{2-7}$$

Notice that there are three representations that belong to the same coupled e_3 representation and to different e_1 and e_2 representations.

The connection between the representations of $SU(N)$ and the S_3 group is that each $SU(N)$ representation built from three fundamental representations is also a representation of S_3. For $SU(2)$, $SU(3)$ and $SU(6)$ groups, this leads to

$$SU(2) \quad \mathbf{2} \otimes \mathbf{2} \otimes \mathbf{2} = \mathbf{4}_s + \mathbf{2}_\rho + \mathbf{2}_\lambda, \tag{2-8}$$

$$SU(3) \quad \mathbf{3} \otimes \mathbf{3} \otimes \mathbf{3} = \mathbf{10}_s + \mathbf{8}_\rho + \mathbf{8}_\lambda + \mathbf{1}_a, \tag{2-9}$$

$$SU(6) \quad \mathbf{6} \otimes \mathbf{6} \otimes \mathbf{6} = \mathbf{56}_s + \mathbf{70}_\rho + \mathbf{70}_\lambda + \mathbf{20}_a \tag{2-10}$$

where the indicies s, ρ, λ and a show the corresponding S_3 basis for each representation and the bold numbers give the dimensionality of the corresponding representation.

More explicitly, the $SU(2)$ spin wavefunctions for a system composed of three spin-$\frac{1}{2}$ particles are

$$\chi^s(S_z = \frac{3}{2}) = \uparrow\uparrow\uparrow \tag{2-11}$$

$$\chi^\rho(S_z = \frac{1}{2}) = \frac{1}{\sqrt{2}}(\uparrow\downarrow\uparrow - \downarrow\uparrow\uparrow) \tag{2-12}$$

$$\chi^\lambda(S_z = \frac{1}{2}) = \frac{1}{\sqrt{6}}(2\uparrow\uparrow\downarrow - \downarrow\uparrow\uparrow - \uparrow\downarrow\uparrow) \tag{2-13}$$

where χ^s has a total spin $S = \frac{3}{2}$, and χ^ρ and χ^λ have a total spin $S = \frac{1}{2}$. Because χ^ρ and χ^λ have the same spin S, a further quantum number is need to distinguish these two bases. This is where the permutation group is important; these wavefunctions are representations of the permutation group S_3 too: χ^s is a totally symmetric vector, while χ^ρ and χ^λ are the two mixed vectors that have the eigenvalues under the permutation P_{12} of -1 and $+1$ respectively. Furthermore, there is no totally antisymmetric basis of S_3 because the dimension of the fundamental representation for spin $\frac{1}{2}$ is 2 ($S_z = \pm\frac{1}{2}$).

For the flavour symmetry $SU(3)$, the fundamental representation is

$$\phi = \begin{pmatrix} u \\ d \\ s \end{pmatrix}, \tag{2-14}$$

which has dimension 3. The corresponding $SU(3)$ flavour wavefunctions for a three-quark system are

$$\phi(\mathbf{10}^s) = \begin{cases} \{ddd\}^s,\ \{ddu\}^s,\ \{duu\}^s,\ \{uuu\}^s & \text{for } \Delta^-,\ \Delta^0,\ \Delta^+,\ \Delta^{++} \\ \{dds\}^s,\ \{dus\}^s,\ \{uus\}^s & \text{for } \Sigma^{-*},\ \Sigma^{0*},\ \Sigma^{+*} \\ \{dss\}^s,\ \{uss\}^s & \text{for } \Xi^{-*},\ \Xi^{0*} \\ \{sss\}^s & \text{for } \Omega^- \end{cases} \tag{2-15}$$

where

$$\{abc\}^s = \sum_{\text{perm}} a(1)b(2)c(3) \tag{2-16}$$

while the mixed symmetry octet wavefunctions are

$$\phi(\mathbf{8}^\lambda) = \begin{cases} \frac{1}{\sqrt{6}}(2uud - duu - udu) & \text{for p} \\ \frac{1}{\sqrt{6}}(dud + udd - 2ddu) & \text{for n} \\ \frac{1}{\sqrt{6}}(2uus - suu - usu) & \text{for } \Sigma^+ \\ \frac{1}{2\sqrt{3}}(sdu + sud + usd + dsu - 2uds - 2dus) & \text{for } \Sigma^0 \\ \frac{1}{\sqrt{6}}(sdd + dsd - 2dds) & \text{for } \Sigma^- \\ \frac{1}{2}(sud + usd - sdu - dsu) & \text{for } \Lambda \\ \frac{1}{\sqrt{6}}(2ssu - sus - uss) & \text{for } \Xi^0 \\ \frac{1}{\sqrt{6}}(2ssd - sds - dss) & \text{for } \Xi^- \end{cases} \tag{2-17}$$

and

$$
\phi(\mathbf{8}^\rho) = \begin{cases} \frac{1}{\sqrt{2}}(udu - duu) & \text{for p} \\ \frac{1}{\sqrt{2}}(udd - dud) & \text{for n} \\ \frac{1}{\sqrt{2}}(suu - usu) & \text{for } \Sigma^+ \\ \frac{1}{2}(sud + sdu - usd - dsu) & \text{for } \Sigma^0 \\ \frac{1}{\sqrt{2}}(sdd - dsd) & \text{for } \Sigma^- \\ \frac{1}{2\sqrt{3}}(usd + sdu - sud - dsu - 2dus + 2uds) & \text{for } \Lambda \\ \frac{1}{\sqrt{2}}(sus - uss) & \text{for } \Xi^0 \\ \frac{1}{\sqrt{2}}(sds - dss) & \text{for } \Xi^- \end{cases} \tag{2-18}
$$

The wavefunction for the singlet state is

$$
\phi(\mathbf{1}^a) = \frac{1}{\sqrt{6}}(uds + dsu + sud - dus - usd - sdu) \tag{2-19}
$$

which is totally antisymmetric.

Utilizing Eqs. 2-4,5,6,7 one can obtain $SU(6)$ wavefunctions that combine the spin ($SU(2)$) and flavour ($SU(3)$) degree freedoms. Denoting the $SU(6)$ wavefunction by $|\mathbf{N}_6,\ {}^{2S+1}\mathbf{N}_3\rangle$, where $\mathbf{N}_6(\mathbf{N}_3)$ represents the $SU(6)$ ($SU(3)$) representation and S stands for the total spin of the wavefunction, we have

$$
|\mathbf{56},\ {}^2\mathbf{8}\rangle = \frac{1}{\sqrt{2}}(\phi^\rho\chi^\rho + \phi^\lambda\chi^\lambda) \tag{2-20}
$$

and

$$
|\mathbf{56},\ {}^4\mathbf{10}\rangle = \phi^s\chi^s. \tag{2-21}
$$

Note that for the symmetric **56** representation the total spin for the decuplet flavour state can only be $\frac{3}{2}$, while for the octet states it should be $\frac{1}{2}$. The mixed symmetry representations **70** can be written as

$$
|\mathbf{70},\ {}^2\mathbf{8}\rangle^\rho = \frac{1}{\sqrt{2}}(\phi^\rho\chi^\lambda + \phi^\lambda\chi^\rho), \tag{2-22}
$$

$$|\mathbf{70},\ {}^4\mathbf{8}\rangle^\rho = \phi^\rho \chi^s, \tag{2-23}$$

$$|\mathbf{70},\ {}^2\mathbf{10}\rangle^\rho = \phi^s \chi^\rho, \tag{2-24}$$

$$|\mathbf{70},\ {}^2\mathbf{1}\rangle^\rho = \phi^a \chi^\lambda, \tag{2-25}$$

$$|\mathbf{70},\ {}^2\mathbf{8}\rangle^\lambda = \frac{1}{\sqrt{2}}(\phi^\rho \chi^\rho - \phi^\lambda \chi^\lambda), \tag{2-26}$$

$$|\mathbf{70},\ {}^4\mathbf{8}\rangle^\lambda = \phi^\lambda \chi^s, \tag{2-27}$$

$$|\mathbf{70},\ {}^2\mathbf{10}\rangle^\lambda = \phi^s \chi^\lambda \tag{2-28}$$

and

$$|\mathbf{70},\ {}^2\mathbf{1}\rangle^\lambda = \phi^a \chi^\rho. \tag{2-29}$$

For the totally antisymmetric representation **20** the wavefunctions are

$$|\mathbf{20},\ {}^2\mathbf{8}\rangle = \frac{1}{\sqrt{2}}(\phi^\rho \chi^\lambda - \phi^\lambda \chi^\rho) \tag{2-30}$$

and

$$|\mathbf{20},\ {}^4\mathbf{1}\rangle = \phi^a \chi^s. \tag{2-31}$$

2.2 Spatial Wavefunctions.

Without a spin-dependent interaction in the Hamiltonian for three-body systems, the total orbital angular momentum **L** is conserved, may be added to the total quark spin **S** to give the total angular momentum **J** of the baryon. Therefore, the spatial wavefunctions possess O_3 symmetry. At the same time, the Hamiltonian for a three-body system can also be invariant under the permutation group S_3, so the spatial

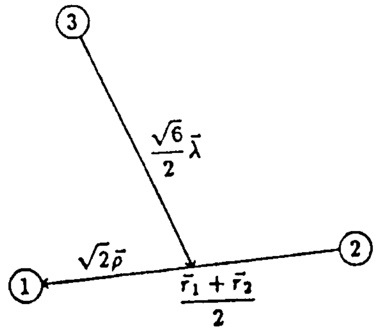

Fig. 1. The natural three body coordinates $\boldsymbol{\rho}$ and $\boldsymbol{\lambda}$

wavefunctions can be written as a representation of the S_3 group. The levels and their symmetries are dependent on the potential, but quite generally the ground state should be a symmetric basis of S_3 with $L^P = 0^+$, and the next excited states are of mixed symmetry with $L^P = 1^-$. Such wavefunctions are often established in the harmonic oscillator basis, which can be used as a first-order approximation. In this section we shall set up the spatial wavefunction in the harmonic oscillator basis up to $N = 2$.

The harmonic oscillator Hamiltonian for a three body system with equal masses is

$$H = \sum_{i=1}^{3} \frac{\mathbf{p}_i^2}{2m} + \frac{1}{6} m\omega^2 \sum_{i<j} (\mathbf{r}_j - \mathbf{r}_i)^2 \tag{2-32}$$

The three coordinates can be rewritten in a basis of S_3 symmetry. The symmetric coordinates $\mathbf{R}$ (or $\mathbf{P}_R$ in momentum space), which describe the usual center of mass motion, and two mixed coordinates $\boldsymbol{\rho}$ and $\boldsymbol{\lambda}$ (or $\mathbf{p}_\rho$ and $\mathbf{p}_\lambda$ in momentum space), which are associated with the internal motion of the three-quark system, are defined as (see Fig. 1)

$$\mathbf{R} = \frac{1}{3}(\mathbf{r}_1 + \mathbf{r}_2 + \mathbf{r}_3) \quad \text{or} \quad \mathbf{P}_R = \mathbf{p}_1 + \mathbf{p}_2 + \mathbf{p}_3, \tag{2-33}$$

$$\boldsymbol{\rho} = \frac{1}{\sqrt{2}}(\mathbf{r}_1 - \mathbf{r}_2) \quad \text{or} \quad \mathbf{p}_\rho = \frac{1}{\sqrt{2}}(\mathbf{r}_1 - \mathbf{r}_2) \tag{2-34}$$

and

$$\boldsymbol{\lambda} = \frac{1}{\sqrt{6}}(\mathbf{r}_1 + \mathbf{r}_2 - 2\mathbf{r}_3) \quad \text{or} \quad \mathbf{p}_\lambda = \frac{1}{\sqrt{6}}(\mathbf{p}_1 + \mathbf{p}_2 - 2\mathbf{p}_3). \tag{2-35}$$

In terms of new coordinates, the harmonic oscillator Hamiltonian Eq. 2-32 is

$$H = \frac{\mathbf{P}^2}{6m} + \frac{\mathbf{p}_\rho^2}{2m} + \frac{\mathbf{p}_\lambda^2}{2m} + \frac{1}{2}m\omega^2(\boldsymbol{\rho}^2 + \boldsymbol{\lambda}^2). \tag{2-36}$$

The corresponding spatial wavefunction can be written as

$$\psi(\mathbf{r}_1, \mathbf{r}_2, \mathbf{r}_3) = \frac{1}{(2\pi)^{\frac{3}{2}}} e^{i\mathbf{P}_R \cdot \mathbf{R}} \psi^\sigma_{NLM_z}(\boldsymbol{\rho}, \boldsymbol{\lambda}) \tag{2-37}$$

where $\psi^\sigma_{NLM_z}(\boldsymbol{\rho}, \boldsymbol{\lambda})$ is the harmonic oscillator wavefunction and $\sigma = s, \rho, \lambda, a$ labels the representation of the S_3 group. The harmonic oscillator wavefunction (see Karl and Obryk 1968) can be rewritten as

$$\psi^\sigma_{NLM_z}(\boldsymbol{\rho}, \boldsymbol{\lambda}) = P^\sigma_{NLM_z} \frac{\alpha^3}{\pi^{\frac{3}{2}}} \exp\left(-\frac{\boldsymbol{\rho}^2 + \boldsymbol{\lambda}^2}{2\alpha^2}\right) \tag{2-38}$$

where $P^\sigma_{NLM_z}$ is polynomial of $\boldsymbol{\lambda}$ and $\boldsymbol{\rho}$, and $\alpha^2 = 1/m\omega$. For the ground state ($N = 0$ $L = 0$) we have

$$P^s_{000} = 1 \tag{2-39}$$

which is the symmetric basis of S_3. For first excited states ($N = 1$) there are two mixed symmetry states with $\mathbf{L}^P = 1^-$:

$$P^\rho_{111} = \alpha\rho_+ \tag{2-40}$$

and

$$P^{\lambda}_{111} = \alpha\lambda_+ \tag{2-41}$$

where $\rho_+ = -(\rho_x + i\rho_y)$ and $\lambda_+ = -(\lambda_x + i\lambda_y)$. For $N = 2$, we have

$$P^{s}_{200} = \frac{1}{\sqrt{3}}\alpha^2(\rho^2 + \lambda^2 - 3\alpha^{-2}) \tag{2-42}$$

which is the radially excited state,

$$P^{\rho}_{200} = \frac{1}{\sqrt{3}}\alpha^2(2\boldsymbol{\rho}\cdot\boldsymbol{\lambda}) \tag{2-43}$$

and

$$P^{\lambda}_{200} = \frac{1}{\sqrt{3}}(\rho^2 - \lambda^2) \tag{2-44}$$

with $L^P = 0^+$,

$$P^{s}_{222} = \frac{1}{2}\alpha^2(\rho_+^2 + \lambda_+^2), \tag{2-45}$$

$$P^{\rho}_{222} = \alpha^2\rho_+\lambda_+ \tag{2-46}$$

and

$$P^{\lambda}_{222} = \frac{1}{2}\alpha^2(\rho_+^2 - \lambda_+^2) \tag{2-47}$$

with $L^P = 2^+$, and

$$P^{a}_{211} = \alpha^2(\rho_+\lambda_z - \lambda_+\rho_z) \tag{2-48}$$

with $L^P = 1^+$. Only the wavefunctions with $M_z = L$ are given here; other states follow the Condon–Shortley convention.

2.3 Total Wavefunction of Baryons.

The $SU(6) \otimes O(3)$ wavefunction can be written as

$$|SU(6) \otimes O(3)\rangle = |\mathbf{N}_6,\ {}^{2S+1}\mathbf{N}_3,\ N, L, J\rangle \tag{2-49}$$

where N and L are the quantum numbers for spatial wavefunctions and the orbital angular momentum L couples with the spin S to give the total angular momentum J. Because the color wavefunction of a three-quark system is totally antisymmetric, the combined $SU(6)$ and spatial wavefunction should be a totally symmetric basis of the S_3 group. Following Eq. 2-4, one only has a symmetric **56** representation of $SU(6)$ wavefunction for the ground state with $N = 0$ and $L^P = 0^+$

$$|\mathbf{56},\ {}^2\mathbf{8},\ 0,\ 0,\ \tfrac{1}{2}\rangle = \frac{1}{\sqrt{2}}(\phi^\rho\chi^\rho + \phi^\lambda\chi^\lambda)\psi^s_{000}(\boldsymbol{\rho},\boldsymbol{\lambda}) \tag{2-50}$$

and

$$|\mathbf{56},\ {}^4\mathbf{10},\ 0,\ 0,\ \tfrac{3}{2}\rangle = \phi^s\chi^s\psi^s_{000}(\boldsymbol{\rho},\boldsymbol{\lambda}). \tag{2-51}$$

The spin assignment for the ground state baryons indeed correspond to the **56** representations of $SU(6)$ symmetry. In particular, for the nonstrange baryons the proton and neutron correspond to the ${}^2\mathbf{8}$ representation, while the Δ resonance $P_{33}(1232)$ has isospin $\frac{3}{2}$, spin $\frac{3}{2}$, and mass 1.232 GeV.

For the first excited states with $N = 1$ and $L^P = 1^-$ only the **70** of $SU(6)$ is possible because of the mixed symmetric spatial wavefunction, so one gets the negative parity baryons:

$$|\mathbf{70},\ {}^2\mathbf{8},\ 1,\ 1,\ J\rangle = \frac{1}{2}[(\phi^\rho\chi^\lambda + \phi^\lambda\chi^\rho)\psi^\rho_{11M}(\boldsymbol{\rho},\boldsymbol{\lambda}) + (\phi^\rho\chi^\rho - \phi^\lambda\chi^\lambda)\psi^\lambda_{11M}(\boldsymbol{\rho},\boldsymbol{\lambda})]_J, \tag{2-52}$$

$$|\mathbf{70},\ ^4\mathbf{8},\ 1,\ 1,\ J\rangle = \frac{1}{\sqrt{2}}[\phi^\rho\chi^s\psi^\rho_{11M}(\boldsymbol{\rho},\boldsymbol{\lambda}) + \phi^\lambda\chi^s\psi^\lambda_{11M}(\boldsymbol{\rho},\boldsymbol{\lambda})]_J, \tag{2-53}$$

$$|\mathbf{70},\ ^2\mathbf{10},\ 1,\ 1,\ J\rangle = \frac{1}{\sqrt{2}}[\phi^s\chi^\rho\psi^\rho_{11M}(\boldsymbol{\rho},\boldsymbol{\lambda}) + \phi^s\chi^\lambda\psi^\lambda_{11M}(\boldsymbol{\rho},\boldsymbol{\lambda})]_J \tag{2-54}$$

and

$$|\mathbf{70}\ ^2\mathbf{1},\ 1,\ 1,\ J\rangle = \frac{1}{\sqrt{2}}[\phi^a\chi^\lambda\psi^\rho_{11M}(\boldsymbol{\rho},\boldsymbol{\lambda}) - \phi^a\chi^\rho\psi^\lambda_{11M}(\boldsymbol{\rho},\boldsymbol{\lambda})]_J \tag{2-55}$$

where the index J inside the bracket means that the spatial and spin wavefunctions are coupled by Clebsch–Gordan coefficients to get a total angular momentum J. Most of these states have been found in experiments; in particular, for the nonstrange baryons these states appear to correspond to

$$^2\mathbf{8}:\ S_{11}(1535),\ D_{13}(1520) \tag{2-56}$$

$$^4\mathbf{8}:\ S_{11}(1650),\ D_{13}(1700),\ D_{15}(1670) \tag{2-57}$$

$$^2\mathbf{10}:\ S_{31}(1650),\ D_{33}(1670) \tag{2-58}$$

where $S_{IS}(M)$ denotes the resonance state with isospin $\frac{I}{2}$, spin $\frac{S}{2}$, and mass M.

For $N = 2$ the spatial wavefunction can be symmetric, antisymmetric, or mixed symmetric, so the **56**, **70**, and **20** representations of $SU(6)$ symmetry are allowed. For the **56** representation of $SU(6)$ the corresponding baryon wavefunctions are

$$|\mathbf{56},\ ^2\mathbf{8},\ 2,\ 0\ \tfrac{1}{2}\rangle = \frac{1}{\sqrt{2}}(\phi^\rho\chi^\rho + \phi^\lambda\chi^\lambda)\psi^s_{200}(\boldsymbol{\rho},\boldsymbol{\lambda}), \tag{2-59}$$

$$|\mathbf{56},\ ^4\mathbf{10},\ 2,\ 0\ \tfrac{3}{2}\rangle = \psi^s\chi^s\psi^s_{200}(\boldsymbol{\rho},\boldsymbol{\lambda}), \tag{2-60}$$

which correspond to radial excitations from the ground states, and

$$|\mathbf{56},\ ^2\mathbf{8},\ 2,\ 2,\ J\rangle = \frac{1}{\sqrt{2}}[(\phi^\rho\chi^\rho + \phi^\lambda\chi^\lambda)\psi^s_{22M}(\boldsymbol{\rho},\boldsymbol{\lambda})]_J, \tag{2-61}$$

$$|\mathbf{56},\ {}^4\mathbf{10},\ 2,\ 2,\ J\rangle = [\psi^s\chi^s\psi^s_{22M}(\boldsymbol{\rho},\boldsymbol{\lambda})]_J. \tag{2-62}$$

For the **70** representation of $SU(6)$, we have

$$|\mathbf{70},\ {}^2\mathbf{8},\ 2,\ 0,\ \tfrac{1}{2}\rangle = \frac{1}{2}[(\phi^\rho\chi^\lambda + \phi^\lambda\chi^\rho)\psi^\rho_{200}(\boldsymbol{\rho},\boldsymbol{\lambda}) + (\phi^\rho\chi^\rho - \phi^\lambda\chi^\lambda)\psi^\lambda_{200}(\boldsymbol{\rho},\boldsymbol{\lambda})], \tag{2-63}$$

$$|\mathbf{70},\ {}^4\mathbf{8},\ 2,\ 0,\ \tfrac{3}{2}\rangle = \frac{1}{\sqrt{2}}[\phi^\rho\chi^s\psi^\rho_{200}(\boldsymbol{\rho},\boldsymbol{\lambda}) + \phi^\lambda\chi^s\psi^\lambda_{200}(\boldsymbol{\rho},\boldsymbol{\lambda})], \tag{2-64}$$

$$|\mathbf{70},\ {}^2\mathbf{8},\ 2,\ 2,\ J\rangle = \frac{1}{2}[(\phi^\rho\chi^\lambda + \phi^\lambda\chi^\rho)\psi^\rho_{22M}(\boldsymbol{\rho},\boldsymbol{\lambda}) + (\phi^\rho\chi^\rho - \phi^\lambda\chi^\lambda)\psi^\lambda_{22M}(\boldsymbol{\rho},\boldsymbol{\lambda})]_J, \tag{2-65}$$

$$|\mathbf{70},\ {}^4\mathbf{8},\ 2,\ 2\ J\rangle = [\phi^\rho\chi^s\psi^\rho_{22M}(\boldsymbol{\rho},\boldsymbol{\lambda}) + \phi^\lambda\chi^s\psi^\lambda_{22M}(\boldsymbol{\rho},\boldsymbol{\lambda})]_J, \tag{2-66}$$

$$|\mathbf{70}\ {}^2\mathbf{10},\ 2,\ 0,\ \tfrac{1}{2}\rangle = \frac{1}{\sqrt{2}}[(\phi^s\chi^\rho\psi^\rho_{200}(\boldsymbol{\rho},\boldsymbol{\lambda}) + \phi^s\chi^\lambda\psi^\lambda_{200}(\boldsymbol{\rho},\boldsymbol{\lambda})]_J, \tag{2-67}$$

$$|\mathbf{70},\ {}^2\mathbf{10}\ 2,\ 2,\ J\rangle = \frac{1}{\sqrt{2}}[(\phi^s\chi^\rho\psi^\rho_{220}(\boldsymbol{\rho},\boldsymbol{\lambda}) + \phi^s\chi^\lambda\psi^\lambda_{220}(\boldsymbol{\rho},\boldsymbol{\lambda})]_J, \tag{2-68}$$

$$|\mathbf{70},\ {}^2\mathbf{1},\ 2,\ 0,\ \tfrac{1}{2}\rangle = \frac{1}{\sqrt{2}}[\phi^a\chi^\lambda\psi^\rho_{200}(\boldsymbol{\rho},\boldsymbol{\lambda}) - \phi^a\chi^\rho\psi^\lambda_{200}(\boldsymbol{\rho},\boldsymbol{\lambda})] \tag{2-69}$$

and

$$|\mathbf{70},\ {}^2\mathbf{1},\ 2,\ 2,\ J\rangle = \frac{1}{\sqrt{2}}[\phi^a\chi^\lambda\psi^\rho_{22M}(\boldsymbol{\rho},\boldsymbol{\lambda}) - \phi^a\chi^\rho\psi^\lambda_{22M}(\boldsymbol{\rho},\boldsymbol{\lambda})]_J. \tag{2-70}$$

For the representation **20**, we have

$$|\mathbf{20},\ {}^2\mathbf{8},\ 2,\ 1,\ J\rangle = \frac{1}{\sqrt{2}}[(\phi^\rho\chi^\lambda - \phi^\lambda\chi^\chi)\psi^a_{21M}(\boldsymbol{\rho},\boldsymbol{\lambda})]_J \tag{2-71}$$

$$|\mathbf{20},\ {}^4\mathbf{1},\ 2,\ 1,\ J\rangle = [\chi^s\phi^a\psi^a_{21M}(\boldsymbol{\rho},\boldsymbol{\lambda})]_J. \tag{2-72}$$

Some of the resonance states corresponding to these representations have been seen in experiments. For the **56** representation, these resonance states are

$${}^2\mathbf{8}:\ P_{11}(1470) \tag{2-73}$$

$${}^4\mathbf{10}:\ P_{33}(1600) \tag{2-74}$$

corresponding to radial excitations with $L = 0$, and the states

$$^2\mathbf{8}: \; P_{13}(1730), \; F_{15}(1688) \tag{2-75}$$

$$^4\mathbf{10}: \; P_{31}(1910), \; P_{33}(1920), \; F_{35}(1905), \; F_{37}(1950) \tag{2-76}$$

with $L = 2$. Only one resonance state has been found that corresponds to the **70** representation; it is $P_{11}(1705)$, with $L = 0$. No resonance state has yet been found that corresponds to the **20** $SU(6)$ representation. Presumably the masses of these states should be higher and the transition rate between these states and the ground states is expected to be very small.

2.4 The Potential Quark Model Of Isgur and Karl.

The quark model is very successful in classification of the baryon spectrum according to $SU(6) \otimes O(3)$ symmetry, but the symmetry limit does not give a quantitative description of baryon spectroscopy; for example, the radial excitation state $P_{11}(1470)$, which has $N = 2$, has lower mass than the negative-parity resonances with $N = 1$. The first systematic and quantitative attempt to describe the baryon spectrum was made by Isgur and Karl (Isgur and Karl, 1978, 1979), who solved the Schrödinger equation for the baryon states with the Hamiltonian

$$H = \sum_i (m_i + \frac{\mathbf{p}_i^2}{2m_i}) + \sum_{i<j} (V^{ij}_{\text{conf}} + H^{ij}_{\text{hyp}}). \tag{2-77}$$

The potential V^{ij} produces confinemant and has the form

$$V^{ij} = C_{qqq} + \frac{1}{2} b r_{ij} - \frac{2}{3} \frac{\alpha_s}{r_{ij}}, \tag{2-78}$$

where $r_{ij} = |\mathbf{r}_i - \mathbf{r}_j|$, and b and α_s are parameters. In a harmonic oscillator basis, V^{ij} can be written in terms of the harmonic oscillator potential plus an anharmonic perturbation:

$$V_{\text{conf}}^{ij} = \frac{1}{2}Kr_{ij}^2 + U_{ij}, \tag{2-79}$$

with

$$U_{ij} = [V_{\text{conf}}^{ij} - \frac{1}{2}Kr_{ij}^2]. \tag{2-80}$$

The hyperfine interaction H_{hyp}^{ij} has the form

$$H_{\text{hyp}}^{ij} = \frac{2\alpha_s}{3m_i m_j}\left\{\frac{8\pi}{3}\mathbf{S}_i\cdot\mathbf{S}_j\delta^3(\mathbf{r}_{ij}) + \frac{1}{r_{ij}^3}\left[\frac{3\mathbf{S}_i\cdot\mathbf{r}_{ij}\mathbf{S}_j\cdot\mathbf{r}_{ij}}{r_{ij}^2} - \mathbf{S}_i\cdot\mathbf{S}_j\right]\right\}, \tag{2-81}$$

where the first term is called the contact term and the second is called the tensor term. The physical origin of the hyperfine interaction is the Breit–Fermi generalization of the one-gluon exchange of QCD, which also includes the spin–orbit force that has been omitted in Eq. 2-81.

The perturbation U_{ij} and the hyperfine interaction play different roles in this model. The perturbations U_{ij} of the potential are anharmonic for different $SU(6)\otimes O(3)$ representations in first-order perturbation; as shown in Fig. 2, the largest energy shift is for the $SU(6)\otimes O(3)$ state $(56', 0^+)$, while it vanishes for the $SU(6)\otimes O(3)$ state $(20, 1^+)$. This gives a good explanation of why the resonance $P_{11}(1470)$ has relatively low mass while the $SU(6)\otimes O(3)$ state $(20, 1^+)$ has not been observed experimentally, in part because the mass scale is predicted to be relatively high. For the hyperfine interaction, the contact term causes the splittings between the

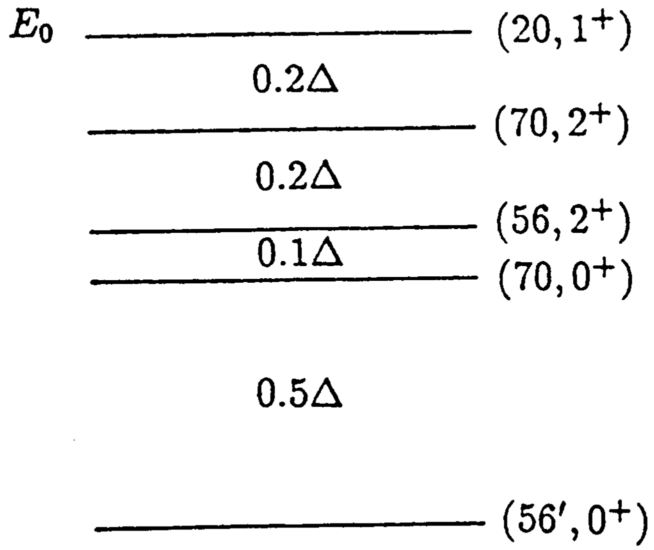

Fig. 2. The pattern of splitting of the N=2 band states in first order for a general anharmonic perturbation U_{ij}. The notation (μ, L^P) gives the $SU(6)$ multiplet μ, the angular momentum L, and parity P of the multiplets. The unperturbed level has the same energy as the state $(20, 1^+)$.

L=0 states $\Delta - N$ because of their different spins. Furthermore, the total spin and total orbital angular momentum are no longer conserved separately because of the tensor structure of the interaction, which induces $SU(6) \otimes O(3)$ configuration mixings. Therefore, one has to diagonalise a matrix for each of the resulting spin-parity sectors; the resulting baryon states are a superposition of the $SU(6) \otimes O(3)$ states

$$|\Psi_{Baryon}\rangle = \sum_i C_i |\Psi^i_{SU(6)\otimes O(3)}\rangle. \qquad (2\text{-}82)$$

For the ground state nucleon, the wavefunction is (Isgur, Karl, and Koniuk, 1978)

$$\begin{aligned}|\Psi_N\rangle \simeq\, & 0.90|\mathbf{56},{}^2\mathbf{8},\ 0,\ 0,\ \tfrac{1}{2}\rangle - 0.34|\mathbf{56},{}^2\mathbf{8},\ 2,\ 0,\ \tfrac{1}{2}\rangle \\ & -0.27|\mathbf{70},{}^2\mathbf{8},\ 2,\ 0,\ \tfrac{1}{2}\rangle - 0.06|\mathbf{70},{}^4\mathbf{8},\ 2,\ 2,\ \tfrac{1}{2}\rangle \end{aligned} \qquad (2\text{-}83)$$

where N and L are the principle quantum number of the harmonic oscillator and total orbital angular momentum, respectively. For the Δ resonance $P_{33}(1232)$ we have

$$\begin{aligned}|\Psi_\Delta\rangle \simeq & 0.97|\mathbf{56},^4\mathbf{10},\ 0,\ 0,\ \tfrac{3}{2}\rangle + 0.20|\mathbf{56},^4\mathbf{10},\ 2,\ 0,\ \tfrac{3}{2}\rangle \\ & -0.10|\mathbf{56},^4\mathbf{10},\ 2,\ 2,\ \tfrac{3}{2}\rangle + 0.07|\mathbf{70},^2\mathbf{10},\ 2,\ 2,\ \frac{3}{2}\rangle. \end{aligned} \qquad (2\text{-}84)$$

In Tables 1 and 2 we show the compositions of the $SU(6) \otimes O(3)$ basis for the positive and negative parity baryons, and their predicted masses. The agreement with the data is indeed impressive.

Despite the success of the model in explaining the data, there are some fundamental problems unanswered in the model. For example, it is neccesary to neglect the spin–orbit interaction, which essentially alters the relative strengths of the short-distance potential terms in the Breit–Fermi limit. As a second example, because the energy shift by the potential U_{ij} is so large, the validity of first order perturbation is questionable. During the last decade, there have been improvements in the model, such as the relativized model of Capstick and Isgur (Capstick and Isgur, 1986).

Table 1: The calculated spectrum and composition of the $SU(6) \otimes O(3)$ basis for the nonstrange baryon resonances with positive parity. Notation: N represents the resonances with isospin $\frac{1}{2}$, and Δ the resonances with isospin $\frac{3}{2}$ (Isgur & Karl, 1979). The experimental data are given by the most recent Particle Data Group Compilation (Yost, *et al,* 1988).

States	Mass (MeV)	Exp. Mass (MeV)	Composition					$SU(6) \otimes O(3)$ Basis
$N\frac{7}{2}^+$	1955	1990±?	1					$\|70\ {}^{4}8, 2, 2, \frac{7}{2}\rangle$
$\Delta\frac{7}{2}^+$	1915	1945±25	1					$\|56\ {}^{4}10, 2, 2, \frac{7}{2}\rangle$
$N\frac{5}{2}^+$	1715	1680±10	0.88	-0.48	0.01			$\|56\ {}^{2}8, 2, 2, \frac{5}{2}\rangle$
$N\frac{5}{2}^+$	1955	2000±?	0.48	0.84	0.27			$\|70\ {}^{2}8, 2, 2, \frac{5}{2}\rangle$
$N\frac{5}{2}^+$	2025	?	-0.13	-0.23	0.96			$\|70\ {}^{4}8, 2, 2, \frac{5}{2}\rangle$
$\Delta\frac{5}{2}^+$	1940	1905±15	0.94	0.38				$\|56\ {}^{4}10, 2, 2, \frac{5}{2}\rangle$
$\Delta\frac{5}{2}^+$	1975	2000±?	-0.38	0.94				$\|70\ {}^{2}10, 2, 2, \frac{5}{2}\rangle$
$N\frac{3}{2}^+$	1710	1745±55	-0.17	0.84	-0.52	0.03	0.00	$\|70\ {}^{4}8, 2, 0, \frac{3}{2}\rangle$
$N\frac{3}{2}^+$	1870	?	0.75	0.34	0.28	-0.46	0.16	$\|56\ {}^{2}8, 2, 2, \frac{3}{2}\rangle$
$N\frac{3}{2}^+$	1955	?	0.59	-0.05	-0.23	0.61	-0.48	$\|70\ {}^{2}8, 2, 2, \frac{3}{2}\rangle$
$N\frac{3}{2}^+$	1980	?	-0.23	0.41	0.77	0.28	-0.34	$\|70\ {}^{4}8, 2, 2, \frac{3}{2}\rangle$
$N\frac{3}{2}^+$	2060	?	0.11	0.08	0.12	0.58	0.79	$\|20\ {}^{2}8, 2, 1, \frac{3}{2}\rangle$
$\Delta\frac{3}{2}^+$	1780	1600±?	0.98	0.18	-0.10			$\|56\ {}^{4}10, 2, 0, \frac{3}{2}\rangle$
$\Delta\frac{3}{2}^+$	1925	1910±15	-0.18	0.92	-0.36			$\|56\ {}^{4}10, 2, 2, \frac{3}{2}\rangle$
$\Delta\frac{3}{2}^+$	1975	?	0.03	0.36	0.94			$\|70\ {}^{2}10, 2, 2, \frac{3}{2}\rangle$
$N\frac{1}{2}^+$	1405	1440±40	0.99	0.17	0.01	0.00		$\|56\ {}^{2}8, 2, 0, \frac{1}{2}\rangle$
$N\frac{1}{2}^+$	1705	1710±30	-0.15	0.94	-0.31	-0.07		$\|70\ {}^{2}8, 2, 0, \frac{1}{2}\rangle$
$N\frac{1}{2}^+$	1890	?	-0.06	0.30	0.83	0.46		$\|70\ {}^{4}8, 2, 2, \frac{1}{2}\rangle$
$N\frac{1}{2}^+$	2055	2100±?	0.02	-0.08	-0.45	0.89		$\|20\ {}^{2}8, 2, 1, \frac{1}{2}\rangle$
$\Delta\frac{1}{2}^+$	1875	1900±50	0.64	0.77				$\|70\ {}^{2}10, 2, 0, \frac{1}{2}\rangle$
$\Delta\frac{1}{2}^+$	1925	?	0.77	-0.64				$\|56\ {}^{4}10, 2, 2, \frac{1}{2}\rangle$

Table 2: The calculated spectrum and composition of the $SU(6) \otimes O(3)$ basis for the nonstrange baryon resonances with negative parity. Notation: N represents the resonances with isospin $\frac{1}{2}$, and Δ the resonances with isospin $\frac{3}{2}$ (Isgur & Karl 1978). The experimental data are given by the most recent Particle Data Group Compilation (Yost, *et al,* 1988).

States	Mass (MeV)	Exp. Mass (MeV)	Composition		$SU(6) \otimes O(3)$ Basis
$N\frac{5}{2}^-$	1670	1675±15	1		$\vert 70\ {}^4 8, 1, 1, \frac{5}{2}\rangle$
$N\frac{3}{2}^-$	1535	1520±10	0.99	-0.11	$\vert 70\ {}^2 8, 1, 1, \frac{3}{2}\rangle$
$N\frac{3}{2}^-$	1745	1700±30	0.11	0.99	$\vert 70\ {}^4 8, 1, 1, \frac{3}{2}\rangle$
$\Delta\frac{3}{2}^-$	1685	1685±55	1		$\vert 70\ {}^2 10, 1, 1, \frac{3}{2}\rangle$
$N\frac{1}{2}^-$	1490	1540±20	0.85	0.53	$\vert 70\ {}^2 8, 1, 1, \frac{1}{2}\rangle$
$N\frac{1}{2}^-$	1655	1650±30	0.53	-0.85	$\vert 70\ {}^4 8, 1, 1, \frac{1}{2}\rangle$
$\Delta\frac{1}{2}^-$	1685	1625±25	1		$\vert 70\ {}^2 10, 1, 1, \frac{1}{2}\rangle$

CHAPTER 3

The Photoproduction of Baryon Resonances

In this chapter we shall follow the work of Copley, Karl and Obryk (Copley *et al* 1969). The basic assumption in the quark model for the photoexcitations of baryon resonances is that a single quark absorbs a photon and is excited. The nonrelativistic electromagnetic interaction is given by Eq. 1-1. The constituent quark mass m_i is chosen to be 330 MeV for the light quarks u and d, and the magnetic moment μ_i is

$$\mu_i = g\frac{e_i}{2m_i} = \mu_0\frac{e_i}{e} \tag{3-1}$$

where μ_0 is taken to be equal to the proton's magnetic moment, and hence $\mu_0 =$ 0.13 GeV^{-1}. The electromagnetic field $\mathbf{A}(r_i)$ of a photon of momentum $\mathbf{k}$ and polarization $\boldsymbol{\epsilon}$ is defined to have the usual expansion:

$$\mathbf{A}_\mathbf{k}(r_i) = \sqrt{4\pi}\sqrt{\frac{1}{2k_0}}\,\boldsymbol{\epsilon}\,[a_\mathbf{k}^\dagger e^{i\mathbf{k}\cdot\mathbf{r}_i} + a_\mathbf{k}e^{-i\mathbf{k}\cdot\mathbf{r}_i}]. \tag{3-2}$$

Eq. 1-1 can be simplified by taking the photon momentum $\mathbf{k}$ as the quantization axis, restricting (without losing generality) to photons with right handed polarization

$$\epsilon = -\frac{1}{\sqrt{2}}(1,\ i,\ 0). \tag{3-3}$$

Further taking advantage of the permutation symmetry of baryon wavefunctions,

$$\begin{aligned}\langle\Psi_f|H_1 + H_2 + H_3|\Psi_i\rangle &= \langle\Psi_f|P_{13}H_3P_{13}^{-1} + P_{23}H_3P_{23}^{-1} + H_3|\Psi_i\rangle \\ &= 3\langle\Psi_f|H_3|\Psi_i\rangle \end{aligned}\tag{3-4}$$

where we note that $P_{13}|\Psi\rangle = P_{23}|\Psi\rangle = -|\Psi\rangle$: i.e, the baryon wavefunctions are totally antisymmetric under exchange among the particles. Hence Eq. 1-1 can be rewritten as

$$\begin{aligned}H_{em} &= \sum_{i=1}^{3} H_i \\ &= 3H_3 \\ &= 6\sqrt{\frac{\pi}{k_0}}\mu_0\ q^{(3)}\ e^{ikz(3)}[kS_+^{(3)} + \frac{1}{g}P_+^{(3)}],\end{aligned}\tag{3-5}$$

where $S_+ = S_x + iS_y$ and $P_+ = P_x + iP_y$. The first term in Eq. 3-5 is the magnetic interaction with a quark and flips the quark's spin projection S_z by one unit, while the second term is the electric multipole interaction that raises L_z of the system by one unit. Therefore, according to the symmetry properties, Eq. 3-5 can be written as

$$H_{em} = q^{(3)}(AL_+ + BS_+) \tag{3-6}$$

with

$$A = 6\sqrt{\frac{\pi}{k_0}}\mu_0\frac{1}{g}\langle\Psi_f|e^{ikz(3)}P_+^{(3)}|\Psi_i\rangle \tag{3-7}$$

and

$$B = 6\sqrt{\frac{\pi}{k_0}}\mu_0 k \langle \Psi_f | e^{ikz(3)} | \Psi_i \rangle \tag{3-8}$$

where $|\Psi_i\rangle$ and $|\Psi_f\rangle$ are the initial and final state wavefunctions.

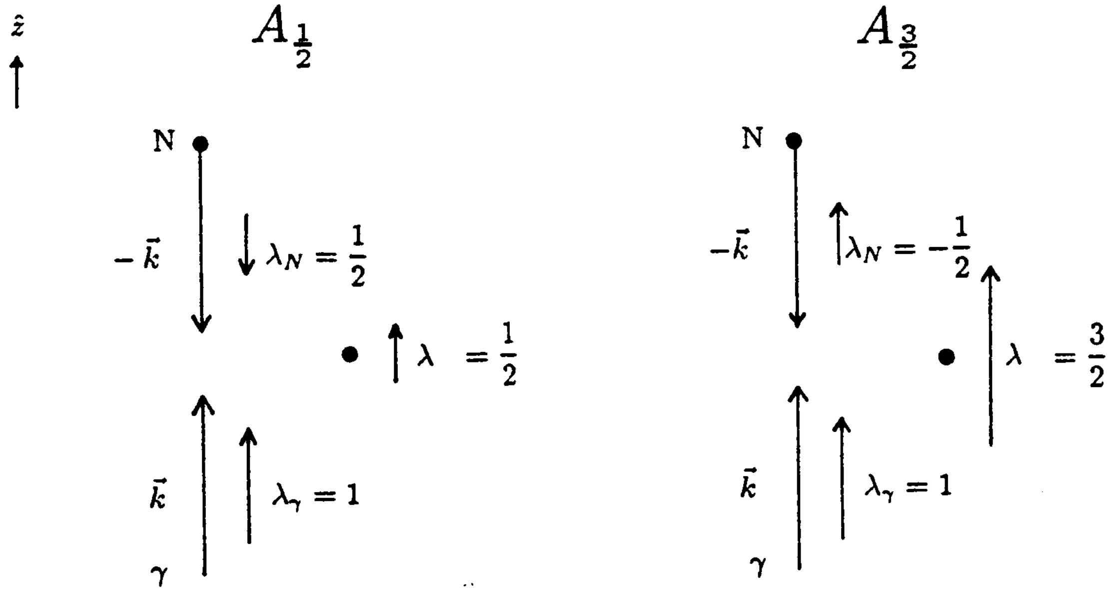

Fig. 3 **Helicity assignments in the rest frame of baryon resonances.**

The transition matrix elements of Eq. 3-6 can be specified completely by the helicity $\frac{1}{2}$ and $\frac{3}{2}$ amplitudes (see Figure 3.), which are defined as

$$A_{\frac{1}{2}} = \langle \Psi_f(J,\ J_z = \frac{1}{2}) | H_{em} | \Psi_i(J,\ J_z = -\frac{1}{2}) \rangle \tag{3-9}$$

and

$$A_{\frac{1}{2}} = \langle \Psi_f(J,\ J_z = \frac{3}{2}) | H_{em} | \Psi_i(J,\ J_z = \frac{1}{2}) \rangle. \tag{3-10}$$

For the helicity $\frac{1}{2}$ amplitude $A_{\frac{1}{2}}$, the initial nucleon has a spin projection $J_z = -\frac{1}{2}$ and a final state $J_z = \frac{1}{2}$, while for the helicity $\frac{3}{2}$ amplitude $A_{\frac{3}{2}}$ the initial state has $J_z = \frac{1}{2}$ and the final state $J_z = \frac{3}{2}$.

The helicity amplitudes $A_{\frac{1}{2}}$ and $A_{\frac{3}{2}}$ are sufficient to determine the rate of excitation, or radiative decay, of a resonance state. Consider a resonance state with spin J and spin projection M along some fixed direction z-axis that decayes into γN. The decay amplitude along a direction z' is a superposition of helicity amplitudes A_λ

$$|A_M^J(\theta)|^2 = \sum_{\lambda=-\frac{3}{2}}^{\frac{3}{2}} |A_{|\lambda|} d^J_{\lambda\ M}(\theta)|^2 \tag{3-11}$$

where $d^J_{\lambda\ M}(\theta)$ is the rotation matrix. The corresponding decay width is

$$\Gamma_\gamma = 2\pi \int |A_M^J(\theta)|^2 \frac{k^2 dk d\Omega}{(2\pi)^3} \frac{m_N}{E_N} \delta(k + E_N - M_R), \tag{3-12}$$

which leads to

$$\Gamma_\gamma = \frac{k^2}{4\pi} \frac{m_N}{M_R} \frac{8}{2J+1} \left\{ |A_{\frac{1}{2}}|^2 + |A_{\frac{3}{2}}|^2 \right\} \tag{3-13}$$

where m_N and M_R are the masses of the nucleon and resonance, respectively. We can relate the width Γ_γ to the total cross section σ_T for the process $\gamma N \to N^* \to N\pi$. In particular, for π^0 photoproduction, we have

$$\sigma_T(\gamma p \to N^* \to p\pi^0) = \left\{ \begin{matrix} \frac{1}{3} \\ \frac{2}{3} \end{matrix} \right\} \frac{m_N}{M_R} \frac{\Gamma_\pi}{\Gamma^2} 2\{|A_{\frac{1}{2}}|^2 + |A_{\frac{3}{2}}|^2\} \tag{3-14}$$

where Γ_π is the partial width for the resonance decay into πN and Γ is the total decay width of the resonance; the factors $\frac{1}{3}$ and $\frac{2}{3}$ correspond to isospin $\frac{1}{2}$ and $\frac{3}{2}$ resonance states, respectively.

The photoexcitation amplitudes $A_{\frac{1}{2}}$ and $A_{\frac{3}{2}}$ can then be calculated in terms of A and B from Eqs. 3-9, 10 in the symmetry limit. The initial state is a proton or neutron, for which the wavefunction is given by Eq. 2-50. For the resonances $S_{11}(1535)$ and $D_{13}(1520)$ the wavefunctions are given by Eq. 2-52, so the helicity amplitude $A_{\frac{1}{2}}$ is

$$A_{\frac{1}{2}}^{P,N} = \frac{1}{2\sqrt{2}}\Big\{\langle 1\ 0, \frac{1}{2}\ \frac{1}{2}|J\ \frac{1}{2}\rangle B[\langle\phi^{\rho}|q^{(3)}|\phi^{\rho}\rangle\langle\chi^{\rho}_{\frac{1}{2}}|S_{+}^{(3)}|\chi^{\rho}_{-\frac{1}{2}}\rangle$$
$$- \langle\phi^{\lambda}|q^{(3)}|\phi_{\lambda}\rangle\langle\chi^{\lambda}_{\frac{1}{2}}|S_{+}^{(3)}|\chi^{\lambda}_{-\frac{1}{2}}\rangle]$$
$$+ \langle 1\ 1, \frac{1}{2}\ -\frac{1}{2}|J\ \frac{1}{2}\rangle A[\langle\phi^{\rho}|q^{(3)}|\phi^{\rho}\rangle - \langle\phi^{\lambda}|q^{(3)}|\phi^{\lambda}\rangle]\Big\}. \quad (3\text{-}15)$$

Notice that

$$\langle\Psi^{\rho}|O^{(3)}|\Psi^{\lambda}\rangle \equiv \langle\Psi^{\lambda}|O^{(3)}|\Psi^{\rho}\rangle \equiv 0 \quad (3\text{-}16)$$

because of the symmetry property $P_{12}O^{(3)}P_{12}^{-1} = O^{(3)}$, where $O^{(3)}$ is the single particle operator of the third particle, which can either be in spin, flavour or spatial space. The matrix elements in Eq. 3-15 are

$$\langle\phi^{\lambda}|q^{(3)}|\phi^{\lambda}\rangle = 0\ (P),\ \frac{1}{3}\ (N), \quad (3\text{-}17)$$

$$\langle\phi^{\rho}|q^{(3)}|\phi^{\rho}\rangle = \frac{2}{3}\ (P),\ -\frac{1}{3}\ (N), \quad (3\text{-}18)$$

$$\langle\chi^{\rho}_{\frac{1}{2}}|S_{+}^{(3)}|\chi^{\rho}_{-\frac{1}{2}}\rangle = 1 \quad (3\text{-}19)$$

and

$$\langle\chi^{\lambda}_{\frac{1}{2}}|S_{+}^{(3)}|\chi^{\lambda}_{-\frac{1}{2}}\rangle = -\frac{1}{3}. \quad (3\text{-}20)$$

This leads to

$$A_{\frac{1}{2}}\begin{pmatrix}P\\N\end{pmatrix} = \frac{2}{3}\left\{A\langle 1\ 1, \frac{1}{2}\ -\frac{1}{2}|J\ \frac{1}{2}\rangle\begin{pmatrix}1\\-1\end{pmatrix} + B\langle 1\ 0, \frac{1}{2}\ \frac{1}{2}|J\ \frac{1}{2}\rangle\begin{pmatrix}1\\-\frac{1}{3}\end{pmatrix}\right\} \quad (3\text{-}21)$$

Therefore, for $J=\frac{3}{2}$ (the resonance $D_{13}(1520)$), the helicity $A_{\frac{1}{2}}$ is

$$A_{\frac{1}{2}}\begin{pmatrix}P\\N\end{pmatrix}=\begin{pmatrix}\frac{1}{3\sqrt{6}}A+\frac{1}{6\sqrt{3}}B\\-\frac{1}{3\sqrt{6}}A-\frac{1}{9\sqrt{3}}B\end{pmatrix} \tag{3-22}$$

while for $J=\frac{1}{2}$ ($S_{11}(1535)$),

$$A_{\frac{1}{2}}\begin{pmatrix}P\\N\end{pmatrix}=\begin{pmatrix}\frac{1}{3\sqrt{3}}A-\frac{1}{3\sqrt{6}}B\\-\frac{1}{3\sqrt{3}}A+\frac{1}{9\sqrt{6}}B\end{pmatrix}. \tag{3-23}$$

Similarly, one can calculate the helicity amplitude $A_{\frac{3}{2}}$:

$$A_{\frac{3}{2}}^{P,N}=\frac{1}{2\sqrt{2}}\langle 1\ 1,\frac{1}{2}\ \frac{1}{2}|J\frac{3}{2}\rangle A[\langle\phi^{\rho}|q^{(3)}|\phi^{\rho}\rangle-\langle\phi^{\lambda}|q^{(3)}|\phi^{\lambda}\rangle]. \tag{3-24}$$

Obviously, only $J=\frac{3}{2}$ ($D_{13}(1520)$) is possible in this case, so one has

$$A_{\frac{3}{2}}\begin{pmatrix}P\\N\end{pmatrix}=\frac{1}{3\sqrt{2}}A\begin{pmatrix}+1\\-1\end{pmatrix}. \tag{3-25}$$

Notice the relation

$$A_{\frac{3}{2}}^{p}=-A_{\frac{3}{2}}^{n} \tag{3-26}$$

in the symmetry limit.

Upon inserting the spatial wavefunction given by Eqs. 2-37, 38, 40 and 41, one can evaluate the coefficients A and B. Explicitly, we have

$$\begin{aligned}&\langle\Psi_f|e^{ikz(3)}P_{+}^{(3)}|\Psi_i\rangle\\&=\frac{\alpha^7}{(2\pi^2)^3}\int d^3Rd^3\rho d^3\lambda e^{-\frac{1}{2}\alpha^2(\lambda^2+\rho^2)}\lambda_{+}\ e^{-i\sqrt{\frac{2}{3}}k\lambda_z}P_{+}^{(3)}e^{-\frac{1}{2}\alpha^2(\lambda^2+\rho^2)}e^{i(\mathbf{P}_f-\mathbf{P}_i-\mathbf{k})\cdot\mathbf{R}}\\&=\delta^3_{(\mathbf{P}_f-\mathbf{P}_i-\mathbf{k})}\frac{\alpha^7}{2\pi^3}\int d^3\rho d^3\lambda\lambda_{+}\ e^{-i\sqrt{\frac{2}{3}}k\lambda_z}P_{+}^{(3)}e^{-\alpha^2(\lambda^2+\rho^2)}.\end{aligned} \tag{3-27}$$

Integrating by parts gives

$$\begin{aligned}
&\langle \Psi_f | e^{ikz(3)} P_+^{(3)} | \Psi_i \rangle \\
&= -\delta^3_{(\mathbf{P}_f - \mathbf{P}_i - \mathbf{k})} \frac{\alpha^7}{2\pi^3} \int d^3\rho \int d^3\lambda e^{-\alpha^2(\lambda^2+\rho^2)} e^{-i\sqrt{\frac{2}{3}}k\lambda_z} P_-^{(3)} \lambda_+ .
\end{aligned} \tag{3-28}$$

Note that

$$\begin{aligned}
P_-^{(3)} \lambda_+ &= -i\sqrt{\frac{2}{3}} \left(\frac{\partial}{\partial \lambda_x} - i \frac{\partial}{\partial \lambda_y} \right) (\lambda_x + i\lambda_y) \\
&= -i2\sqrt{\frac{2}{3}}
\end{aligned} \tag{3-29}$$

and

$$e^{-i\sqrt{\frac{2}{3}}k\lambda_z} = \sum_{l=0}^{\infty} (-i)^l (2l+1) P_l(\cos\theta) j_l(\sqrt{\frac{2}{3}}k\lambda) \tag{3-30}$$

where $P_l(\cos\theta)$ and $j_l(\sqrt{\frac{2}{3}}k\lambda)$ are a Legendre polynomial and a spherical Bessel function, respectively. Substitute Eqs. 3-29, 30 and integrate $d^3\rho$ and the angular part of λ to give

$$\langle \Psi_f | e^{ikz(3)} P_+^{(3)} | \Psi_i \rangle = i\delta^3_{(\mathbf{P}_f - \mathbf{P}_i - \mathbf{k})} \frac{4\alpha^4}{(\pi)^{\frac{1}{2}}} \sqrt{\frac{2}{3}} \int_0^{\infty} j_0(\sqrt{\frac{2}{3}}k\lambda) \lambda^2 \exp\left(-\frac{\lambda^2}{\alpha^2} \right) d\lambda. \tag{3-31}$$

Using the formula

$$\int_0^{\infty} d\lambda \lambda^{\nu+2} e^{-\alpha^2\lambda^2} j_\nu(k\lambda) = \left(\frac{k}{2\alpha} \right)^{\nu} \left(\frac{\sqrt{\pi}}{4\alpha^3} \right) \exp\left(-\frac{k^2}{4\alpha^2} \right), \tag{3-32}$$

the explicit expression for A is

$$A = 6\sqrt{\frac{2}{3}} \mu \sqrt{\frac{\pi}{k_0}} \frac{1}{g} \alpha \exp\left(-\frac{k^2}{6\alpha^2} \right). \tag{3-33}$$

where the phase factor i has been removed from the integral. Similarly, one can show that

$$B = -\frac{6}{\sqrt{3}}\mu\sqrt{\frac{\pi}{k_0}}\,\frac{k^2}{\alpha}\,\exp\left(-\frac{k^2}{6\alpha^2}\right). \tag{3-34}$$

The helicity amplitudes $A_{\frac{1}{2}}$ and $A_{\frac{3}{2}}$ for other resonances are shown in the Table 3, and the expression for the coefficients A and B are given in Table 4. From Table 3, one can obtain the following selection rules and constraints among the helicity amplitudes without further numerical calculation:

1) For the resonance $P_{33}(1230)$ the transition is pure magnetic, which only is proportional to the B term so one has the relation

$$\frac{A_{\frac{3}{2}}}{A_{\frac{1}{2}}} = \sqrt{3}, \tag{3-35}$$

which is consistent with the experimental data.

2) For the resonance $P_{11}(1470)$ we should have the relation,

$$\frac{A^p_{\frac{1}{2}}}{A^n_{\frac{1}{2}}} = -\frac{3}{2} \tag{3-36}$$

which is the ratio of the magnetic moments between the proton and neutron. As shown in chapter 2, the resonance $P_{11}(1470)$ is the radial excitation of the proton and neutron; the wavefunction for this resonance is exactly the same as that of the ground state of protons and neutrons except for the spatial wavefunction. Therefore, the magnetic transition would be proportional to the magnetic moments of the proton and neutron.

3) For the $SU(6)\otimes O(3)$ states $|\mathbf{56}\ {}^2\mathbf{8},\ 2,\ 2,\ J\rangle$, (the resonances $F_{15}(1688)$ and

Table 3: Photon-decay amplitudes between $[56,0^+]_0$ and excited basis state for Eq. 3-6 in naive SU(6) model. These are coefficients multiplying A, B for which the expressions are given in Table 4.

Multiplet	States	$A^p_{\frac{1}{2}}$		$A^p_{\frac{3}{2}}$		$A^n_{\frac{1}{2}}$		$A^n_{\frac{3}{2}}$	
		A	B	A	B	A	B	A	B
$[70,1^-]_1$	$N(^2P_M)\frac{1}{2}^-$	$\frac{1}{3\sqrt{3}}$	$\frac{-1}{3\sqrt{6}}$			$\frac{-1}{3\sqrt{3}}$	$\frac{1}{9\sqrt{6}}$		
	$N(^2P_M)\frac{3}{2}^-$	$\frac{1}{3\sqrt{6}}$	$\frac{1}{6\sqrt{3}}$	$\frac{1}{3\sqrt{2}}$	0	$\frac{-1}{3\sqrt{6}}$	$\frac{-1}{9\sqrt{3}}$	$\frac{-1}{3\sqrt{2}}$	0
	$N(^4P_M)\frac{1}{2}^-$	0	0			0	$\frac{-\sqrt{2}}{18\sqrt{3}}$		
	$N(^4P_M)\frac{3}{2}^-$	0	0	0	0	0	$\frac{-1}{9\sqrt{30}}$	0	$\frac{-1}{3\sqrt{10}}$
	$N(^4P_M)\frac{5}{2}^-$	0	0	0	0	0	$\frac{1}{3\sqrt{30}}$	0	$\frac{1}{3\sqrt{15}}$
	$\Delta(^2P_M)\frac{1}{2}^-$	$\frac{1}{3\sqrt{3}}$	$\frac{-1}{9\sqrt{6}}$						
	$\Delta(^2P_M)\frac{3}{2}^-$	$\frac{-1}{3\sqrt{6}}$	$\frac{1}{9\sqrt{3}}$	$\frac{-1}{3\sqrt{2}}$	0				
$[56,2^+]_2$	$N(^2D_S)\frac{3}{2}^+$	$\frac{\sqrt{3}}{3\sqrt{5}}$	$\frac{-\sqrt{2}}{3\sqrt{5}}$	$\frac{-1}{3\sqrt{5}}$	0	0	$\frac{2\sqrt{2}}{9\sqrt{5}}$	0	0
	$N(^2D_S)\frac{5}{2}^+$	$\frac{\sqrt{2}}{3\sqrt{5}}$	$\frac{\sqrt{3}}{3\sqrt{5}}$	$\frac{2}{3\sqrt{5}}$	0	0	$\frac{-2\sqrt{3}}{9\sqrt{5}}$	0	0
	$\Delta(^4D_S)\frac{1}{2}^+$	0	$\frac{-\sqrt{2}}{9\sqrt{5}}$						
	$\Delta(^4D_S)\frac{3}{2}^+$	0	$\frac{\sqrt{2}}{9\sqrt{5}}$	0	$\frac{-\sqrt{6}}{9\sqrt{5}}$				
	$\Delta(^4D_S)\frac{5}{2}^+$	0	$\frac{\sqrt{6}}{9\sqrt{35}}$	0	$\frac{2}{\sqrt{105}}$				
	$\Delta(^4D_S)\frac{7}{2}^+$	0	$\frac{-2}{3\sqrt{35}}$	0	$\frac{-2\sqrt{3}}{9\sqrt{7}}$				
$[56,0^+]_2$	$N(^2S'_S)\frac{1}{2}^+$	0	$\frac{1}{3}$			0	$\frac{-2}{9}$		
	$\Delta(^4S'_S)\frac{3}{2}^+$	0	$\frac{-\sqrt{2}}{9}$	0	$\frac{-\sqrt{6}}{9}$				
$[56,0^+]_0$	$\Delta(^4S_S)\frac{3}{2}^+$	0	$\frac{-\sqrt{2}}{9}$	0	$\frac{-\sqrt{6}}{9}$				
$[70,0^+]_2$	$N(^2S_M)\frac{1}{2}^+$	0	$\frac{1}{3\sqrt{2}}$			0	$\frac{-1}{9\sqrt{2}}$		
	$N(^4S_M)\frac{3}{2}^+$	0	0	0	0	0	$\frac{\sqrt{2}}{18}$	0	$\frac{\sqrt{6}}{18}$

Table 4: The coefficients of table 1 expressed in a harmonic oscillator basis.

Multiplet	Expression
$[70,1^-]_1$	$A = 6\sqrt{\frac{2}{3}}\mu\sqrt{\frac{\pi}{k_0}}\ \frac{1}{g}\ \alpha \exp\left(-\frac{k^2}{6\alpha^2}\right)$
	$B = -\frac{6}{\sqrt{3}}\mu\sqrt{\frac{\pi}{k_0}}\ \frac{k^2}{\alpha}\ \exp\left(-\frac{k^2}{6\alpha^2}\right)$
$[56,2^+]_2$	$A = -2\mu\sqrt{\frac{\pi}{k_0}}\ \frac{1}{g}\ k \exp\left(-\frac{k^2}{6\alpha^2}\right)$
	$B = \sqrt{\frac{2}{3}}\mu\sqrt{\frac{\pi}{k_0}} k\ \left(\frac{k}{\alpha}\right)^2\ \exp\left(-\frac{k^2}{6\alpha^2}\right)$
$[56,0^+]_2$	$B = -\sqrt{\frac{2}{3}}\mu\sqrt{\frac{\pi}{k_0}}\ k\ \left(\frac{k}{\alpha}\right)^2\ \exp\left(-\frac{k^2}{6\alpha^2}\right)$
$[56,0^+]_0$	$B = -6\mu\sqrt{\frac{\pi}{k_0}} \exp\left(-\frac{k^2}{6\alpha^2}\right)$
$[70,0^+]_2$	$B = \frac{1}{\sqrt{3}}\mu\sqrt{\frac{\pi}{k_0}}\ k\ \left(\frac{k}{\alpha}\right)^2\ \exp\left(-\frac{k^2}{6\alpha^2}\right)$

$P_{13}(1720)$), the amplitudes $A^n_{\frac{3}{2}}$ vanish. In order to have $J_z = \frac{3}{2}$ the wavefunction must have $L_z \neq 0$ and so the transition can only proceed by L_z flip (i.e, by the A term in Eq. 3-6), and the A term in $SU(6)$ space is proportional to the charge operator. Because the $SU(6)$ wavefunction for the resonances $F_{15}(1688)$ and $P_{13}(1720)$ is the same as the $SU(6)$ wavefunction of the proton and neutron, we should have

$$\langle (F_{15},\ P_{13})|q^{(3)}|n\rangle = \langle n|q^{(3)}|n\rangle = 0. \tag{3-37}$$

The data are consistent with this selection rule.

4) Furthermore, for the representation ${}^4\mathbf{8}$, **70** the photoexcitations from the proton vanish. This is called the Moorhouse selection rule (Moorhouse 1966). Since such an excitation changes the quark spin from $S = \frac{1}{2}$ to $S = \frac{3}{2}$, it must take place via a magnetic transition; i.e, through the B term in Eq. 3-8. From Eqs. 2-48, 51, we should have

$$A_{S_z} = \frac{1}{2}B\langle 1\ 0, \frac{3}{2}, S_z|J\ S_z\rangle\langle\phi^\lambda|q^{(3)}|\phi^\lambda\rangle\langle\chi^s_{S_z}|S^{(3)}_+|\chi^\lambda_{S_z-1}\rangle. \tag{3-38}$$

Notice that from Eq. 3-16,

$$\langle\Psi^\rho_f|e^{ikz(3)}|\Psi^s_i\rangle = 0 \tag{3-39}$$

because of permutation symmetry. From Eq. 3-19, we have that A_{S_z} is zero for proton.

These selection rules are determined by the symmetry; there are also the dynamical selection rules proposed by Copley Karl and Obryk. Notice the explicit amplitude $A^p_{\frac{1}{2}}$ from Table 3 and 4

$$A^p_{\frac{1}{2}} \propto \begin{cases} 1 - \frac{k^2}{\alpha^2} & \text{for } D_{13}(1520) \\ 1 - \frac{k^2}{2\alpha^2} & \text{for } F_{15}(1688). \end{cases} \tag{3-40}$$

Empirically these amplitudes are small and may be forced to vanish in the center mass of frame by choosing a value for the oscillator strength $\alpha^2 = 0.175$ GeV^2, where

$$k = \frac{M_R^2 - m_N^2}{2M_R} \tag{3-41}$$

in the center of mass frame. In the symmetry limit the excited energies of baryon resonances can be described qualitatively by this value, so the calculation is consistent within the nonrelativistic framework. Indeed, the photoproduction of baryon resonances provides strong evidence for the underlying $SU(6) \otimes O(3)$ symmetry of the baryon spectrum in the nonrelativistic limit.

CHAPTER 4

Electromagnetic Interaction For Three–body Systems

In this chapter we shall investigate relativistic effects in the electromagnetic interaction for a bound system of three spin-$\frac{1}{2}$ particles. It has long been known that the $H_{\rm em}$ used in chapter 3 is inconsistent, as manifested by its failure to satisfy general low energy theorem for Compton scattering. The spin dependent (DHG) sum rule for a real photon

$$\int \frac{d\omega}{\omega}[\sigma_{\frac{1}{2}} - \sigma_{\frac{3}{2}}] = -\frac{2\alpha\pi^2\kappa^2}{m^2} \tag{4-1}$$

(κ is the anomalous magnetic moment for a target of mass m) provides us with an important criteria for the underlying dynamics of photoexcitations; the corresponding electromagnetic interaction requires the inclusion of relativistic effects up to $O(v^2/c^2)$ in order to satisfy this sum rule, even for systems of free particles. The question is how to obtain $H_{\rm em}$ (including the relativistic effects) from a Dirac Hamiltonian with a binding potential that, as Le. Yaouanc *et al* pointed out, may play an explicit role in H_{em}. The standard procedure in deriving nonrelativistic electromagnetic interactions from the Dirac Hamiltonian is the Foldy–Wouthuysen transformation (see Bjorken and Drell 1964), but this transformation is only adequate for one particle systems. Complications arise from the correlation between the center mass and the internal motions (the so called Wigner rotation) for many body systems. The approach adopted here will be to transform the Dirac equation so that the four-component Dirac spinors are reduced to two-component spin wavefunction satisfying a Shrödinger equation. First, we are going to develop a procedure which is different from the Foldy–Wouthuysen transformation for a one particle system and can be generalized easily to three particle systems. A new H_{em} up to $O(v^2/c^2)$ will be derived, which satisfies the DHG sum rule and low energy theorem. Furthermore, we will discuss the role of the binding potential and show that it may not play an explicit role in H_{em} under the longwavelength approximation, which is valid for real photon interactions.

Generally, one can approximate a four component Dirac wavefunction as

$$\Psi = N(p)\begin{pmatrix} 1 \\ \frac{\boldsymbol{\sigma}\cdot\mathbf{p}}{m+E} \end{pmatrix}\Phi\chi_s \tag{4-2}$$

where $N(p) = \sqrt{\frac{E+m}{2m}}$ with $E = \sqrt{\mathbf{p}^2 + m}$ is the normalization factor, Φ is the spatial wavefunction, and χ is a two component spin wavefunction. The corresponding

Dirac equation can be written as

$$
\begin{aligned}
H\begin{pmatrix} 1 \\ \frac{\boldsymbol{\sigma}\cdot\mathbf{p}}{m+E} \end{pmatrix}\Phi\chi_s N(p) &= i\frac{\partial}{\partial t}\begin{pmatrix} 1 \\ \frac{\boldsymbol{\sigma}\cdot\mathbf{p}}{m+E} \end{pmatrix}\Phi\chi_s N(p) \\
&= i\left(\frac{\partial}{\partial t}\begin{pmatrix} 1 \\ \frac{\boldsymbol{\sigma}\cdot\mathbf{p}}{m+E} \end{pmatrix}N(p)\right)\Phi\chi_s + i\begin{pmatrix} 1 \\ \frac{\boldsymbol{\sigma}\cdot\mathbf{p}}{m+E} \end{pmatrix}N(p)\left(\frac{\partial}{\partial t}\Phi\chi_s\right).
\end{aligned} \tag{4-3}
$$

Multiplying each side of the Eq. 4-3 by $N(p)\left(1,\ \frac{\boldsymbol{\sigma}\cdot\mathbf{p}}{E+m}\right)$ gives

$$
H_{\mathrm{NR}}\Phi\chi_s = i\frac{\partial}{\partial t}\Phi\chi_s \tag{4-4}
$$

where

$$
H_{\mathrm{NR}} = N(p)\left(1,\ \frac{\boldsymbol{\sigma}\cdot\mathbf{p}}{m+E}\right)(H - i\frac{\partial}{\partial t})\begin{pmatrix} 1 \\ \frac{\boldsymbol{\sigma}\cdot\mathbf{p}}{m+E} \end{pmatrix}N(p) \tag{4-5}
$$

is the nonrelativistic Hamiltonian in the corresponding two component Schrödinger equation, and the H_{NR} should be expanded in terms of p/m. Assume that the Hamiltonian in Eq. 4-3 has the form

$$
H = \boldsymbol{\alpha}\cdot(\mathbf{p} - e\mathbf{A}) + \beta m + e\phi \tag{4-6}
$$

where $\mathbf{A}$ and ϕ are electromagnetic fields, and

$$
\boldsymbol{\alpha} = \begin{pmatrix} 0 & \boldsymbol{\sigma} \\ \boldsymbol{\sigma} & 0 \end{pmatrix},\quad \beta = \begin{pmatrix} I & 0 \\ 0 & -I \end{pmatrix} \tag{4-7}
$$

are Dirac matrices. In the case of electromagnetic fields the momentum $\mathbf{p}_i$ in Eq. 4-2 should be replaced by $\mathbf{p} - e\mathbf{A}$. Substitute Eqs. 4-6,7 into Eq. 4-5, expand H_{NR} up to order p^2/m^2, and note that $N(p) \simeq 1 + \frac{\mathbf{p}^2}{8m^2}$ to obtain

$$
\begin{aligned}
H_{\mathrm{NR}} = m &+ \frac{(\mathbf{p} - e\mathbf{A})^2}{2m} - \frac{(\mathbf{p} - e\mathbf{A})^4}{8m^3} + e\phi - \frac{e}{2m}\boldsymbol{\sigma}\cdot\mathbf{B} \\
&+ \frac{e}{8m^2}\boldsymbol{\sigma}\cdot(\mathbf{E}\times\mathbf{p} - \mathbf{p}\times\mathbf{E}) - \frac{e}{8m^2}\nabla\cdot\mathbf{E}.
\end{aligned} \tag{4-8}
$$

This indeed agrees with the result of the Foldy–Wouthuysen transformation for one-particle systems.

For three particle systems, the Dirac wavefunction (Brodsky and Primack 1969) is not simply the product of single particle wavefunctions, and there are additional terms in the spinor because of the correlation between the center of mass and internal motion. It has the form

$$\Psi = N(p_1, p_2, p_3) \prod_{i=1}^{3} \begin{bmatrix} 1 + \frac{\boldsymbol{\sigma}_i \cdot \mathbf{P}}{2M_T+T} \frac{\boldsymbol{\sigma}_i \cdot \mathbf{p}'_i}{2m_i+t_i} \\ \boldsymbol{\sigma} \cdot \left(\frac{\mathbf{P}}{2M_T+T} + \frac{\mathbf{p}'_i}{2m_i+t_i} \right) \end{bmatrix} \Phi \chi_s \tag{4-9}$$

where $\mathbf{P}$ is the total momentum of the system, $\mathbf{p}'_i = \mathbf{p}_i - \frac{m_i}{M_T}\mathbf{P}$, T (t_i) is the kinetic energy of the center of mass system (the particle i), which can be neglected to order $O(1/m^2)$, and $N(p_1, p_2, p_3)$ is the normalization factor for the spinor. In the presence of the binding potential the Hamiltonian for three-body systems is

$$\begin{aligned} H = & \sum_{i=1}^{3} [\boldsymbol{\alpha}_i \cdot (\mathbf{p}_i - e_i \mathbf{A}_i) + \beta_i m_i + e_i \phi_i] \\ & + \sum_{i<j} [V_v(\mathbf{r}_i - \mathbf{r}_j)(1 - \frac{1}{2}\boldsymbol{\alpha}_i \cdot \boldsymbol{\alpha}_j) + \frac{1}{2}\boldsymbol{\alpha}_i \cdot \mathbf{r}\, \boldsymbol{\alpha}_j \cdot \mathbf{r} \frac{V'_v}{r} + \beta_i \beta_j V_s(\mathbf{r}_i - \mathbf{r}_j)] \end{aligned} \tag{4-10}$$

where $r = |\mathbf{r}_i - \mathbf{r}_j|$,

$$V'_v = \frac{dV_v(\mathbf{r}_i - \mathbf{r}_j)}{d|\mathbf{r}_i - \mathbf{r}_j|}, \tag{4-11}$$

and $V_v(\mathbf{r}_i - \mathbf{r}_j)$ and $V_s(\mathbf{r}_i - \mathbf{r}_j)$ denote vector and scalar binding potentials for the quark system (later we will write simply V_v and V_s for brevity). In a typical example, V_s could be a long range scalar harmonic potential and V_v could be a single-gluon exchange potential. Gauge invariance requires the vector potential V_v

to have the form in Eq. 4-10. Similarly, the two-component Hamiltonian for three-body systems can be written as

$$H_{\rm NR} = N(p_1,p_2,p_3)\left(\prod_{i=1}^{3}\begin{bmatrix} 1+\frac{\boldsymbol{\sigma}_i\cdot\mathbf{P}}{2M_T+T}\frac{\boldsymbol{\sigma}_i\cdot\mathbf{p}_i'}{2m_i+t_i} \\ \boldsymbol{\sigma}_i\cdot\left(\frac{\mathbf{P}}{2M_T+T}+\frac{\mathbf{p}_i'}{2m_i+t_i}\right)\end{bmatrix}\right)^{\dagger}\times$$

$$(H-\frac{\partial}{i\partial t})\prod_{i=1}^{3}\begin{bmatrix} 1+\frac{\boldsymbol{\sigma}_i\cdot\mathbf{P}}{2M_T+T}\frac{\boldsymbol{\sigma}_i\cdot\mathbf{p}_i'}{2m_i+t_i} \\ \boldsymbol{\sigma}_i\cdot\left(\frac{\mathbf{P}}{2M_T+T}+\frac{\mathbf{p}_i'}{2m_i+t_i}\right)\end{bmatrix}N(p_1,p_2,p_3). \qquad (4\text{-}12)$$

The resulting nonrelativistic Hamiltonian $H_{\rm NR}$ corresponding to Eq. 4-10 can be divided into two parts: the nonrelativistic binding potential $H_{\rm b}$ and the electromagnetic interaction $H_{\rm em}$. Up to order p^4/m^4 the binding potential H_b is

$$\begin{aligned} H_{\rm b} =& \sum_{i=1}^{3}\left(\frac{p_i^2}{2m_i}-\frac{p_i^4}{8m_i^3}\right)+ \\ & \sum_{i<j}\Bigg\{V_v+V_s+\frac{1}{8m_i^2}\,\nabla^2\,V_v+\frac{1}{4m_i^2}\boldsymbol{\sigma}_i\cdot[\nabla(V_v-V_s)\times\mathbf{p}_i] \\ & -\frac{1}{4m_j^2}\boldsymbol{\sigma}_j\cdot[\nabla(V_v-V_s)\times\mathbf{p}_j]-\{(\frac{1}{8m_i^2}p_i^2+\frac{1}{8m_j^2}p_j^2),V_s\} \\ & -\frac{1}{4m_i^2}\mathbf{p}_i\cdot V_s\mathbf{p}_i-\frac{1}{4m_j^2}\mathbf{p}_jV_s\cdot\mathbf{p}_j+\frac{1}{4M_T}\left(\frac{\boldsymbol{\sigma}_i}{m_i}-\frac{\boldsymbol{\sigma}_j}{m_j}\right)\cdot[\nabla(V_v+V_s)\times\mathbf{P}] \\ & +\frac{1}{2m_im_j}\Bigg[-\frac{1}{4}\{\mathbf{p}_i,\ \{\mathbf{p}_j,\ V_v\}\}+\frac{1}{4}\{\mathbf{p}_j,\ \{\mathbf{p}_i,\ \mathbf{r}\mathbf{r}\frac{V_v'}{r}\}\}+\boldsymbol{\sigma}_j\cdot(\mathbf{p}_i\times\nabla V_v) \\ & \quad -\boldsymbol{\sigma}_i\cdot(\mathbf{p}_j\times\nabla V_v)-\boldsymbol{\sigma}_i\cdot\boldsymbol{\sigma}_j\,\nabla^2\,V_v+(\boldsymbol{\sigma}_i\cdot\nabla)(\boldsymbol{\sigma}_j\cdot\nabla)V_v\Bigg]\Bigg\} \end{aligned} \qquad (4\text{-}13)$$

where

$$\{\mathbf{p}_i,\ \{\mathbf{p}_j,\ V_v\}\} = \mathbf{p}_i\cdot\mathbf{p}_jV_v+\mathbf{p}_i\cdot V_v\mathbf{p}_j+\mathbf{p}_j\cdot V_v\mathbf{p}_i+V_v\mathbf{p}_i\cdot\mathbf{p}_j, \qquad (4\text{-}14)$$

$$\begin{aligned}\{\mathbf{p}_j,\ \{\mathbf{p}_i,\ \mathbf{r}\mathbf{r}\frac{V_v'}{r}\}\} =& \mathbf{p}_i\cdot(\mathbf{p}_j\cdot\mathbf{r})\mathbf{r}\frac{V_v'}{r}+\mathbf{p}_i\cdot\mathbf{r}\frac{V_v'}{r}\mathbf{r}\cdot\mathbf{p}_j \\ & +\mathbf{p}_j\cdot\mathbf{r}\frac{V_v'}{r}\mathbf{r}\cdot\mathbf{p}_i+\frac{V_v'}{r}\mathbf{r}\cdot(\mathbf{r}\cdot\mathbf{p}_j)\mathbf{p}_i. \end{aligned} \qquad (4\text{-}15)$$

and $\{A, B\}$ represents the anticommutator. If the vector potential is $V_v = \frac{1}{r}$, the terms associated with V_v in Eq. 4-13 are

$$H_{ij}(V_v) = \frac{1}{r} - \frac{1}{2m_i m_j}\left(\frac{\mathbf{p}_i \cdot \mathbf{p}_j}{r} + \frac{\mathbf{r}\cdot(\mathbf{r}\cdot\mathbf{p}_i)\mathbf{p}_j}{r^3}\right) - \frac{\pi}{2}\delta^3(\mathbf{r})\left(\frac{1}{m_i^2} + \frac{1}{m_j^2} + \frac{4\boldsymbol{\sigma}_i\cdot\boldsymbol{\sigma}_j}{3m_i m_j}\right)$$
$$- \frac{1}{4r^3}\Bigg\{\frac{1}{m_i^2}\boldsymbol{\sigma}_i \cdot \mathbf{r}\times\mathbf{p}_i - \frac{1}{m_j^2}\boldsymbol{\sigma}_j\cdot\mathbf{r}\times\mathbf{p}_j + \frac{1}{m_i m_j}[2\boldsymbol{\sigma}_j\cdot\mathbf{r}\times\mathbf{p}_i - 2\boldsymbol{\sigma}_i\cdot\mathbf{r}\times\mathbf{p}_j$$
$$-\boldsymbol{\sigma}_i\cdot\boldsymbol{\sigma}_j + \frac{3(\boldsymbol{\sigma}_i\cdot\mathbf{r})(\boldsymbol{\sigma}_j\cdot\mathbf{r})}{r^2}]\Bigg\} \tag{4-16}$$

which is the standard Breit–Fermi interaction. For H_{em} it has the form

$$H_{\mathrm{em}} = \sum_{i=1}^{3}\{-\frac{e_i}{2m_i}(\mathbf{A}_i\cdot\mathbf{p}_i + \mathbf{p}_i\cdot\mathbf{A}_i) - \frac{e_i}{2m_i}\boldsymbol{\sigma}_i\cdot\mathbf{B}_i + e_i\phi_i$$
$$+\frac{e_i}{4m_i}\boldsymbol{\sigma}_i\cdot(\mathbf{E}_i\times\frac{\mathbf{p}_i}{2m_i} - \frac{\mathbf{p}_i}{2m_i}\times\mathbf{E}_i)$$
$$+\frac{e_i}{8m_i^3}\{p_i^2, \mathbf{A}_i\cdot\mathbf{p}_i + \mathbf{p}_i\cdot\mathbf{A}_i + \boldsymbol{\sigma}_i\cdot\mathbf{B}_i\}\}+$$
$$\sum_{i<j}\Bigg\{-\frac{e_i}{4m_i^2}\boldsymbol{\sigma}_i\cdot[\nabla(V_v - V_s)\times\mathbf{A}_i] + \frac{e_j}{4m_j^2}\boldsymbol{\sigma}_j\cdot[\nabla(V_v - V_s)\times\mathbf{A}_j]$$
$$+\{V_s, \frac{1}{8m_i^2}(\mathbf{p}_i\cdot\mathbf{A}_i + \mathbf{A}_i\cdot\mathbf{p}_i) + \frac{1}{8m_j^2}(\mathbf{p}_j\cdot\mathbf{A}_j + \mathbf{A}_j\cdot\mathbf{p}_j)\}$$
$$+(\frac{e_i}{2m_i^2}\boldsymbol{\sigma}_i\cdot\mathbf{B}_i + \frac{e_j}{2m_j^2}\boldsymbol{\sigma}_j\cdot\mathbf{B}_j)V_s + \frac{e_i}{4m_i^2}(\mathbf{p}_i\cdot\mathbf{A}_iV_s + V_s\mathbf{A}_i\cdot\mathbf{p}_i)$$
$$+\frac{e_j}{4m_j^2}(\mathbf{p}_j\cdot\mathbf{A}_jV_s + V_s\mathbf{A}_j\cdot\mathbf{p}_j) + \frac{1}{4M_T}\left(\frac{\boldsymbol{\sigma}_i}{m_i} - \frac{\boldsymbol{\sigma}_j}{m_j}\right)\cdot[e_j\mathbf{E}_j\times\mathbf{p}_i$$
$$-e_i\mathbf{E}_i\times\mathbf{p}_j - \nabla(V_v + V_s)\times(e_1\mathbf{A}_1 + e_2\mathbf{A}_2 + e_3\mathbf{A}_3)]$$
$$-\frac{1}{2m_i m_j}\Bigg[-\frac{1}{2}e_i\mathbf{A}_i\cdot\{\mathbf{p}_j,\ V_v\} - \frac{1}{2}e_j\mathbf{A}_j\cdot\{\mathbf{p}_i,\ V_v\}$$
$$+\frac{1}{2}\{\mathbf{p}_j, \mathbf{r}(e_i\mathbf{A}_i\cdot\mathbf{r})\frac{V_v'}{r}\} + \frac{1}{2}\{\mathbf{p}_i, \mathbf{r}(e_j\mathbf{A}_j\cdot\mathbf{r})\frac{V_v'}{r}\}$$
$$+\boldsymbol{\sigma}_j\cdot(e_i\mathbf{A}_i\times\nabla V_v) - \boldsymbol{\sigma}_i\cdot(e_j\mathbf{A}_j\times\nabla V_v)\Bigg]\Bigg\} \tag{4-17}$$

The effects of the anomalous magnetic moment have been excluded in this calculation and will be included later; terms with higher powers of $\mathbf{A}_i$ also have been excluded.

From this calculation we can see that the nonrelativistic electromagnetic interaction can be divided into two parts: the first part is associated with the gauge invariance of the nonrelativistic H_b in which $\mathbf{p}_i$ is replaced by $\mathbf{p}_i - e_i\mathbf{A}_i$; the second part is the interaction between the magnetic moments of the quark system and the external magnetic fields. McClary and Byers (McClary and Byers 1983) in their calculation of the transition rates in heavy quarkonium have shown how to avoid the explicit appearance of the binding potential in the first part. Note that the gauge invariant transformation converts the H_b of Eq. 4-13 to

$$H_b(\mathbf{r}_i, \mathbf{p}_i) \xrightarrow{\mathbf{p}_i \to \mathbf{p}_i - e_i\mathbf{A}_i} H_b(\mathbf{r}_i, \mathbf{p}_i - e_i\mathbf{A}_i). \tag{4-18}$$

Expanding the $H_b(\mathbf{r}_i, \mathbf{p}_i - e_i\mathbf{A}_i)$ in terms of $e_i\mathbf{A}_i$ one has

$$H_b(\mathbf{r}_i, \mathbf{p}_i - e_i\mathbf{A}_i) = H_b(\mathbf{r}_i, \mathbf{p}_i) + H'_{\text{em}} + O(\mathbf{A}_i^2) \tag{4-19}$$

where

$$\begin{aligned} H'_{\text{em}} &= \sum_i -e_i\mathbf{A}_i \cdot \nabla_{\mathbf{p}_i} H_b(\mathbf{r}_i, \mathbf{p}_i) \\ &= \sum_i ie_i\mathbf{A}_i \cdot [H_b(\mathbf{r}_i, \mathbf{p}_i),\ \mathbf{r}_i] \end{aligned} \tag{4-20}$$

and hence Eq. 4-17 becomes

$$\begin{aligned} H_{\text{em}} = &\sum_{i=1}^{3} e_i(-i\frac{1}{2}([H_b, \mathbf{r}_i] \cdot \mathbf{A}_i + \mathbf{A}_i \cdot [H_b, \mathbf{r}_i]) - \frac{e_i}{2m_i}\boldsymbol{\sigma}_i \cdot \mathbf{B}_i + e_i\phi_i + \\ &\frac{e_i}{4m_i}\sigma_i \cdot (\mathbf{E}_i \times \frac{\mathbf{p}_i}{2m_i} - \frac{\mathbf{p}_i}{2m_i} \times \mathbf{E}_i) + \frac{e_i}{8m_i^3}\{p_i^2, \boldsymbol{\sigma}_i \cdot \mathbf{B}_i\}) + \\ &\sum_{i<j}((\frac{e_i}{2m_i^2}\boldsymbol{\sigma}_i \cdot \mathbf{B}_i + \frac{e_j}{2m_j^2}\sigma_j \cdot \mathbf{B}_j)V_s + \\ &\frac{1}{4M_T}\left(\frac{\boldsymbol{\sigma}_i}{m_i} - \frac{\boldsymbol{\sigma}_j}{m_j}\right) \cdot (e_j\mathbf{E}_j \times \mathbf{p}_i - e_i\mathbf{E}_i \times \mathbf{p}_j)). \end{aligned} \tag{4-21}$$

Furthermore, the $\boldsymbol{\sigma}\cdot\mathbf{B}$ terms can be made more transparent:

$$\sum_{i=1}^{3}(-\frac{e_i}{2m_i}\boldsymbol{\sigma}_i\cdot\mathbf{B}_i+\frac{e_i}{8m_i^3}\{p_i^2,\boldsymbol{\sigma}_i\cdot\mathbf{B}_i\})+\sum_{i<j}(\frac{e_i}{2m_i^2}\boldsymbol{\sigma}_i\cdot\mathbf{B}_i+\frac{e_j}{2m_j^2}\boldsymbol{\sigma}_j\cdot B_j)V_s$$
$$=\sum_{i=1}^{3}\frac{e_i}{2m_i^*}\boldsymbol{\sigma}_i\cdot\mathbf{B}_i+O(1/m^2) \qquad (4\text{-}22)$$

where the constituent mass m_i^* is

$$m_i^*=m_i+\frac{p_i^2}{2m_i}+\sum_{j\neq i}V_s(\mathbf{r}_i-\mathbf{r}_j). \qquad (4\text{-}23)$$

Therefore, one can relate the constituent mass to the current quark mass plus the effect of a scalar potential responsible for confinement in the quark model.

After including the contribution of the anomalous magnetic moment, the electromagnetic interaction of the quark system can be written as

$$H_{\mathrm{em}}=\sum_{i=1}^{3}(-ie_i\frac{1}{2}([H_b,\mathbf{r}_i]\cdot\mathbf{A}_i+\mathbf{A}_i\cdot[H_b,\mathbf{r}_i])-\mu_i\boldsymbol{\sigma}_i\cdot\mathbf{B}_i-$$
$$\frac{1}{2}(2\mu_i-\frac{e_i}{2m_i^*})\boldsymbol{\sigma}_i\cdot(\mathbf{E}_i\times\frac{\mathbf{p}_i}{2m_i^*}-\frac{\mathbf{p}_i}{2m_i^*}\times\mathbf{E}_i)+e_i\phi_i)+$$
$$\sum_{i<j}\frac{1}{4M_T}\left(\frac{\boldsymbol{\sigma}_i}{m_i^*}-\frac{\boldsymbol{\sigma}_j}{m_j^*}\right)\cdot(e_j\mathbf{E}_j\times\mathbf{p}_i-e_i\mathbf{E}_i\times\mathbf{p}_j) \qquad (4\text{-}24)$$

which in the long wavelength approximation may be written as

$$H_{\mathrm{em}}=\sum_{i=1}^{3}(e_i\mathbf{r}_i\cdot\mathbf{E}_i+i\frac{e_i}{2m_i^*}(\mathbf{p}_i\cdot\mathbf{k}\mathbf{r}_i\cdot\mathbf{A}_i+\mathbf{r}_i\cdot\mathbf{A}_i\mathbf{p}_i\cdot\mathbf{k})-\mu_i\boldsymbol{\sigma}_i\cdot\mathbf{B}_i-$$
$$\frac{1}{2}(2\mu_i-\frac{e_i}{2m_i^*})\boldsymbol{\sigma}_i\cdot(\mathbf{E}_i\times\frac{\mathbf{p}_i}{2m_i^*}-\frac{p_i}{2m_i^*}\times\mathbf{E}_i)+e_i\phi_i)+$$
$$\sum_{i<j}\frac{1}{4M_T}\left(\frac{\boldsymbol{\sigma}_i}{m_i^*}-\frac{\boldsymbol{\sigma}_j}{m_j^*}\right)\cdot(e_j\mathbf{E}_j\times\boldsymbol{p}_i-e_i\mathbf{E}_i\times\mathbf{p}_j). \qquad (4\text{-}25)$$

This form for H_{em} satisfies the DHG sum rule and low energy theorem (Brodsky, Primack 1969; Close, Osborn 1970; Close, Copley 1970). Note that the second and third lines in Eq. 4-25, omitted in much of the literature, are necessary in this regard.

The physics behind this is very clear, as McClary and Byers pointed out. The first part of the electromagnetic interaction containing the binding potential is generated from the corresponding term in H_b by the gauge-covariant substitution $\mathbf{p} \to \mathbf{p} - e\mathbf{A}$. Thus the tensorial transformation properties of $H_b(\mathbf{p})$ are manifested in $H_{\rm em}(\mathbf{A})$. If there is no configuration mixing in the quark model, the matrix elements of Eq. 4-24 between eigenstates of the binding potential are identical to those of the electromagnetic interaction of Eq. 4-17 neglecting the binding potential $V_{s,v}$ terms. This point has not been consistently addressed in the literature. For example, Ohta (Ohta 1979) generates a spin–orbit term in $H_{\rm em}$ by substituting $\mathbf{p} \to \mathbf{p} - e\mathbf{A}$ into the spin–orbit term of H_b; however, in the Isgur–Karl study of the baryon spectrum it is necessary to ignore the $\mathbf{L}\cdot\mathbf{S}$ terms in H_b in order to fit the data (Isgur and Karl 1978). This can generate an inconsistency in electromagnetic transition operators when the binding potential is included. The binding potential may induce configuration mixing among the $SU(6) \otimes O(3)$ basis states, but need not play an explicit role in $H_{\rm em}$ if Eq. 4-25 is used.

CHAPTER 5

Relativistic Effects

In chapter 4, we saw that relativistic effects exist both in the binding potential H_b, (such as the Breit–Fermi interaction), and in the electromagnetic interaction (which is required to satisfy the low energy theorem and DHG sum rule). The relativistic effect in the binding potential further induces $SU(6) \otimes O(3)$ configuration mixing, as shown by Isgur and Karl; this in turn will affect the transition matrix element. In this chapter we shall show how to calculate the matrix elements of the spin–orbit and non-additive interaction in Eq. 4-24. Further, we shall evaluate the relativistic effects due to QCD configuration mixing, which leads to the presence of large components of the $SU(6) \otimes O(3)$ states $|\mathbf{56},\ {}^2\mathbf{8},\ N = 2,\ L = 0\rangle$ and $|\mathbf{70},\ {}^2\mathbf{8},\ N = 2,\ L = 0\rangle$ in the ground state wavefunction of Eq. 2-81 for the Isgur and Karl model.

Notice that the relativistic effects in the electromagnetic interaction and in the binding potential should have different phenomenlogical consequences; some of the selection rules and constraints among the helicity amplitudes in the symmetry limit should still exist for the electromagnetic interaction of Eq. 4-24, and these selection rules will be broken down by the configuration mixing effects. This should help us to establish the configuration mixing effects in the data, and also tell us about the kind of quark-quark potential that would induce such configuration mixing effects. Therefore, we will study the phenomenological consequences of relativistic effects in the electromagnetic interaction first, and specially try to establish the selection rules and constraints among the helicity amplitudes; then we will use the wavefunction given by the Isgur and Karl potential model to evaluate the configuration mixing effects. The agreement between the theoretical prediction and data will be a crucial test of the model.

Following the procedure of chapter 3, the Eq. 4-24 may be rewritten as

$$H_{\rm em} = H_{\rm NR} + H_{\rm SO} + H_{\rm NA} \tag{5-1}$$

where

$$H_{\rm NR} = \sum_{i=1}^{3}(e_i\mathbf{r}_i \cdot \mathbf{E}_i + i\frac{e_i}{2m_i}(\mathbf{p}_i \cdot \mathbf{k}\mathbf{r}_i \cdot \mathbf{A}_i + \mathbf{r}_i \cdot \mathbf{A}_i\mathbf{p}_i \cdot \mathbf{k}) - \mu_i\boldsymbol{\sigma}_i \cdot \mathbf{B}_i + e_i\phi_i) \tag{5-2}$$

which is essentially the nonrelativistic $H_{\rm em}$ used in most work on the nonrelativistic quark model, but with the first two terms replacing the more usual $\mathbf{p} \cdot \mathbf{A}/m_q$ term in order to take into acount the effects of the binding potential,

$$H_{\rm SO} = \sum_{i=1}^{3} -\frac{1}{2}(2\mu_i - \frac{e_i}{2m_i})\frac{\boldsymbol{\sigma}_i}{2m_i} \cdot (\mathbf{E}_i \times \mathbf{p}_i - \mathbf{p}_i \times \mathbf{E}_i) \tag{5-3}$$

which is the so called spin orbit term, and

$$H_{\rm NA} = \sum_{j\rangle i=1}^{3} \frac{1}{4M_T}\left(\frac{\boldsymbol{\sigma}_i}{m_i} - \frac{\boldsymbol{\sigma}_j}{m_j}\right) \cdot (e_j\mathbf{E}_j \times \mathbf{p}_i - e_i\mathbf{E}_i \times \mathbf{p}_j) \tag{5-4}$$

which is the nonadditive term associated with the Wigner rotation of the quark transformed from the frame of the recoiling quark to the frame of the recoiling baryon. Similarly we can rewrite Eqs. 5-2, 5-3, and 5-4 as

$$H_{\mathrm{NR}} = q^{(3)}(A_n L_+ + B_n S_+) \tag{5-5}$$

$$H_{\mathrm{SO}} = q^{(3)}(B_s S_+ + C_s S_z L_+) \tag{5-6}$$

$$H_{\mathrm{NA}} = q^{(2)}(B_{no} S_+^{(1-2)} - C_{no} S_z^{(1-2)} L_+) \tag{5-7}$$

where

$$A_n = 6\sqrt{\frac{\pi}{k_0}}\mu\frac{im_q}{g}\langle\Psi_f|e^{ikz(3)}r_+^{(3)}(k_0 - \frac{k}{m_q}(P_z^{(3)} + \frac{k}{2}))|\Psi_i\rangle, \tag{5-8}$$

$$B_n = 6\sqrt{\pi k}\mu\langle\Psi_f|e^{ikz(3)}|\Psi_i\rangle, \tag{5-9}$$

$$B_s = -6\sqrt{\pi k}\frac{\mu}{2m_q}(2 - \frac{1}{g})\langle\Psi_f|e^{ikz(3)}(P_z^{(3)} + \frac{k}{2})|\Psi_{i,}\rangle \tag{5-10}$$

$$C_s = 6\sqrt{\pi k}\frac{\mu}{2m_q}(2 - \frac{1}{g})\langle\Psi_f|e^{ikz(3)}P_+^{(3)}|\Psi_i\rangle, \tag{5-11}$$

$$B_{na} = \sqrt{\pi k}\frac{2\mu}{m_q g}\langle\Psi_f|e^{ikz(2)}P_z^{(1)}|\Psi_i\rangle \tag{5-12}$$

and

$$C_{na} = \sqrt{\pi k}\frac{2\mu}{m_q g}\langle\Psi_f|e^{ikz(2)}P_+^{(1)}|\Psi_i\rangle. \tag{5-13}$$

In a way similar to Chapter 3, one can evaluate A, B, C and D in Eqs. 5-8, 9, 10 and 11, but one has to be careful to include the recoil effects properly. To understand this we turn to current conservation in the nonrelativistic limit, which states (Abdullah and Close, 1972)

$$k_\lambda V^\lambda = k_0 V_0 - \mathbf{k}\cdot\mathbf{V} = 0, \tag{5-14}$$

and in the $SU(6)\otimes O(3)$ symmetry limit this leads to

$$k_0\langle\Psi_f(\boldsymbol{\rho},\boldsymbol{\lambda},\mathbf{R})|e^{i\mathbf{k}\cdot\mathbf{r}_3}|\Psi_i(\boldsymbol{\rho},\boldsymbol{\lambda},\mathbf{R})\rangle =$$

$$\frac{1}{2m_q}\mathbf{k}\cdot\langle\Psi_f(\boldsymbol{\rho},\boldsymbol{\lambda},\mathbf{R})|\mathbf{p}_3 e^{i\mathbf{k}\cdot\mathbf{r}_3}+e^{i\mathbf{k}\cdot\mathbf{r}_3}\mathbf{p}_3|\Psi_i(\boldsymbol{\rho},\boldsymbol{\lambda},\mathbf{R})\rangle, \quad (5\text{-}15)$$

where k_λ is the four-momentum transfer to the quark system, and we assume equal mass quarks. Note that

$$\begin{aligned}\mathbf{k}\cdot\mathbf{p}_3 e^{i\mathbf{k}\cdot\mathbf{r}_3}+e^{i\mathbf{k}\cdot\mathbf{r}_3}\mathbf{p}_3\cdot\mathbf{k} &= \mathbf{p}_3\cdot[\mathbf{p}_3,\ e^{i\mathbf{k}\cdot\mathbf{r}_3}]+[\mathbf{p}_3,\ e^{i\mathbf{k}\cdot\mathbf{r}_3}]\cdot\mathbf{p}_3\\ &= [\mathbf{p}_3^2,\ e^{i\mathbf{k}\cdot\mathbf{r}_3}]. \end{aligned}\quad (5\text{-}16)$$

So, one could further write the right hand side of Eq. 5-15 as

$$\begin{aligned}&\frac{1}{2m_q}\langle\Psi_f(\boldsymbol{\rho},\boldsymbol{\lambda},\mathbf{R})|[\mathbf{p}_3^2,\ e^{i\mathbf{k}\cdot\mathbf{r}_3}]|\Psi_i(\boldsymbol{\rho},\boldsymbol{\lambda},\mathbf{R})\rangle\\ &\qquad=\langle\Psi_f(\boldsymbol{\rho},\boldsymbol{\lambda},\mathbf{R})|[\sum_{i=1}^{3}\frac{\mathbf{p}_i^2}{2m_i},\ e^{i\mathbf{k}\cdot\mathbf{r}_3}]|\Psi_i(\boldsymbol{\rho},\boldsymbol{\lambda},\mathbf{R})\rangle\\ &\qquad=\langle\Psi_f(\boldsymbol{\rho},\boldsymbol{\lambda},\mathbf{R})|[H,\ e^{i\mathbf{k}\cdot\mathbf{r}_3}]|\Psi_i(\boldsymbol{\rho},\boldsymbol{\lambda},\mathbf{R})\rangle,\end{aligned}\quad (5\text{-}17)$$

where we assume that the Hamiltonian H for a three quark system is

$$H=\sum_{i=1}^{3}\frac{p_i^2}{2m_i}+\sum_{i<j}V(\mathbf{r}_i-\mathbf{r}_j). \quad (5\text{-}18)$$

This leads to

$$\frac{1}{2m_q}\mathbf{k}\cdot\langle\Psi_f(\boldsymbol{\rho},\boldsymbol{\lambda},\mathbf{R})|\mathbf{p}_3 e^{i\mathbf{k}\cdot\mathbf{r}_3}+e^{i\mathbf{k}\cdot\mathbf{r}_3}\mathbf{p}_3|\Psi_i(\boldsymbol{\rho},\boldsymbol{\lambda},\mathbf{R})\rangle =$$

$$[\frac{1}{6m_q}(\mathbf{P}_f^2-\mathbf{P}_i^2)+(E_f-E_i)]\langle\Psi_f(\boldsymbol{\rho},\boldsymbol{\lambda},\mathbf{R})|e^{i\mathbf{k}\cdot\mathbf{r}_3}|\Psi_i(\boldsymbol{\rho},\boldsymbol{\lambda},\mathbf{R})\rangle \quad (5\text{-}19)$$

where $\mathbf{P}_f(\mathbf{P}_i)$ is the final (initial) momentum of the center of mass, and $E_f(E_i)$is final (initial) internal energy level of the system. Thus Eq. 5-15 implies

$$k_0 = \frac{1}{6m_q}(\mathbf{P}_f^2 - \mathbf{P}_i^2) + E_f - E_i \tag{5-20}$$

which is energy conservation in the first-order nonrelativistic approximation.

For the harmonic oscillator basis the above constraints are satisfied explicitly since

$$E_f - E_i = \frac{(\Delta N)\alpha^2}{m_q} \tag{5-21}$$

where α is the oscillator strength and N is the quantum number of the energy level. Further, if we take $\mathbf{k}$ to be in the z direction we have the relation

$$B_s = -\frac{k}{m_q}\left(2 - \frac{1}{g}\right)[\Delta N + \frac{1}{6\alpha^2}(\mathbf{P}_f^2 - \mathbf{P}_i^2)]B_n. \tag{5-22}$$

The left hand side of Eq. 5-22 was used by Kubota and Ohta (Kubota and Ohta 1976) in calculating matrix elements of the spin-orbit term in the center of mass frame. This integral is frame dependent and $\mathbf{P}_f^2 - \mathbf{P}_i^2 = \mathbf{k}^2$ in the CM frame, so the first term on the right hand side of Eq. 5-22 is not zero; therefore it should be taken into account, but it was ignored in previous calculations. The recoil term can contribute to the transition matrix elements and sometimes it is important.

From Eq. 5-22 it is possible to make the recoil contribution vanish by working in the Breit frame where $|P_f| = |P_i|$ and the amplitudes then correspond to a total internal transition. The result of the calculation will be shown later.

One can also give similar constraints for the coefficient A_n of Eq. 5-8; because

$$
\begin{aligned}
&\frac{k}{m_q}\langle\Psi_f|e^{ikz(3)}r_+(3)(P_z(3)+\frac{k}{2})|\Psi_i\rangle \\
&= \langle\Psi_f|r_+(3)[H,\ e^{ikz(3)}]|\Psi_i\rangle \\
&= \langle\Psi_f|[H,\ r_+(3)e^{ikz(3)}]|\Psi_i\rangle - \frac{i}{m_q}\langle\Psi_f|P_+(3)e^{ikz(3)}|\Psi_i\rangle
\end{aligned}
\qquad (5\text{-}23)
$$

we have

$$
\begin{aligned}
A_n = 6\sqrt{\frac{\pi}{k_0}}\mu\frac{im_q}{g}\langle\Psi_f|e^{ikz(3)}r_+^{(3)}\left\{k_0 - \left[\frac{1}{6m_q}(\mathbf{P}_f^2 - \mathbf{P}_i^2) + E_f - E_i\right]\right\}|\Psi_i\rangle \\
+ 6\sqrt{\frac{\pi}{k_0}}\frac{\mu}{g}\langle\Psi_f|P_+(3)e^{ikz(3)}|\Psi_i\rangle.
\end{aligned}
\qquad (5\text{-}24)
$$

In the nonrelativistic limit the first term in the right hand side of Eq. 5-24 vanishes because of the current conservation, and A_n is the same as A of Eq. 3-9. Therefore, the first term on the right side of Eq. 5-24 may be regarded as the contribution from the binding potential, which is of order $O(v^2/c^2)$.

In Tables 5 and 6 we show analytical expressions for the transition matrix element of H_{em} between the ground state $|\mathbf{56},\ {}^2\mathbf{8},\ N=0, L=0\rangle$ and other $SU(6)\otimes O(3)$ states. Our calculations confirm the results of Koniuk and Isgur (Koniuk and Isgur 1980) for the nonrelativisitic operator H_{NR} if the A_n term is replaced by A of Eq. 3-9; the results of Kubota and Ohta (Kubota and Ohta 1976) incorporating H_{SO} are also confirmed, except for their failure to include the recoil effects properly. The terms $\frac{k_0}{m_q}$ in these expressions comes from the spin-orbit interaction H_{SO} and the nonadditive term H_{NA} (We have chosen $g=1$ in these calculations).

Table 5: Transition matrix elements between the $SU(6) \otimes O(3)$ state $|56,\ ^2 8,\ N = 0, L = 0\rangle$ and the positive parity $SU(6) \otimes O(3)$ states in the Breit frame. The full matrix elements are obtained by multiplying the entries in this table by a factor $\sqrt{\frac{\pi}{k_0}}\mu k \exp\left(-\frac{k^2}{6\alpha^2}\right)$

States	N	$A_{\frac{1}{2}}$	$A_{\frac{3}{2}}$
$N(^2D_S)\frac{3}{2}^+$	p	$\frac{2}{\sqrt{15}}\left[\frac{k_0 m_q}{\alpha^2} - 1 + \frac{1}{3}\left(\frac{k}{\alpha}\right)^2 - \frac{7}{18}\frac{k_0}{m_q}\right]$	$\frac{-2}{3\sqrt{5}}\left[\frac{k_0 m_q}{\alpha^2} - 1 + \frac{1}{12}\frac{k_0}{m_q}\right]$
	n	$\frac{-4\sqrt{3}}{27\sqrt{5}}\left[\left(\frac{k}{\alpha}\right)^2 - \frac{13}{8}\frac{k_0}{m_q}\right]$	$\frac{1}{18\sqrt{5}}\frac{k_0}{m_q}$
$N(^2D_S)\frac{5}{2}^+$	p	$\frac{2\sqrt{2}}{3\sqrt{5}}\left[\frac{k_0 m_q}{\alpha^2} - 1 - \frac{1}{2}\left(\frac{k}{\alpha}\right)^2 + \frac{1}{6}\frac{k_0}{m_q}\right]$	$\frac{4}{3\sqrt{5}}\left[\frac{k_0 m_q}{\alpha^2} - 1 + \frac{1}{6}\frac{k_0}{m_q}\right]$
	n	$\frac{2\sqrt{2}}{9\sqrt{5}}\left[\left(\frac{k}{\alpha}\right)^2 - \frac{1}{4}\frac{k_0}{m_q}\right]$	$\frac{-1}{9\sqrt{5}}\frac{k_0}{m_q}$
$\Delta(^4D_S)\frac{1}{2}^+$	p,n	$\frac{2\sqrt{3}}{27\sqrt{5}}\left[\left(\frac{k}{\alpha}\right)^2 - \frac{5}{4}\frac{k_0}{m_q}\right]$	
$\Delta(^4D_S)\frac{3}{2}^+$	p,n	$\frac{-2}{9\sqrt{15}}\left[\left(\frac{k}{\alpha}\right)^2 - \frac{1}{2}\frac{k_0}{m_q}\right]$	$\frac{2}{9\sqrt{5}}\left[\left(\frac{k}{\alpha}\right)^2 - \frac{k_0}{m_q}\right]$
$\Delta(^4D_S)\frac{5}{2}^+$	p,n	$\frac{-2}{9\sqrt{35}}\left[\left(\frac{k}{\alpha}\right)^2 - \frac{7}{4}\frac{k_0}{m_q}\right]$	$\frac{-2\sqrt{2}}{3\sqrt{35}}\left[\left(\frac{k}{\alpha}\right)^2 - \frac{7}{12}\frac{k_0}{m_q}\right]$
$\Delta(^4D_S)\frac{7}{2}^+$	p,n	$\frac{2\sqrt{2}}{3\sqrt{105}}\left(\frac{k}{\alpha}\right)^2$	$\frac{2\sqrt{2}}{9\sqrt{7}}\left(\frac{k}{\alpha}\right)^2$
$N(^2S'_S)\frac{1}{2}^+$	p	$\frac{-1}{3\sqrt{3}}\left[\left(\frac{k}{\alpha}\right)^2 - \frac{2}{3}\frac{k_0}{m_q}\right]$	
	n	$\frac{-2}{9\sqrt{3}}\left[\left(\frac{k}{\alpha}\right)^2 - \frac{1}{2}\frac{k_0}{m_q}\right]$	
$\Delta(^4S'_S)\frac{3}{2}^+$	p,n	$\frac{-\sqrt{2}}{9\sqrt{3}}\left[\left(\frac{k}{\alpha}\right)^2 - \frac{1}{2}\frac{k_0}{m_q}\right]$	$\frac{2}{9}\left[\left(\frac{k}{\alpha}\right)^2 - \frac{1}{2}\frac{k_0}{m_q}\right]$
$N(^2S_M)\frac{1}{2}^+$	p	$\frac{-1}{3\sqrt{6}}\left[\left(\frac{k}{\alpha}\right)^2 - \frac{k_0}{m_q}\right]$	
	n	$\frac{-1}{9\sqrt{6}}\left[\left(\frac{k}{\alpha}\right)^2 - \frac{k_0}{m_q}\right]$	
$N(^2S_M)\frac{3}{2}^+$	p	$\frac{1}{36\sqrt{6}}\frac{k_0}{m_q}$	$\frac{1}{36\sqrt{2}}\frac{k_0}{m_q}$
	n	$\frac{1}{9\sqrt{6}}\left[\left(\frac{k}{\alpha}\right)^2 - \frac{5}{4}\frac{k_0}{m_q}\right]$	$\frac{1}{9\sqrt{2}}\left[\left(\frac{k}{\alpha}\right)^2 - \frac{5}{4}\frac{k_0}{m_q}\right]$
$N(^2D_M)\frac{3}{2}^+$	p	$\frac{-\sqrt{2}}{\sqrt{15}}\left[\frac{k_0 m_q}{\alpha^2} - 1 + \frac{1}{3}\left(\frac{k}{\alpha}\right)^2 - \frac{1}{4}\frac{k_0}{m_q}\right]$	$\frac{2}{3\sqrt{10}}\left[\frac{k_0 m_q}{\alpha^2} - 1 + \frac{1}{4}\frac{k_0}{m_q}\right]$
	n	$\frac{\sqrt{2}}{\sqrt{15}}\left[\frac{k_0 m_q}{\alpha^2} - 1 - \frac{1}{9}\left(\frac{k}{\alpha}\right)^2 - \frac{1}{4}\frac{k_0}{m_q}\right]$	$\frac{2}{3\sqrt{15}}\left[\frac{k_0 m_q}{\alpha^2} - 1 + \frac{1}{12}\frac{k_0}{m_q}\right]$
$N(^2D_M)\frac{5}{2}^+$	p	$\frac{2}{3\sqrt{5}}\left[\frac{k_0 m_q}{\alpha^2} - 1 - \frac{1}{4}\left(\frac{k}{\alpha}\right)^2 - \frac{1}{2}\frac{k_0}{m_q}\right]$	$\frac{-2\sqrt{2}}{3\sqrt{5}}\left[\frac{k_0 m_q}{\alpha^2} - 1 + \frac{1}{4}\frac{k_0}{m_q}\right]$
	n	$\frac{2}{3\sqrt{5}}\left[\frac{k_0 m_q}{\alpha^2} - 1 - \frac{1}{6}\left(\frac{k}{\alpha}\right)^2 - \frac{1}{12}\frac{k_0}{m_q}\right]$	$\frac{2\sqrt{2}}{3\sqrt{5}}\left[\frac{k_0 m_q}{\alpha^2} - 1 + \frac{1}{12}\frac{k_0}{m_q}\right]$
$\Delta(^4D_M)\frac{3}{2}^+$	p,n	$\frac{-2}{\sqrt{30}}\left[\frac{k_0 m_q}{\alpha^2} - 1 - \frac{1}{9}\left(\frac{k}{\alpha}\right)^2 - \frac{5}{36}\frac{k_0}{m_q}\right]$	$\frac{-2}{3\sqrt{10}}\left[\frac{k_0 m_q}{\alpha^2} - 1 + \frac{1}{12}\frac{k_0}{m_q}\right]$
$\Delta(^4D_M)\frac{5}{2}^+$	p,n	$\frac{2}{3\sqrt{5}}\left[\frac{k_0 m_q}{\alpha^2} - 1 + \frac{1}{6}\left(\frac{k}{\alpha}\right)^2 + \frac{1}{12}\frac{k_0}{m_q}\right]$	$\frac{-2\sqrt{2}}{3\sqrt{5}}\left[\frac{k_0 m_q}{\alpha^2} - 1 + \frac{1}{12}\frac{k_0}{m_q}\right]$

Table 6: Transition matrix elements between the $SU(6) \otimes O(3)$ state $|56,\ ^2 8,\ N = 0, L = 0\rangle$ and the negative parity $SU(6) \otimes O(3)$ states in the Breit frame. The full matrix elements are obtained by multiplying the entries in this table by a factor $\sqrt{\frac{\pi}{k_0}}\mu\alpha \exp\left(-\frac{k^2}{6\alpha^2}\right)$

States	N	$A_{\frac{1}{2}}$	$A_{\frac{3}{2}}$
$N(^2P_M)\frac{1}{2}^-$	p	$\frac{2\sqrt{2}}{3}[\frac{k_0 m_q}{\alpha^2} + \frac{1}{2}\left(\frac{k}{\alpha}\right)^2 - \frac{1}{6}\frac{k_0}{m_q}]$	
	n	$\frac{-2\sqrt{2}}{3}[\frac{k_0 m_q}{\alpha^2} + \frac{1}{6}\left(\frac{k}{\alpha}\right)^2 - \frac{1}{6}\frac{k_0}{m_q}]$	
$N(^2P_M)\frac{3}{2}^-$	p	$\frac{2}{3}[\frac{k_0 m_q}{\alpha^2} - \left(\frac{k}{\alpha}\right)^2 + \frac{1}{12}\frac{k_0}{m_q}]$	$\frac{2}{\sqrt{3}}[\frac{k_0 m_q}{\alpha^2} + \frac{1}{12}\frac{k_0}{m_q}]$
	n	$\frac{-2}{3}[\frac{k_0 m_q}{\alpha^2} - \frac{1}{3}\left(\frac{k}{\alpha}\right)^2 + \frac{1}{12}\frac{k_0}{m_q}]$	$\frac{-2}{\sqrt{3}}[\frac{k_0 m_q}{\alpha^2} + \frac{1}{12}\frac{k_0}{m_q}]$
$N(^4P_M)\frac{1}{2}^-$	p	$\frac{\sqrt{2}}{9}\frac{k_0}{m_q}$	
	n	$\frac{\sqrt{2}}{9}[\left(\frac{k}{\alpha}\right)^2 - \frac{k_0}{m_q}]$	
$N(^4P_M)\frac{3}{2}^-$	p	$\frac{\sqrt{10}}{18}\frac{k_0}{m_q}$	$\frac{5}{3\sqrt{30}}\frac{k_0}{m_q}$
	n	$\frac{2}{9\sqrt{10}}[\left(\frac{k}{\alpha}\right)^2 - \frac{5}{2}\frac{k_0}{m_q}]$	$\frac{2}{\sqrt{30}}[\left(\frac{k}{\alpha}\right)^2 - \frac{6}{5}\frac{k_0}{m_q}]$
$N(^4P_M)\frac{5}{2}^-$	p	0	0
	n	$\frac{-2}{3\sqrt{10}}\left(\frac{k}{\alpha}\right)^2$	$\frac{-2}{3\sqrt{5}}\left(\frac{k}{\alpha}\right)^2$
$\Delta(^2P_M)\frac{1}{2}^-$	p,n	$\frac{-2\sqrt{2}}{3}[\frac{k_0 m_q}{\alpha^2} - \frac{1}{6}\left(\frac{k}{\alpha}\right)^2 + \frac{1}{6}\frac{k_0}{m_q}]$	
$\Delta(^2P_M)\frac{3}{2}^-$	p,n	$\frac{-2}{3}[\frac{k_0 m_q}{\alpha^2} + \frac{1}{3}\left(\frac{k}{\alpha}\right)^2 - \frac{1}{12}\frac{k_0}{m_q}]$	$\frac{-2}{\sqrt{3}}[\frac{k_0 m_q}{\alpha^2} - \frac{1}{12}\frac{k_0}{m_q}]$

Without further numerical calculation, Tables 5 and 6 show that there are interesting constraints implied among some of the amplitudes that are rather general and independent of the binding potential or choice of parameters. First we note that for nonrelativistic spin–orbit and non-additive terms with arbitrary strengths one has

$$D_{15}(1680): \; A^n_{\frac{3}{2}} = \sqrt{2} A^n_{\frac{1}{2}}, \tag{5-25}$$

while the helicity amplitudes for the proton are zero. Data are consistent with this at $q^2 = 0$; if $SU(6)$ symmetry applies for large q^2 then this relationship should hold for all q^2. Second, if the g-factor is chosen to be unity in the harmonic oscillator basis, the relation

$$D_{13}(1520)(^2 8): \; A^p_{\frac{3}{2}} = -A^n_{\frac{3}{2}} \tag{5-26}$$

(which is familiar in the nonrelativistic model, but violated by the *additive* spin–orbit terms) is recovered when the non-additive terms of Eq. 5-6 are included. Furthermore, the constraint for the resonances $P_{33}(1232)$ and $P_{33}(1600)$

$$A_{\frac{3}{2}} = \sqrt{3} A_{\frac{1}{2}} \tag{5-27}$$

survives the relativistic correction.

The most pleasing symmetry among these expressions occurs in the Breit frame where the recoil effects vanish, resulting in simple relations. In particular, in the Breit frame the contributions of the nonadditive terms to the neutron in $^4\mathbf{8}$ of the $[70, 1^-]_1$ resonant states and to the Δ resonances of $[70, 1^-]_1$ are all zero. Thus, in other frames the non-additive terms contribute to these particular excitations only through recoil effects. These constraints and selection rules are frame independent. The violation of these relations in the data could give us information on configuration mixing effects. For the resonance $P_{33}(1232)$ Eq. 5-22 results from a pure magnetic dipole transition, and the presence of the electric quadrupole transition in the data indicates mixing of the configuration with non-zero orbital angular momentum in the ground state or $P_{33}(1232)$ state wavefunction.

According to Eq. 2-83, there are significant contribution from $SU(6) \otimes O(3)$ states $|\mathbf{56},\ ^2\mathbf{8},\ N=2,\ L=0\rangle$ and $|\mathbf{70},\ ^2\mathbf{8},\ N=2,\ L=0\rangle$ in the ground state wavefunction of the Isgur and Karl model. We show the analytical expressions for the transition matrix elements between the $SU(6)\otimes O(3)$ state $|\mathbf{56},\ ^2\mathbf{8},\ N=2,\ L=0\rangle$ and the excited states in Tables 7 and 8, and between the $SU(6) \otimes O(3)$ state $|\mathbf{70},\ ^2\mathbf{8},\ N=2,\ L=0\rangle$ and the other excited states in Tables 9 and 10.

In Tables 11 and 12 we show the numerical result of our calculation of the photoproduction amplitudes for the P wave baryon resonance and the positive parity baryon resonances with and without QCD mixing effects. We show how these magnitudes are built up: the nonrelativistic results and the relativistic contribution (spin–orbit and non-additive terms combined) were calculated in the center of mass frame with harmonic oscillator strength $\alpha^2 = 0.175$ GeV^2 — the value used in earlier electromagnetic calculations (Koniuk and Isgur 1980; Copley, Karl and Obryk 1969). The calculation including the QCD mixing effects is performed in the Breit

Table 7: Transition matrix elements between $SU(6)\otimes O(3)$ state $|56,\ ^2 8,\ N=2, L=0\rangle$ and the positive parity $SU(6)\otimes O(3)$ states in the Breit frame. The full matrix elements are obtained by multiplying the entries in this table by a factor $\sqrt{\frac{\pi}{k_0}}\mu\ k\ \exp\left(-\frac{k^2}{6\alpha^2}\right)$

States	A^N_λ	A
$N(^2D_S)\frac{3}{2}^+$	$A^p_{\frac12}$	$\frac{4}{3\sqrt5}\left\{[\frac{k_0 m_q}{\alpha^2}+\frac13\left(\frac{k}{\alpha}\right)^2](1-\frac{1}{12}\left(\frac{k}{\alpha}\right)^2)-\frac{1}{12}\left(\frac{k}{\alpha}\right)^2(1-\frac13\frac{k_0}{m_q})\right\}$
	$A^n_{\frac12}$	$\frac{-8\sqrt3}{27\sqrt5}\left(\frac{k}{\alpha}\right)^2\left\{1-\frac{3}{32}\frac{k_0}{m_q}-\frac{1}{12}\left(\frac{k}{\alpha}\right)^2\right\}$
	$A^p_{\frac32}$	$\frac{-4}{3\sqrt5}\left\{\frac{k_0 m_q}{\alpha^2}(1-\frac{1}{12}\left(\frac{k}{\alpha}\right)^2)-\frac{1}{12}\left(\frac{k}{\alpha}\right)^2(1+\frac16\frac{k_0}{m_q})\right\}$
	$A^n_{\frac32}$	$\frac{1}{108\sqrt{15}}\frac{k_0}{m_q}\left(\frac{k}{\alpha}\right)^2$
$N(^2D_S)\frac{5}{2}^+$	$A^p_{\frac12}$	$\frac{4\sqrt2}{3\sqrt{15}}\left\{[\frac{k_0 m_q}{\alpha^2}-\frac12\left(\frac{k}{\alpha}\right)^2](1-\frac{1}{12}\left(\frac{k}{\alpha}\right)^2)-\frac{1}{12}\left(\frac{k}{\alpha}\right)^2(1-\frac13\frac{k_0}{m_q})\right\}$
	$A^n_{\frac12}$	$\frac{4\sqrt2}{9\sqrt{15}}\left(\frac{k}{\alpha}\right)^2\left\{(1-\frac{1}{12}\left(\frac{k}{\alpha}\right)^2)+\frac{1}{12}\frac{k_0}{m_q}\right\}$
	$A^p_{\frac32}$	$\frac{8}{3\sqrt{15}}\left\{\frac{k_0 m_q}{\alpha^2}(1-\frac{1}{12}\left(\frac{k}{\alpha}\right)^2)-\frac{1}{12}\left(\frac{k}{\alpha}\right)^2(1+\frac13\frac{k_0}{m_q})\right\}$
	$A^n_{\frac32}$	$\frac{-1}{54\sqrt{15}}\frac{k_0}{m_q}\left(\frac{k}{\alpha}\right)^2$
$\Delta(^4D_S)\frac{1}{2}^+$	$A^{p,n}_{\frac12}$	$\frac{4}{27\sqrt5}\left\{\left(\frac{k}{\alpha}\right)^2(1-\frac{1}{12}\left(\frac{k}{\alpha}\right)^2)+\frac{1}{16}\frac{k_0}{m_q}\left(\frac{k}{\alpha}\right)^2\right\}$
$\Delta(^4D_S)\frac{3}{2}^+$	$A^{p,n}_{\frac12}$	$\frac{-4}{27\sqrt5}\left(\frac{k}{\alpha}\right)^2\left\{1-\frac{1}{12}\left(\frac{k}{\alpha}\right)^2\right\}$
	$A^{p,n}_{\frac32}$	$\frac{4\sqrt3}{27\sqrt5}\left\{\left(\frac{k}{\alpha}\right)^2(1-\frac{1}{12}\left(\frac{k}{\alpha}\right)^2)-\frac{1}{24}\frac{k_0}{m_q}\left(\frac{k}{\alpha}\right)^2\right\}$
$\Delta(^4D_S)\frac{5}{2}^+$	$A^{p,n}_{\frac12}$	$\frac{-4}{9\sqrt{105}}\left\{\left(\frac{k}{\alpha}\right)^2(1-\frac{1}{12}\left(\frac{k}{\alpha}\right)^2)+\frac{5}{48}\frac{k_0}{m_q}\left(\frac{k}{\alpha}\right)^2\right\}$
	$A^{p,n}_{\frac32}$	$\frac{-4\sqrt6}{9\sqrt{35}}\left\{\left(\frac{k}{\alpha}\right)^2(1-\frac{1}{12}\left(\frac{k}{\alpha}\right)^2)+\frac{1}{144}\frac{k_0}{m_q}\left(\frac{k}{\alpha}\right)^2\right\}$
$\Delta(^4D_S)\frac{7}{2}^+$	$A^{p,n}_{\frac12}$	$\frac{4\sqrt2}{9\sqrt{35}}\left\{\left(\frac{k}{\alpha}\right)^2(1-\frac{1}{12}\left(\frac{k}{\alpha}\right)^2)-\frac{1}{24}\frac{k_0}{m_q}\left(\frac{k}{\alpha}\right)^2\right\}$
	$A^{p,n}_{\frac32}$	$\frac{4\sqrt2}{9\sqrt{21}}\left\{\left(\frac{k}{\alpha}\right)^2(1-\frac{1}{12}\left(\frac{k}{\alpha}\right)^2)-\frac{1}{24}\frac{k_0}{m_q}\left(\frac{k}{\alpha}\right)^2\right\}$
$N(^2S'_S)\frac{1}{2}^+$	$A^p_{\frac12}$	$2\left\{1-\frac19\left(\frac{k}{\alpha}\right)^2+\frac{1}{108}\left(\frac{k}{\alpha}\right)^4\right\}$
	$A^n_{\frac12}$	$\frac{-4}{3}\left\{1-\frac19\left(\frac{k}{\alpha}\right)^2+\frac{1}{108}\left(\frac{k}{\alpha}\right)^4\right\}$
$\Delta(^4S'_S)\frac{3}{2}^+$	$A^{p,n}_{\frac12}$	$\frac{-2\sqrt2}{3}\left\{1-\frac19\left(\frac{k}{\alpha}\right)^2+\frac{1}{108}\left(\frac{k}{\alpha}\right)^4\right\}$
	$A^{p,n}_{\frac32}$	$\frac{-2\sqrt2}{\sqrt3}\left\{1-\frac19\left(\frac{k}{\alpha}\right)^2+\frac{1}{108}\left(\frac{k}{\alpha}\right)^4\right\}$
$\Delta(^2D_M)\frac{3}{2}^+$	$A^{p,n}_{\frac12}$	$\frac{-2\sqrt2}{3\sqrt5}\left\{[\frac{k_0 m_q}{\alpha^2}-\frac19\left(\frac{k}{\alpha}\right)^2](1-\frac{1}{12}\left(\frac{k}{\alpha}\right)^2)-\frac{1}{12}\left(\frac{k}{\alpha}\right)^2(1-\frac{13}{36}\frac{k_0}{m_q})\right\}$
	$A^{p,n}_{\frac32}$	$\frac{-4}{3\sqrt{30}}\left\{\frac{k_0 m_q}{\alpha^2}(1-\frac{1}{12}\left(\frac{k}{\alpha}\right)^2)-\frac{1}{12}\left(\frac{k}{\alpha}\right)^2(1-\frac{1}{12}\frac{k_0}{m_q})\right\}$

Table 7 continued.

States	A^N_λ	A
$\Delta(^2D_M)\frac{5}{2}^+$	$A^{p,n}_{\frac{1}{2}}$	$\frac{4}{3\sqrt{15}}\left\{\left[\frac{k_0 m_q}{\alpha^2}+\frac{1}{6}\left(\frac{k}{\alpha}\right)^2\right]\left(1-\frac{1}{12}\left(\frac{k}{\alpha}\right)^2\right)-\frac{1}{12}\left(\frac{k}{\alpha}\right)^2\left(1-\frac{1}{12}\frac{k_0}{m_q}\right)\right\}$
	$A^{p,n}_{\frac{3}{2}}$	$\frac{-4\sqrt{2}}{3\sqrt{5}}\left\{\frac{k_0 m_q}{\alpha^2}\left(1-\frac{1}{12}\left(\frac{k}{\alpha}\right)^2\right)-\frac{1}{12}\left(\frac{k}{\alpha}\right)^2\left(1-\frac{1}{12}\frac{k_0}{m_q}\right)\right\}$
$N(^2S_M)\frac{1}{2}^+$	$A^p_{\frac{1}{2}}$	$\frac{\sqrt{2}}{9}\left\{\left(\frac{k}{\alpha}\right)^2\left(1-\frac{1}{12}\left(\frac{k}{\alpha}\right)^2\right)+\frac{1}{9}\frac{k_0}{m_q}\left(\frac{k}{\alpha}\right)^2\right\}$
	$A^n_{\frac{1}{2}}$	$\frac{-\sqrt{2}}{27}\left(\frac{k}{\alpha}\right)^2\left\{1-\frac{1}{12}\left(\frac{k}{\alpha}\right)^2\right\}$
$N(^2D_M)\frac{3}{2}^+$	$A^p_{\frac{1}{2}}$	$\frac{-2\sqrt{2}}{3\sqrt{5}}\left\{\left[\frac{k_0 m_q}{\alpha^2}+\frac{1}{3}\left(\frac{k}{\alpha}\right)^2\right]\left(1-\frac{1}{12}\left(\frac{k}{\alpha}\right)^2\right)-\frac{1}{12}\left(\frac{k}{\alpha}\right)^2\left(1-\frac{1}{12}\frac{k_0}{m_q}\right)\right\}$
	$A^n_{\frac{1}{2}}$	$\frac{2\sqrt{2}}{3\sqrt{5}}\left\{\left[\frac{k_0 m_q}{\alpha^2}-\frac{1}{9}\left(\frac{k}{\alpha}\right)^2\right]\left(1-\frac{1}{12}\left(\frac{k}{\alpha}\right)^2\right)-\frac{1}{12}\left(\frac{k}{\alpha}\right)^2\left(1-\frac{1}{9}\frac{k_0}{m_q}\right)\right\}$
	$A^p_{\frac{3}{2}}$	$\frac{4}{3\sqrt{30}}\left\{\frac{k_0 m_q}{\alpha^2}\left(1-\frac{1}{12}\left(\frac{k}{\alpha}\right)^2\right)-\frac{1}{12}\left(\frac{k}{\alpha}\right)^2\left(1+\frac{1}{4}\frac{k_0}{m_q}\right)\right\}$
	$A^n_{\frac{3}{2}}$	$\frac{4}{3\sqrt{30}}\left\{\frac{k_0 m_q}{\alpha^2}\left(1-\frac{1}{12}\left(\frac{k}{\alpha}\right)^2\right)-\frac{1}{12}\left(\frac{k}{\alpha}\right)^2\left(1+\frac{1}{9}\frac{k_0}{m_q}\right)\right\}$
$N(^2D_M)\frac{5}{2}^+$	$A^p_{\frac{1}{2}}$	$\frac{4}{3\sqrt{15}}\left\{\left[\frac{k_0 m_q}{\alpha^2}-\frac{1}{2}\left(\frac{k}{\alpha}\right)^2\right]\left(1-\frac{1}{12}\left(\frac{k}{\alpha}\right)^2\right)-\frac{1}{12}\left(\frac{k}{\alpha}\right)^2\left(1+\frac{1}{12}\frac{k_0}{m_q}\right)\right\}$
	$A^n_{\frac{1}{2}}$	$\frac{4}{3\sqrt{15}}\left\{\left[\frac{k_0 m_q}{\alpha^2}-\frac{1}{6}\left(\frac{k}{\alpha}\right)^2\right]\left(1-\frac{1}{12}\left(\frac{k}{\alpha}\right)^2\right)-\frac{1}{12}\left(\frac{k}{\alpha}\right)^2\left(1-\frac{1}{12}\frac{k_0}{m_q}\right)\right\}$
	$A^p_{\frac{3}{2}}$	$\frac{-4\sqrt{2}}{3\sqrt{15}}\left\{\frac{k_0 m_q}{\alpha^2}\left(1-\frac{1}{12}\left(\frac{k}{\alpha}\right)^2\right)-\frac{1}{12}\left(\frac{k}{\alpha}\right)^2\left(1+\frac{1}{4}\frac{k_0}{m_q}\right)\right\}$
	$A^n_{\frac{3}{2}}$	$\frac{4\sqrt{2}}{3\sqrt{15}}\left\{\frac{k_0 m_q}{\alpha^2}\left(1-\frac{1}{12}\left(\frac{k}{\alpha}\right)^2\right)-\frac{1}{12}\left(\frac{k}{\alpha}\right)^2\left(1+\frac{1}{12}\frac{k_0}{m_q}\right)\right\}$

Table 8: Transition matrix elements between the $SU(6) \otimes O(3)$ state $|56,\ {}^28,\ N = 2, L = 0\rangle$ and the negative parity $SU(6) \otimes O(3)$ states in the Breit frame. The full matrix elements are obtained by multiplying the entries in this table by a factor $\sqrt{\frac{\pi}{k_0}}\mu\alpha\ \exp\left(-\frac{k^2}{6\alpha^2}\right)$.

States	A^N_λ	A
$N(^2P_M)\frac{1}{2}^-$	$A^p_{\frac{1}{2}}$	$\frac{2\sqrt{2}}{3\sqrt{3}}\{[\frac{k_0 m_q}{\alpha^2} + \frac{1}{2}\left(\frac{k}{\alpha}\right)^2 + \frac{1}{6}\frac{k_0}{m_q}](1 - \frac{1}{6}\left(\frac{k}{\alpha}\right)^2) - \frac{1}{3}\left(\frac{k}{\alpha}\right)^2\}$
	$A^n_{\frac{1}{2}}$	$\frac{-2\sqrt{2}}{3\sqrt{3}}\{[\frac{k_0 m_q}{\alpha^2} + \frac{1}{6}\left(\frac{k}{\alpha}\right)^2](1 - \frac{1}{6}\left(\frac{k}{\alpha}\right)^2) + \frac{1}{6}\frac{k_0}{m_q} - \frac{1}{3}\left(\frac{k}{\alpha}\right)^2\}$
$N(^2P_M)\frac{3}{2}^-$	$A^p_{\frac{1}{2}}$	$\frac{2}{3\sqrt{3}}\{[\frac{k_0 m_q}{\alpha^2} - \left(\frac{k}{\alpha}\right)^2 - \frac{1}{12}\frac{k_0}{m_q}](1 - \frac{1}{6}\left(\frac{k}{\alpha}\right)^2) - \frac{1}{3}\left(\frac{k}{\alpha}\right)^2(1 - \frac{1}{4}\frac{k_0}{m_q})\}$
	$A^n_{\frac{1}{2}}$	$\frac{-2}{3\sqrt{3}}\{[\frac{k_0 m_q}{\alpha^2} - \frac{1}{3}\left(\frac{k}{\alpha}\right)^2 - \frac{1}{12}\frac{k_0}{m_q}](1 - \frac{1}{6}\left(\frac{k}{\alpha}\right)^2) - \frac{1}{3}\left(\frac{k}{\alpha}\right)^2(1 - \frac{1}{12}\frac{k_0}{m_q})\}$
	$A^p_{\frac{3}{2}}$	$\frac{2}{3}\{\frac{k_0 m_q}{\alpha^2}(1 - \frac{1}{6}\left(\frac{k}{\alpha}\right)^2) - \frac{1}{3}\left(\frac{k}{\alpha}\right)^2 - \frac{1}{12}\frac{k_0}{m_q}(1 + \frac{1}{6}\left(\frac{k}{\alpha}\right)^2)\}$
	$A^n_{\frac{3}{2}}$	$\frac{-2}{3}\{\frac{k_0 m_q}{\alpha^2}(1 - \frac{1}{6}\left(\frac{k}{\alpha}\right)^2) - \frac{1}{3}\left(\frac{k}{\alpha}\right)^2 - \frac{1}{12}\frac{k_0}{m_q}(1 + \frac{1}{6}\left(\frac{k}{\alpha}\right)^2)\}$
$N(^4P_M)\frac{1}{2}^-$	$A^p_{\frac{1}{2}}$	$\frac{-\sqrt{2}}{9\sqrt{3}}\frac{k_0}{m_q}\{1 + \frac{1}{6}\left(\frac{k}{\alpha}\right)^2\}$
	$A^n_{\frac{1}{2}}$	$\frac{\sqrt{2}}{9\sqrt{3}}\{\left(\frac{k}{\alpha}\right)^2 + \frac{k_0}{m_q}\}(1 - \frac{1}{6}\left(\frac{k}{\alpha}\right)^2)$
$N(^4P_M)\frac{3}{2}^-$	$A^p_{\frac{1}{2}}$	$\frac{-\sqrt{10}}{18\sqrt{3}}\frac{k_0}{m_q}\{1 + \frac{1}{6}\left(\frac{k}{\alpha}\right)^2\}$
	$A^n_{\frac{1}{2}}$	$\frac{2}{9\sqrt{30}}\{\left(\frac{k}{\alpha}\right)^2(1 - \frac{1}{6}\left(\frac{k}{\alpha}\right)^2) + \frac{5}{2}\frac{k_0}{m_q}(1 + \frac{1}{6}\left(\frac{k}{\alpha}\right)^2)\}$
	$A^p_{\frac{3}{2}}$	$\frac{-5}{9\sqrt{10}}\frac{k_0}{m_q}\{1 + \frac{1}{6}\left(\frac{k}{\alpha}\right)^2\}$
	$A^n_{\frac{3}{2}}$	$\frac{2}{3\sqrt{10}}\{\left(\frac{k}{\alpha}\right)^2(1 - \frac{1}{6}\left(\frac{k}{\alpha}\right)^2) + \frac{5}{6}\frac{k_0}{m_q}(1 + \frac{1}{15}\left(\frac{k}{\alpha}\right)^2)\}$
$N(^4P_M)\frac{5}{2}^-$	$A^p_{\frac{1}{2}}$	0
	$A^n_{\frac{1}{2}}$	$\frac{-2}{3\sqrt{30}}\{\left(\frac{k}{\alpha}\right)^2(1 - \frac{1}{6}\left(\frac{k}{\alpha}\right)^2) + \frac{1}{12}\left(\frac{k}{\alpha}\right)^2\frac{k_0}{m_q}\}$
	$A^p_{\frac{3}{2}}$	0
	$A^n_{\frac{3}{2}}$	$\frac{-2}{3\sqrt{15}}\{\left(\frac{k}{\alpha}\right)^2(1 - \frac{1}{6}\left(\frac{k}{\alpha}\right)^2) + \frac{1}{12}\left(\frac{k}{\alpha}\right)^2\frac{k_0}{m_q}\}$
$\Delta(^2P_M)\frac{1}{2}^-$	$A^{p,n}_{\frac{1}{2}}$	$\frac{-2\sqrt{2}}{3\sqrt{3}}\{[\frac{k_0 m_q}{\alpha^2} - \frac{1}{6}\left(\frac{k}{\alpha}\right)^2](1 - \frac{1}{6}\left(\frac{k}{\alpha}\right)^2) - \frac{1}{3}\left(\frac{k}{\alpha}\right)^2 - \frac{1}{6}\frac{k_0}{m_q}(1 + \frac{1}{6}\left(\frac{k}{\alpha}\right)^2\}$
$\Delta(^2P_M)\frac{3}{2}^-$	$A^{p,n}_{\frac{1}{2}}$	$\frac{-2}{3\sqrt{3}}\{[\frac{k_0 m_q}{\alpha^2} + \frac{1}{3}\left(\frac{k}{\alpha}\right)^2](1 - \frac{1}{6}\left(\frac{k}{\alpha}\right)^2) - \frac{1}{3}\left(\frac{k}{\alpha}\right)^2 + \frac{1}{12}\frac{k_0}{m_q}(1 + \frac{1}{6}\left(\frac{k}{\alpha}\right)^2)\}$
	$A^{p,n}_{\frac{3}{2}}$	$\frac{-2}{3}\{\frac{k_0 m_q}{\alpha^2}(1 - \frac{1}{6}\left(\frac{k}{\alpha}\right)^2) - \frac{1}{3}\left(\frac{k}{\alpha}\right)^2 + \frac{1}{12}\frac{k_0}{m_q}(1 + \frac{1}{6}\left(\frac{k}{\alpha}\right)^2\}$

Table 9: Transition matrix elements between the $SU(6) \otimes O(3)$ state $|70,\ ^2 8,\ N = 2, L = 0\rangle$ and the positive parity $SU(6) \otimes O(3)$ states in the Breit frame. The full matrix elements are obtained by multiplying the entries in this table by a factor $\sqrt{\frac{\pi}{k_0}}\mu k \exp\left(-\frac{k^2}{6\alpha^2}\right)$

States	A^N_λ	A
$N(^2D_S)\frac{3}{2}^+$	$A^p_{\frac{1}{2}}$	$\frac{-2\sqrt{2}}{3\sqrt{5}}\left\{[\frac{k_0 m_q}{\alpha^2} + \frac{1}{3}\left(\frac{k}{\alpha}\right)^2](1 - \frac{1}{12}\left(\frac{k}{\alpha}\right)^2) - \frac{1}{12}\left(\frac{k}{\alpha}\right)^2(1 - \frac{1}{6}\frac{k_0}{m_q})\right\}$
	$A^n_{\frac{1}{2}}$	$\frac{2\sqrt{2}}{3\sqrt{15}}\left\{[\frac{k_0 m_q}{\alpha^2} - \frac{1}{9}\left(\frac{k}{\alpha}\right)^2](1 - \frac{1}{12}\left(\frac{k}{\alpha}\right)^2) - \frac{1}{12}\left(\frac{k}{\alpha}\right)^2(1 - \frac{1}{9}\left(\frac{k}{\alpha}\right)^2)\right\}$
	$A^p_{\frac{3}{2}}$	$\frac{2\sqrt{2}}{3\sqrt{15}}\left\{\frac{k_0 m_q}{\alpha^2}(1 - \frac{1}{12}\left(\frac{k}{\alpha}\right)^2) - \frac{1}{12}\left(\frac{k}{\alpha}\right)^2(1 + \frac{1}{6}\frac{k_0}{m_q})\right\}$
	$A^n_{\frac{3}{2}}$	$\frac{-2\sqrt{2}}{3\sqrt{15}}\left\{\frac{k_0 m_q}{\alpha^2}(1 - \frac{1}{12}\left(\frac{k}{\alpha}\right)^2) - \frac{1}{12}\left(\frac{k}{\alpha}\right)^2(1 + \frac{1}{12}\frac{k_0}{m_q})\right\}$
$N(^2D_S)\frac{5}{2}^+$	$A^p_{\frac{1}{2}}$	$\frac{-4}{3\sqrt{15}}\left\{[\frac{k_0 m_q}{\alpha^2} - \frac{1}{2}\left(\frac{k}{\alpha}\right)^2](1 - \frac{1}{12}\left(\frac{k}{\alpha}\right)^2) - \frac{1}{12}\left(\frac{k}{\alpha}\right)^2(1 - \frac{1}{3}\frac{k_0}{m_q})\right\}$
	$A^n_{\frac{1}{2}}$	$\frac{4}{3\sqrt{15}}\left\{[\frac{k_0 m_q}{\alpha^2} - \frac{1}{6}\left(\frac{k}{\alpha}\right)^2](1 - \frac{1}{12}\left(\frac{k}{\alpha}\right)^2) - \frac{1}{12}\left(\frac{k}{\alpha}\right)^2(1 - \frac{1}{12}\frac{k_0}{m_q})\right\}$
	$A^p_{\frac{3}{2}}$	$\frac{-4\sqrt{2}}{3\sqrt{15}}\left\{\frac{k_0 m_q}{\alpha^2}(1 - \frac{1}{12}\left(\frac{k}{\alpha}\right)^2) - \frac{1}{12}\left(\frac{k}{\alpha}\right)^2(1 + \frac{1}{6}\frac{k_0}{m_q})\right\}$
	$A^n_{\frac{3}{2}}$	$\frac{4\sqrt{2}}{3\sqrt{15}}\left\{\frac{k_0 m_q}{\alpha^2}(1 - \frac{1}{12}\left(\frac{k}{\alpha}\right)^2) - \frac{1}{12}\left(\frac{k}{\alpha}\right)^2(1 + \frac{1}{6}\frac{k_0}{m_q})\right\}$
$\Delta(^4D_S)\frac{1}{2}^+$	$A^{p,n}_{\frac{1}{2}}$	$\frac{2\sqrt{2}}{27\sqrt{5}}\left\{\left(\frac{k}{\alpha}\right)^2(1 - \frac{1}{12}\left(\frac{k}{\alpha}\right)^2) + \frac{1}{16}\frac{k_0}{m_q}\left(\frac{k}{\alpha}\right)^2\right\}$
$\Delta(^4D_S)\frac{3}{2}^+$	$A^{p,n}_{\frac{1}{2}}$	$\frac{-2\sqrt{2}}{27\sqrt{5}}\left\{\left(\frac{k}{\alpha}\right)^2(1 - \frac{1}{12}\left(\frac{k}{\alpha}\right)^2) + \frac{1}{24}\frac{k_0}{m_q}\left(\frac{k}{\alpha}\right)^2\right\}$
	$A^{p,n}_{\frac{3}{2}}$	$\frac{2\sqrt{2}}{9\sqrt{15}}\left\{\left(\frac{k}{\alpha}\right)^2(1 - \frac{1}{12}\left(\frac{k}{\alpha}\right)^2) + \frac{1}{12}\frac{k_0}{m_q}\left(\frac{k}{\alpha}\right)^2\right\}$
$\Delta(^4D_S)\frac{5}{2}^+$	$A^{p,n}_{\frac{1}{2}}$	$\frac{-2\sqrt{2}}{9\sqrt{105}}\left\{\left(\frac{k}{\alpha}\right)^2(1 - \frac{1}{12}\left(\frac{k}{\alpha}\right)^2) + \frac{5}{48}\frac{k_0}{m_q}\left(\frac{k}{\alpha}\right)^2\right\}$
	$A^{p,n}_{\frac{3}{2}}$	$\frac{-4}{3\sqrt{105}}\left\{\left(\frac{k}{\alpha}\right)^2(1 - \frac{1}{12}\left(\frac{k}{\alpha}\right)^2) + \frac{1}{144}\frac{k_0}{m_q}\left(\frac{k}{\alpha}\right)^2\right\}$
$\Delta(^4D_S)\frac{7}{2}^+$	$A^{p,n}_{\frac{1}{2}}$	$\frac{4}{9\sqrt{35}}\left\{\left(\frac{k}{\alpha}\right)^2(1 - \frac{1}{12}\left(\frac{k}{\alpha}\right)^2) - \frac{1}{24}\frac{k_0}{m_q}\left(\frac{k}{\alpha}\right)^2\right\}$
	$A^{p,n}_{\frac{3}{2}}$	$\frac{4}{9\sqrt{21}}\left\{\left(\frac{k}{\alpha}\right)^2(1 - \frac{1}{12}\left(\frac{k}{\alpha}\right)^2) - \frac{1}{24}\frac{k_0}{m_q}\left(\frac{k}{\alpha}\right)^2\right\}$
$N(^2S'_S)\frac{1}{2}^+$	$A^p_{\frac{1}{2}}$	$\frac{\sqrt{2}}{9}\left\{\left(\frac{k}{\alpha}\right)^2 - \frac{1}{36}\left(\frac{k}{\alpha}\right)^2\frac{k_0}{m_q}\right\}$
	$A^n_{\frac{1}{2}}$	$\frac{-2\sqrt{2}}{27}\left\{\left(\frac{k}{\alpha}\right)^2 - \frac{k_0}{m_q}\right\}$
$\Delta(^4S'_S)\frac{3}{2}^+$	$A^{p,n}_{\frac{1}{2}}$	$\frac{2}{27}\left\{\left(\frac{k}{\alpha}\right)^2(1 - \frac{1}{12}\left(\frac{k}{\alpha}\right)^2) + \frac{1}{24}\left(\frac{k}{\alpha}\right)^2\frac{k_0}{m_q}\right\}$
	$A^{p,n}_{\frac{3}{2}}$	$\frac{-2}{9\sqrt{3}}\left\{\left(\frac{k}{\alpha}\right)^2(1 - \frac{1}{12}\left(\frac{k}{\alpha}\right)^2) + \frac{1}{24}\left(\frac{k}{\alpha}\right)^2\frac{k_0}{m_q}\right\}$

Table 9 continued.

States	A^N_λ	A
$\Delta(^2D_M)\frac{3}{2}^+$	$A^{p,n}_{\frac{1}{2}}$	$\frac{-1}{18\sqrt{5}}\left\{\left(\frac{k}{\alpha}\right)^2\left(\frac{k_0 m_q}{\alpha^2}+\frac{11}{3}+\frac{1}{9}\left(\frac{k}{\alpha}\right)^2\right)-\frac{1}{6}\frac{k_0}{m_q}\left(1+\frac{5}{12}\frac{k_0}{m_q}\right)\right\}$
	$A^{p,n}_{\frac{3}{2}}$	$\frac{-1}{18\sqrt{15}}\left\{\left(\frac{k}{\alpha}\right)^2\left(\frac{k_0 m_q}{\alpha^2}+1\right)+2\frac{k_0}{m_q}\left(1-\frac{1}{8}\left(\frac{k}{\alpha}\right)^2\right)\right\}$
$\Delta(^2D_M)\frac{5}{2}^+$	$A^{p,n}_{\frac{1}{2}}$	$\frac{\sqrt{2}}{18\sqrt{15}}\left\{\left(\frac{k}{\alpha}\right)^2\left(\frac{k_0 m_q}{\alpha^2}-7-\frac{1}{6}\left(\frac{k}{\alpha}\right)^2\right)+4\frac{k_0}{m_q}\left(1-\frac{1}{24}\left(\frac{k}{\alpha}\right)^2\right)\right\}$
	$A^{p,n}_{\frac{3}{2}}$	$\frac{-1}{9\sqrt{15}}\left\{\left(\frac{k}{\alpha}\right)^2\left(\frac{k_0 m_q}{\alpha^2}+1\right)-\frac{k_0}{m_q}\right\}$
$N(^2S_M)\frac{1}{2}^+$	$A^{p}_{\frac{1}{2}}$	$\frac{2}{3}\left\{1-\frac{1}{9}\left(\frac{k}{\alpha}\right)^2+\frac{1}{72}\left(\frac{k}{\alpha}\right)^4+\frac{2}{3}\frac{k_0}{m_q}\left(1-\frac{1}{12}\left(\frac{k}{\alpha}\right)^2\right)\right\}$
	$A^{n}_{\frac{1}{2}}$	$\frac{1}{3}\left\{1-\frac{1}{9}\left(\frac{k}{\alpha}\right)^2-\frac{1}{324}\left(\frac{k}{\alpha}\right)^4\right\}$
$N(^2D_M)\frac{3}{2}^+$	$A^{p}_{\frac{1}{2}}$	$\frac{4}{3\sqrt{5}}\left\{\frac{k_0 m_q}{\alpha^2}+\frac{5}{72}\left(\frac{k}{\alpha}\right)^2+\frac{1}{18}\frac{k_0}{m_q}-\frac{1}{24}\left(\frac{k}{\alpha}\right)^2\left(\frac{k_0 m_q}{\alpha^2}+\frac{1}{3}\left(\frac{k}{\alpha}\right)^2+\frac{1}{36}\frac{k_0}{m_q}\right)\right\}$
	$A^{n}_{\frac{1}{2}}$	$\frac{2}{3\sqrt{5}}\left\{\frac{k_0 m_q}{\alpha^2}\left(1-\frac{1}{12}\left(\frac{k}{\alpha}\right)^2\right)+\frac{1}{9}\left(\frac{k}{\alpha}\right)^2\left(1+\frac{1}{12}\left(\frac{k}{\alpha}\right)^2\right)+\frac{1}{144}\frac{k_0}{m_q}\left(\frac{k}{\alpha}\right)^2\right\}$
	$A^{p}_{\frac{3}{2}}$	$\frac{4}{3\sqrt{15}}\left\{\frac{k_0 m_q}{\alpha^2}\left(1-\frac{1}{24}\left(\frac{k}{\alpha}\right)^2\right)-\frac{1}{24}\left(\frac{k}{\alpha}\right)^2+\frac{1}{12}\frac{k_0}{m_q}\left(1-\frac{1}{6}\left(\frac{k}{\alpha}\right)^2\right)\right\}$
	$A^{n}_{\frac{3}{2}}$	$\frac{2}{3\sqrt{15}}\left\{\frac{k_0 m_q}{\alpha^2}\left(1-\frac{1}{12}\left(\frac{k}{\alpha}\right)^2\right)-\frac{1}{108}\left(\frac{k}{\alpha}\right)^2\frac{k_0}{m_q}\right\}$
$N(^2D_M)\frac{5}{2}^+$	$A^{p}_{\frac{1}{2}}$	$\frac{4\sqrt{2}}{3\sqrt{15}}\left\{\frac{k_0 m_q}{\alpha^2}-\frac{5}{24}\left(\frac{k}{\alpha}\right)^2-\frac{1}{2}\frac{k_0}{m_q}-\frac{1}{24}\left(\frac{k}{\alpha}\right)^2\left(\frac{k_0 m_q}{\alpha^2}-\frac{1}{2}\left(\frac{k}{\alpha}\right)^2-\frac{13}{12}\frac{k_0}{m_q}\right)\right\}$
	$A^{n}_{\frac{1}{2}}$	$\frac{2\sqrt{2}}{3\sqrt{15}}\left\{\frac{k_0 m_q}{\alpha^2}\left(1-\frac{1}{12}\left(\frac{k}{\alpha}\right)^2\right)-\frac{1}{6}\left(\frac{k}{\alpha}\right)^2\left(1+\frac{1}{12}\left(\frac{k}{\alpha}\right)^2\right)-\frac{1}{72}\frac{k_0}{m_q}\left(\frac{k}{\alpha}\right)^2\right\}$
	$A^{p}_{\frac{3}{2}}$	$\frac{-8}{3\sqrt{15}}\left\{\frac{k_0 m_q}{\alpha^2}\left(1-\frac{1}{24}\left(\frac{k}{\alpha}\right)^2\right)-\frac{1}{24}\left(\frac{k}{\alpha}\right)^2-\frac{1}{6}\frac{k_0}{m_q}\left(1-\frac{1}{16}\left(\frac{k}{\alpha}\right)^2\right)\right\}$
	$A^{n}_{\frac{3}{2}}$	$\frac{-4}{3\sqrt{15}}\left\{\frac{k_0 m_q}{\alpha^2}\left(1-\frac{1}{12}\left(\frac{k}{\alpha}\right)^2\right)-\frac{1}{72}\frac{k_0}{m_q}\left(\frac{k}{\alpha}\right)^2\right\}$

Table 10: Transition matrix elements between the $SU(6) \otimes O(3)$ state $|70,\ ^2 8,\ N = 2, L = 0\rangle$ and the negative parity $SU(6) \otimes O(3)$ states in the Breit frame. The full matrix elements are obtained by multiplying the entries in this table by a factor $\sqrt{\frac{\pi}{k_0}}\mu\alpha \exp\left(-\frac{k^2}{6\alpha^2}\right)$.

States	A_λ^N	A
$N(^2P_M)\frac{1}{2}^-$	$A_{\frac{1}{2}}^p$	$\frac{-1}{9\sqrt{3}}\left\{\left[\frac{k_0 m_q}{\alpha^2} + \frac{1}{2}\left(\frac{k}{\alpha}\right)^2 + 4\right]\left(\frac{k}{\alpha}\right)^2 + 4\frac{k_0}{m_q}(1 + \frac{1}{12}\left(\frac{k}{\alpha}\right)^2)\right\}$
	$A_{\frac{1}{2}}^n$	$\frac{2}{3\sqrt{3}}\left\{\frac{k_0 m_q}{\alpha^2}(1 + \frac{1}{6}\left(\frac{k}{\alpha}\right)^2) - \frac{1}{2}\left(\frac{k}{\alpha}\right)^2(1 + \frac{1}{9}\left(\frac{k}{\alpha}\right)^2) + \frac{1}{2}\frac{k_0}{m_q}(1 - \frac{1}{6}\left(\frac{k}{\alpha}\right)^2)\right\}$
$N(^2P_M)\frac{3}{2}^-$	$A_{\frac{1}{2}}^p$	$\frac{1}{9\sqrt{6}}\left\{\left[-\frac{k_0 m_q}{\alpha^2} + \left(\frac{k}{\alpha}\right)^2 + 8\right]\left(\frac{k}{\alpha}\right)^2 + 2\frac{k_0}{m_q}(1 - \frac{1}{24}\left(\frac{k}{\alpha}\right)^2)\right\}$
	$A_{\frac{1}{2}}^n$	$\frac{\sqrt{2}}{3\sqrt{3}}\left\{[\frac{k_0 m_q}{\alpha^2}(1 + \frac{1}{6}\left(\frac{k}{\alpha}\right)^2) + \left(\frac{k}{\alpha}\right)^2(1 + \frac{1}{9}\left(\frac{k}{\alpha}\right)^2) + \frac{k_0}{m_q}(1 + \frac{1}{8}\left(\frac{k}{\alpha}\right)^2)\right\}$
	$A_{\frac{3}{2}}^p$	$\frac{\sqrt{2}}{18}\left\{-\frac{k_0 m_q}{\alpha^2}\left(\frac{k}{\alpha}\right)^2 + \frac{k_0}{m_q}(1 + \frac{1}{8}\left(\frac{k}{\alpha}\right)^2)\right\}$
	$A_{\frac{3}{2}}^n$	$\frac{\sqrt{2}}{3}\left\{\frac{k_0 m_q}{\alpha^2}(1 + \frac{1}{6}\left(\frac{k}{\alpha}\right)^2) - \frac{1}{2}\frac{k_0}{m_q}\right\}$
$N(^4P_M)\frac{1}{2}^-$	$A_{\frac{1}{2}}^p$	$\frac{2}{9\sqrt{3}}\left\{\left(\frac{k}{\alpha}\right)^2 + \frac{3}{4}\frac{k_0}{m_q}(1 + \frac{1}{9}\left(\frac{k}{\alpha}\right)^2)\right\}$
	$A_{\frac{1}{2}}^n$	$\frac{1}{54\sqrt{3}}\left(\frac{k}{\alpha}\right)^2\left\{\left(\frac{k}{\alpha}\right)^2 + \frac{k_0}{m_q}\right\}$
$N(^4P_M)\frac{3}{2}^-$	$A_{\frac{1}{2}}^p$	$\frac{2}{9\sqrt{15}}\left\{\left(\frac{k}{\alpha}\right)^2 + \frac{k_0}{m_q}(1 + \frac{1}{8}\left(\frac{k}{\alpha}\right)^2)\right\}$
	$A_{\frac{1}{2}}^n$	$\frac{1}{54\sqrt{15}}\left(\frac{k}{\alpha}\right)^2\left\{\left(\frac{k}{\alpha}\right)^2 + \frac{1}{2}\frac{k_0}{m_q}\right\}$
	$A_{\frac{3}{2}}^p$	$\frac{2}{3\sqrt{5}}\left\{\left(\frac{k}{\alpha}\right)^2 + \frac{1}{6}\frac{k_0}{m_q}(1 + \frac{5}{6}\left(\frac{k}{\alpha}\right)^2)\right\}$
	$A_{\frac{3}{2}}^n$	$\frac{1}{18\sqrt{5}}\left(\frac{k}{\alpha}\right)^2\left\{\left(\frac{k}{\alpha}\right)^2 + \frac{1}{2}\frac{k_0}{m_q}\right\}$
$N(^4P_M)\frac{5}{2}^-$	$A_{\frac{1}{2}}^p$	$\frac{-2\sqrt{3}}{9\sqrt{5}}\left\{\left(\frac{k}{\alpha}\right)^2 - \frac{1}{4}\frac{k_0}{m_q}\right\}$
	$A_{\frac{1}{2}}^n$	$\frac{-\sqrt{3}}{54\sqrt{5}}\left(\frac{k}{\alpha}\right)^2\left\{\left(\frac{k}{\alpha}\right)^2 + \frac{1}{2}\frac{k_0}{m_q}\right\}$
	$A_{\frac{3}{2}}^p$	$\frac{-2\sqrt{6}}{9\sqrt{5}}\left\{\left(\frac{k}{\alpha}\right)^2 - \frac{1}{4}\frac{k_0}{m_q}\right\}$
	$A_{\frac{3}{2}}^n$	$\frac{-\sqrt{6}}{54\sqrt{5}}\left(\frac{k}{\alpha}\right)^2\left\{\left(\frac{k}{\alpha}\right)^2 + \frac{1}{2}\frac{k_0}{m_q}\right\}$
$\Delta(^2P_M)\frac{1}{2}^-$	$A_{\frac{1}{2}}^{p,n}$	$\frac{-4}{3\sqrt{3}}\left\{\frac{k_0 m_q}{\alpha^2}(1 + \frac{1}{12}\left(\frac{k}{\alpha}\right)^2) + \frac{1}{6}\left[\left(\frac{k}{\alpha}\right)^2 - \frac{k_0}{m_q}\right](1 + \frac{1}{12}\left(\frac{k}{\alpha}\right)^2)\right\}$
$\Delta(^2P_M)\frac{3}{2}^-$	$A_{\frac{1}{2}}^{p,n}$	$\frac{-2\sqrt{2}}{3\sqrt{3}}\left\{\frac{k_0 m_q}{\alpha^2}(1 + \frac{1}{12}\left(\frac{k}{\alpha}\right)^2) - \frac{1}{3}\left[\left(\frac{k}{\alpha}\right)^2 + \frac{k_0}{m_q}\right](1 - \frac{1}{12}\left(\frac{k}{\alpha}\right)^2)\right\}$
	$A_{\frac{3}{2}}^{p,n}$	$\frac{-2\sqrt{2}}{3}\left\{\frac{k_0 m_q}{\alpha^2}(1 + \frac{1}{12}\left(\frac{k}{\alpha}\right)^2) - \frac{1}{12}\frac{k_0}{m_q}(1 - \frac{1}{12}\left(\frac{k}{\alpha}\right)^2)\right\}$

Table 11: Photon-decay amplitudes of the P wave baryon resonances (theory versus experiment). The experimental data are given by the most recent Particle Data Group Compilation (Yost, *et al*, 1988). A^{NR} is the nonrelativistic result, A^{RE} is the nonrelativistic results plus the relativistic correction. Both A^{NR} and A^{RE} are calculated in the CM frame with harmonic oscillator strength $\alpha^2 = 0.175$ GeV^2, see ref. 8. The A_1^M is the result with QCD mixing effects and the relativistic corrections, in which the harmonic oscillator strength is $\alpha^2 = 0.175$ GeV^2. A_2^M is the same as A_1^M except the α^2 is 0.09 GeV^2. All amplitudes have 100 GeV$^{\frac{1}{2}}$ units.

Multiplet	States	A_J^N	A^{NR}	A^{RE}	A_1^M	A_2^M	A^{exp}
$[70,1^-]_1$	$S_{11}(1535)$	$A^p_{\frac{1}{2}}$	174	163	142	162	73 ± 14
		$A^n_{\frac{1}{2}}$	-128	-106	-77	-90	-76 ± 32
	$D_{13}(1520)$	$A^p_{\frac{1}{2}}$	-20	-30	-47	-51	-22 ± 10
		$A^n_{\frac{1}{2}}$	-43	-49	-75	-79	-65 ± 13
		$A^p_{\frac{3}{2}}$	131	146	117	133	167 ± 10
		$A^n_{\frac{3}{2}}$	-131	-146	-127	-153	-144 ± 14
	$S_{11}(1700)$	$A^p_{\frac{1}{2}}$	0	25	78	97	48 ± 16
		$A^n_{\frac{1}{2}}$	28	10	-47	-60	-17 ± 37
	$D_{13}(1700)$	$A^p_{\frac{1}{2}}$	0	-27	-16	-1	-22 ± 12
		$A^n_{\frac{1}{2}}$	-13	12	35	11	0 ± 56
		$A^p_{\frac{3}{2}}$	0	-47	-42	-18	0 ± 19
		$A^n_{\frac{3}{2}}$	-66	-36	10	-15	-2 ± 44
	$D_{15}(1675)$	$A^p_{\frac{1}{2}}$	0	0	8	8	19 ± 12
		$A^n_{\frac{1}{2}}$	-37	-47	-30	-31	-47 ± 23
		$A^p_{\frac{3}{2}}$	0	0	11	11	19 ± 12
		$A^n_{\frac{3}{2}}$	-52	-66	-42	-44	-69 ± 19
	$S_{31}(1620)$	$A^{p,n}_{\frac{1}{2}}$	68	109	72	40	19 ± 16
	$D_{33}(1675)$	$A^{p,n}_{\frac{1}{2}}$	100	68	81	74	116 ± 17
		$A^{p,n}_{\frac{3}{2}}$	104	78	58	60	77 ± 28

Table 12: Photon-decay amplitudes for the positive parity baryon resonances. The experimental data are given by the most recent Particle Data Group Compilation (Yost, *et al,* 1988). For significance of A^{NR}, A^{RE}, A_1^M and A_2^M, see caption to Table 11.

Multiplet	States	A_J^N	A^{NR}	A^{RE}	A_1^M	A_2^M	A^{exp}
$[56, 2^+]_2$	$P_{13}(1720)$	$A^p_{\frac{1}{2}}$	-113	-75	-68	-112	52 ± 39
		$A^n_{\frac{1}{2}}$	32	16	-4	24	-2 ± 26
		$A^p_{\frac{3}{2}}$	38	49	53	55	-35 ± 24
		$A^n_{\frac{3}{2}}$	0	-5	-33	-17	-43 ± 94
	$F_{15}(1680)$	$A^p_{\frac{1}{2}}$	0	6	-8	-15	-17 ± 10
		$A^n_{\frac{1}{2}}$	36	37	11	15	31 ± 13
		$A^p_{\frac{3}{2}}$	76	98	105	107	127 ± 12
		$A^n_{\frac{3}{2}}$	0	-11	-43	-36	-30 ± 14
	$P_{31}(1910)$	$A^{p,n}_{\frac{1}{2}}$	-21	-19	-28	-27	-12 ± 30
	$P_{33}(1920)$	$A^{p,n}_{\frac{1}{2}}$	-21	-20	-14	-26	43±?
		$A^{p,n}_{\frac{3}{2}}$	36	21	-7	18	23±?
	$F_{35}(1905)$	$A^{p,n}_{\frac{1}{2}}$	-14	-1	24	13	27 ± 13
		$A^{p,n}_{\frac{3}{2}}$	-60	-53	25	-9	-47 ± 19
	$F_{37}(1950)$	$A^{p,n}_{\frac{1}{2}}$	-36	-47	-28	-35	-73 ± 14
		$A^{p,n}_{\frac{3}{2}}$	-48	-65	-36	-45	-90 ± 13
$[56, 0^+]_2$	$P_{11}(1470)$	$A^p_{\frac{1}{2}}$	26	10	-93	-80	-69 ± 7
		$A^n_{\frac{1}{2}}$	-18	-11	67	60	37 ± 19
	$P_{33}(1600)$	$A^{p,n}_{\frac{1}{2}}$	-22	-15	-38	-33	-22 ± 29
		$A^{p,n}_{\frac{3}{2}}$	-38	-25	-70	-64	1 ± 22
$[56, 0^+]_0$	$P_{33}(1232)$	$A^{p,n}_{\frac{1}{2}}$	-101	-113	-94	-93	-141 ± 5
		$A^{p,n}_{\frac{3}{2}}$	-173	-195	-162	-160	-258 ± 19
$[70, 0^+]_2$	$P_{11}(1705)$	$A^p_{\frac{1}{2}}$	-40	-18	-18	-16	5 ± 16
		$A^n_{\frac{1}{2}}$	13	4	-22	-23	-5 ± 23

frame, in which recoil effects vanish and so electromagnetic transitions correspond directly to internal excitations. (We have also made similar calculations in the center of mass frame; some differences are found, but they generally do not affect the qualitative behavior of the photoproduction amplitudes.) The phase convention is chosen to be the same as in the work of Koniuk and Isgur (Koniuk and Isgur 1980), and the values of the parameters are the same *except for the harmonic oscillator strength* which we fix at $\alpha^2 = 0.09$ GeV^2, *which is the value used in fitting the spectrum* when QCD mixings are included. Thus to the extent that the A^M (the calculated amplitudes including mixing and (v^2/c^2) effects) agree with A^{exp} we have, for the first time, a unified consistent description of spectroscopy and electromagnetic transitions. (The small component $|N^2 D_M\rangle$ in Eq. (2-75) is neglected in our calculation.)

The highlight of the original nonrelativistic calculation by Copley, Karl and Obryk is that there are dynamical selection rules in addition to the selection rules dictated by $SU(6) \otimes O(3)$ symmetry. These arise because the photoproduction amplitudes for the resonances $D_{13}(1520)$ and $F_{15}(1688)$ have the form

$$A^p_{\frac{1}{2}} \simeq \begin{cases} 1 - \frac{k^2}{\alpha^2} & \text{for } D_{13}(1520) \\ 1 - \frac{k^2}{2\alpha^2} & \text{for } F_{15}(1688). \end{cases} \tag{5-28}$$

Empirically these amplitudes are small and Copley *et al* forced this in the center of mass frame by choosing a value for the oscillator strength $\alpha^2 = 0.175$ GeV^2. The excited energies of baryon resonances can be described qualitatively with this value, so the calculation is consistent within the nonrelativistic framework. These dynamical selection rules become nontrivial with the addition of QCD mixing effects; the formalism becomes more complicated because of large configuration mixing and relativistic corrections, and the harmonic oscillator strength required to fit the resonance mass spectrum is changed due to the anharmonic perturbation of the hyperfine interaction.

In some cases the QCD mixings make significant contributions. Probably the most noticeable example is in the amplitudes for the Roper resonance, $P_{11}(1470)$. According to the results of Isgur and Karl, the $SU(6) \otimes O(3)$ state $|\mathbf{56},\ ^2\mathbf{8},\ N = 2,\ L = 0\rangle$ dominates the wavefunction of the resonance $P_{11}(1470)$, and the transition matrix elements between the $SU(6) \otimes O(3)$ components $|\mathbf{56},\ ^2\mathbf{8},\ N = 2,\ L = 0\rangle$ in the ground state and in the resonance $P_{11}(1470)$ contributes significantly to the photoproduction amplitudes. Indeed, the QCD mixing effects play a crucial role in determining the mass and photoproduction amplitudes of these states. But it is premature to say that the nature of the Roper resonance has been fully understood; the calculation for the pionic decay of the resonance including relativistic correction and the mixed wavefunction has not yet been done. Presumbly one could expect that QCD mixing effects might also play an important role in the pion decay of the Roper resonance. Furthermore, without the relativistic correction the ratio between the Roper excitation amplitudes $A^p_{\frac{1}{2}}$ and $A^n_{\frac{1}{2}}$ should be $-\frac{2}{3}$, which is the ratio of the magnetic moments of the proton and neutron; however this relationship is destroyed by the relativistic correction. Therefore, more accurate experimental information on the Roper excitation amplitudes could help to establish the importance of relativistic effects.

For the L=1 negative parity baryon resonances we find a large contribution from the matrix element between the state $|N^2S_M\rangle$ in Eq. 2-75 and $|N^2P_M\rangle$. There is a major unresolved problem with the most prominent of these resonances: the photoproduction amplitudes for the resonance $S_{11}(1535)$. These were found to be too large in the nonrelativistic model, and remained large even after QCD mixing was incorporated. Our inclusion of $H_{\mathrm{em(rel)}}$ does not change this essentially. The transition from $|N^2P_M\rangle$ to the ground state dominates the photoproduction amplitudes of the resonance $S_{11}(1700)$, so QCD mixing affects these amplitudes significantly; in comparison, the effect of $H_{\mathrm{em(rel)}}$ is small here.

It is interesting to notice that the relation

$$D_{15}(1675);\ A_{\frac{3}{2}} = \sqrt{2}A_{\frac{1}{2}} \tag{5-29}$$

for both the neutron and proton survives the QCD mixing effects, is independent of the choice of the frame, and is consistent with the data. This has been shown previously by Koniuk *et al.* The result presented here shows that this relation survives the use of $H_{\mathrm{em(rel)}}$ as well, though the absolute magnitudes have changed because of our relativistic corrections and the change of the harmonic oscillator strength. This is very important. In Isgur and Karl's model the resonance $D_{15}(1675)$ is a pure $SU(6)\otimes O(3)$ state; therefore, the relation 5-29 is determined by the symmetry, and the experimental data are consistent with this relation. The QCD mixing and the use of $H_{em(rel)}$ play an important role for the resonances $S_{31}(1620)$ and $D_{33}(1675)$, as can be seen in Table 11.

Another important resonance is the $P_{33}(1600)$; it is the partner of the Roper resonance in the 56plet of SU(6) in the unmixed spectrum, but the QCD mixing plays an essential role in making these states so light and one may expect that photoproduction amplitudes may also be significantly modified. If the state $|\Delta^4 S_{S'}\rangle$ dominates the $P_{33}(1600)$ resonance (as implied by Isgur and Karl's calculation), then the photoproduction amplitude should satisfy the relation

$$A_{\frac{3}{2}} = \sqrt{3}A_{\frac{1}{2}} \tag{5-30}$$

because it is a pure magnetic dipole transition. This result obtains in calculations with or without QCD mixing; the data look as if they may violate this, though the error bars are too great to draw this conclusion definitively. Clearly this is an example where better data may be crucial. The status of the resonance $P_{33}(1600)$ is far from clear, and more accurate information is needed; good data on the electromagnetic transitions could help to establish both the existence and the internal symmetry structure of this state.

Notice that for the $P_{33}(1232)$ the calculated magnitudes after the inclusion of both relativistic corrections and the QCD mixing effects are essentially unchanged from the nonrelativistic magnitudes (see Table 12), and as such remain unsatisfactory.

There has been a suggestion that the resonance $P_{11}(1705)$ could be the lightest hybrid baryon in view of a selection rule (Barnes and Close 1983) that says this hybrid state is not photoproduced from proton targets. The data were consistent with this zero and inconsistent with the predictions of the nonrelativistic quark model (column 1 of Table 12). However, we see that the relativistic effect and QCD mixing change the predicted magnitudes significantly such that they are now in better agreement with data. Improved data and extension to electroproduction may help to elucidate the nature of this resonance.

Overall the results show that the success of the nonrelativistic calculation is preserved by the QCD mixing and corresponding relativistic effects, and there are improvements for some cases where the QCD mixing effects become important. In the next chapter we discuss electroproduction, where we expect that the QCD mixing effects may become more noticeable as q^2 increases.

CHAPTER 6

Electroproduction

We shall follow the procedure of Foster and Hughes (Foster and Hughes 1982), whose calculations were for an equal velocity frame (EVF) (which is very close to the Breit frame). When the calculation is extended to electroproduction it becomes highly relativistic, and these authors introduced a Lorentz boost factor in the spatial integrals of Eqs. 3-33,34 (Licht and Pagnamenta 1972):

$$R(k) \rightarrow \frac{1}{\gamma^2} R(\frac{k}{\gamma}). \tag{6-1}$$

In the EVF the Lorentz boost factor is

$$\gamma = \left(1 + \frac{k^2}{(M_r + M_p)^2}\right)^{\frac{1}{2}} \tag{6-2}$$

where M_r and M_p are the masses and the resonance and nucleon, respectively. The relation of the momentum k of the mass of the virtual photon in the EVF is

$$k^2(EVF) = \frac{(M_r^2 - M_p^2)^2}{4M_rM_p} + \frac{q^2(M_r + M_p)^2}{4M_rM_p}. \tag{6-3}$$

In the $SU(6) \otimes O(3)$ basis the photoproduction amplitudes can be derived analytically, so we can easily extend our calculation to electroproduction with the help of Eqs. 6-1,2,3. In Figs. 4-a,b,c,d we show the results of our calculations of the transverse amplitudes for the resonances $S_{11}(1535)$, $D_{13}(1520)$, $F_{15}(1688)$ and the Roper resonance $P_{11}(1470)$.

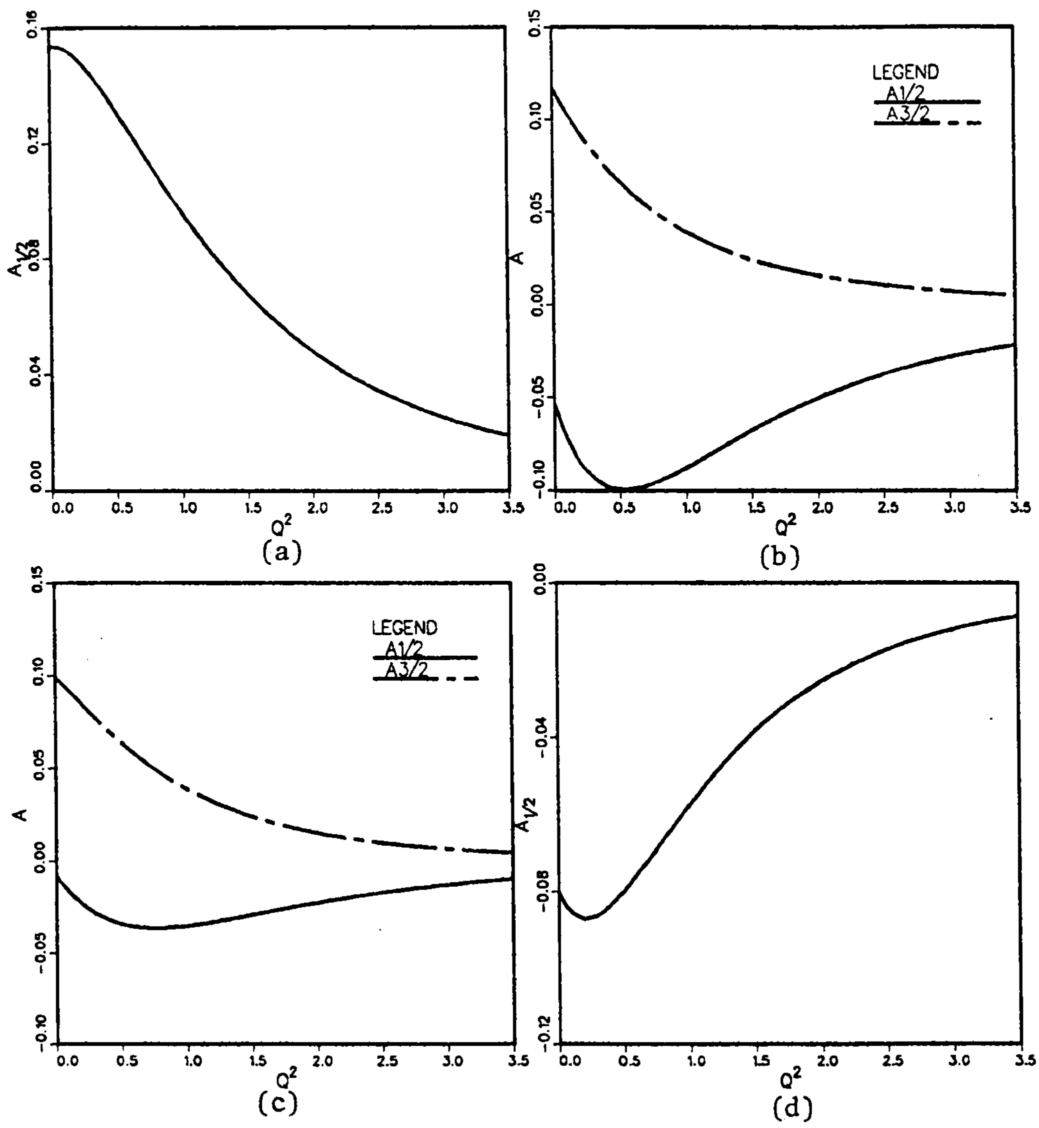

Fig. 4. **The q^2 dependence of the helicity amplitudes (a) $A^p_{\frac{1}{2}}$ for the $S_{11}(1535)$, (b) A for the $D_{13}(1520)$, (c) $F_{15}(1568)$, where solid (dot-dash) line represents $A^p_{\frac{1}{2}}$ ($A^p_{\frac{3}{2}}$) and (d) $A^p_{\frac{1}{2}}$ for the $P_{11}(1470)$. The QCD mixing effects and relativistic corrections are included.**

For real photoproduction the amplitudes are not particularly sensitive to the value of α^2 in the range 0.09 to 0.175 GeV^2. However for electroproduction α^2 determines the scale of q^2 at which the form factor begins to die off and, in particular, controls the charge radius of the nucleon. If one chooses $\alpha^2 = 0.175$ GeV^2 the corresponding charge radius of the nucleon is about 0.5 fm, which is too small compared to the data; therefore one can not expect the nonrelativistic calculation to give a good description of the q^2 dependence. In order to overcome this, Foster and Hughes introduced an *ad hoc* form factor, which is outside of the model and fitted to the data. If a smaller value of α^2, such as 0.09 GeV^2, is used, there is no need for such an *ad hoc* form factor and the corresponding charge radius is closer to the data, as indicated by Isgur and Karl.

The relative importance of different components in the mixed wavefunctions varies with q^2 for the following reason. The form factors for transitions to components with large N quantum numbers have larger threshold behaviors and hence fall less rapidly with q^2 than do the small N components. Therefore large q^2 electroproduction increasingly feels the large N components in the wavefunctions that could cause the ratios of helicity amplitudes to vary, perhaps significantly.

Comparing our calculation with the data (Burkert 1988), we find that the QCD mixing effects have improved the photoproduction amplitude for the Roper resonance, but they do not solve the problem of why this amplitude empirically appears to change sign with increasing q^2. A similar result has been shown by Warn *et al* (Warn *et al*, 1990). This might imply that the wavefunctions given by the calculation of Isgur and Karl do not have the correct internal structure for the Roper resonance, or that we need another dynamical approach to electroproduction. Gavela *et al* (Gavela *et al* 1981) have shown that the quark-pair-creation model (QPCM) may give a natural explanation for such behavior. It would be a challenge to show that the success of the QPCM survives the QCD mixing effect, and also gives a consistent description for other baryon resonances. Therefore, the q^2 dependence of helicity amplitudes may help us to distinguish among different dynamical approaches. Furthermore, because of the large QCD mixing effect for the Roper resonance, the restriction of mixing to a single harmonic shell in the Isgur and Karl calculation becomes unrealistic, especially as q^2 increases. A recent study suggests that two resonances may be associated with the Roper resonance; this might support a scenario where one of these is dominantly a hybrid $gQQQ$ state and other is a conventional QQQ state. Comparison of γN and πN data will be interesting; on proton targets two states would contribute to πN, but only one to γN (Barnes and Close 1983). The reversed process $\pi_- p \to N^* \to \gamma n$ could access the neutron coupling of both conventional and hybrid baryon states. In electroproduction this leads to zero contribution from the proton targets, but non-zero for neutron targets. Further study should be made on the resonance $P_{33}(1600)$. It would be the 56-plet partner of the Roper resonance in the QQQ model, but for the hybrid baryons no such partner exists.

But one has to be cautious about the extension of photoproduction to electroproduction. The nonrelativistic quark model has used for H_{em} Eq. 5-1, and the relativistic corrections to it have to date been limited to Eq. 5-6. In our work we have adopted this formalism and completed it with the necessary non-additive contributions Eq. 5-7. However, our derivation of H_{em} in Chapter 4 shows that in general it has a complicated form with explicit appearance of the binding potentials (Eq. 4-16). McClary and Byers have shown that, if $1/m^2$ employed here, this H_{em} reduces to Eq. 4-25, only to the extent that the long wavelength approximation is valid. If this approximation fails then the H_{em} of Eq. 4-25, and all results following from it, will be inconsistent.

One of the criteria for the long wavelength approximation is that we can expand the common factor $\exp(-\frac{k^2}{6\alpha^2})$ to order k^2, that is

$$\exp\left(-\frac{k^2}{6\alpha^2}\right) \simeq 1 - \frac{k^2}{6\alpha^2}. \tag{6-4}$$

Let η be a factor, defined as;

$$\eta = \frac{1 - \frac{k^2}{6\alpha^2}}{\exp(-\frac{k^2}{6\alpha^2})} \tag{6-5}$$

Then if the longwavelength approximation is a good one, η should be close to unity.

We stress that this thesis, and most papers in the literature, use an approximation for a H_{em} (Eq. 4-25) that is valid only if $\eta \simeq 1$. Essentially, if H_{em} is used to order $(v/c)^2$, then it is only consistent to expand the exponential to order $(k/\alpha)^2$. We show the relation between η^2 and the virtual photon mass in Fig. 5 for three different final states in the Breit frame. From this calculation we can see that for small q^2 the value of η is indeed very close to unity, but it deviates very quickly with increasing q^2. This implies that the longwavelength approximation breaks down in electroproduction and the model's validity becomes dubious. To confront large q^2 for individual amplitudes requires more sophisticated approaches, higher order terms in Eq. 4-25 as in the non-relativistic Hamiltonian, and also detailed evaluation of the role of gluon dynamics. These go far beyond the present paper and highlight the limited application of the model, something that seems not to have been addressed much in the literature.

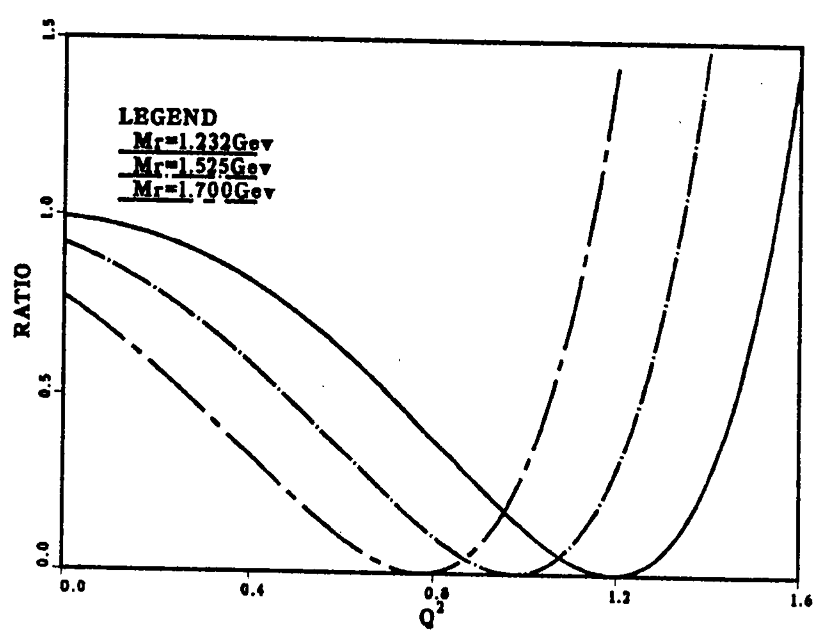

Fig. 5. **The relation η^2 with virtual photon mass Q^2 for three different final states in the Breit frame. A similar result is obtained in the CM frame.**

However, one may still be able to make predictions for the ratios of helicity amplitudes as a function of q^2, where many of the uncertainties may cancel out, and relativistic effects on the structure of the wavefunction become increasingly important. For example, the helicity asymmetry of baryon resonances, which is defined as

$$A = \frac{A^2_{\frac{1}{2}} - A^2_{\frac{3}{2}}}{A^2_{\frac{1}{2}} + A^2_{\frac{3}{2}}}, \tag{6-6}$$

plays a very important role in this regard; the Drell–Hearn–Gerasimov (DHG) sum rule and the Bjorken sum rule (Bjorken 1966) suggest a rather nontrivial dependence on q^2 of helicity asymmetry (Close 1989). Indeed, Close and Gilman have shown using the nonrelativistic quark model that there is a dramatic change of the helicity asymmetry for the resonances $D_{13}(1520)$ and $F_{15}(1688)$ with increase of q^2. Our calculation with the relativistic correction and QCD mixing effects (shown in Fig. 6) has consistently confirmed the prediction of Close and Gilman, which is also in agreement with experimental data. Such behavior shows that the magnetic multipole moments become dominant at high q^2, while the electric multipole transitions dominate the helicity amplitudes $A_{\frac{3}{2}}$ for these resonances. This is a very important result; if the Bloom–Gilman duality assumption is correct (Bloom and Gilman, 1970), the dramatic change in helicity asymmetry implies that the Bjorken structure polarization function $g_1(x)$ could become negative as $x \to 0$. Quantitatively, the QCD mixing effects have improved the agreement with data for the resonance $F_{15}(1688)$, and made little change for $D_{13}(1520)$.

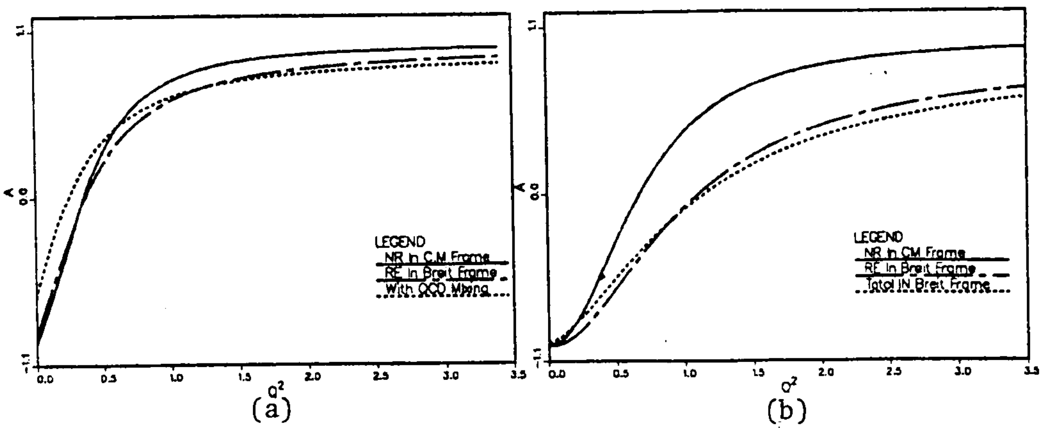

Fig. 6. **The helicity asymmetry for (a) $D_{13}(1520)$ and (b) $F_{15}(1688)$. The solid line represents the nonrelativistic results, dot–dash line is the result with the relativistic correction, and the dotted line is the calculation with QCD mixing effects and the relativistic correction. See text.**

Another interesting quantity is the ratio $A^p_{\frac{1}{2}}(D_{13})/A^p_{\frac{1}{2}}(S_{11})$. In the nonrelativistic quark model both resonances $S_{11}(1535)$ and $D_{13}(1520)$ belong to the same $SU(6)\otimes O(3)$ representation $|N^2P_M\rangle$. Because the magnetic dipole transition dominates at high q^2, this ratio should be the ratio of the magnetic quadrupole matrix elements in $SU(6)\otimes O(3)$ states, which is the Clebsch–Gordon coupling coefficient. Quantitatively, it can be shown that the ratio should be $\sqrt{2}$ with $q^2 \to \infty$ for the $SU(6)\otimes O(3)$ state $|N^2P_M\rangle$; this is also true under the relativistic extension. Certainly, the QCD mixing effect would break down such relations. In Fig. 7 we shown results with the QCD mixing effects and the nonrelativistic calculation of Copley Karl and Obryk. The two calculations are quite close to each other, and neither gives a good description of the experimental data at higher q^2.

The data for the resonances $S_{11}(1535)$ and $D_{13}(1520)$ show that there should be large configuration mixing for $S_{11}(1535)$, but rather little mixing for $D_{13}(1520)$. This behavior is also found in the calculation of Isgur and Karl. Because the matrix element between the state $|N^2P_M\rangle$ and the ground state dominates the transition amplitudes, the qualitative behavior would remain the same as in the nonrelativistic calculation. Therefore, here the QCD mixing effects fail to improve the agreement with data at high q^2. It may be that higher configurations in the QCD mixed wavefunction are becoming increasingly important, and that we are seeing a transition where some other approximation or model approach needs to be developed. One such suggestion (Carlson 1986) is that there are effects arising from perturbative QCD that begin to show up at moderate values of q^2.

One still can test the static symmetry of the quark model in electroproduction in order to understand at what value of q^2 that static symmetry begins to fail. One such example is the helicity asymmetry for the resonance $P_{33}(1232)$, which the model predicts should be $-\frac{1}{2}$, and for $D_{15}(1675)$ which the model predicts to be $-\frac{1}{3}$ for neutrons and protons, independent of QCD mixing effects.

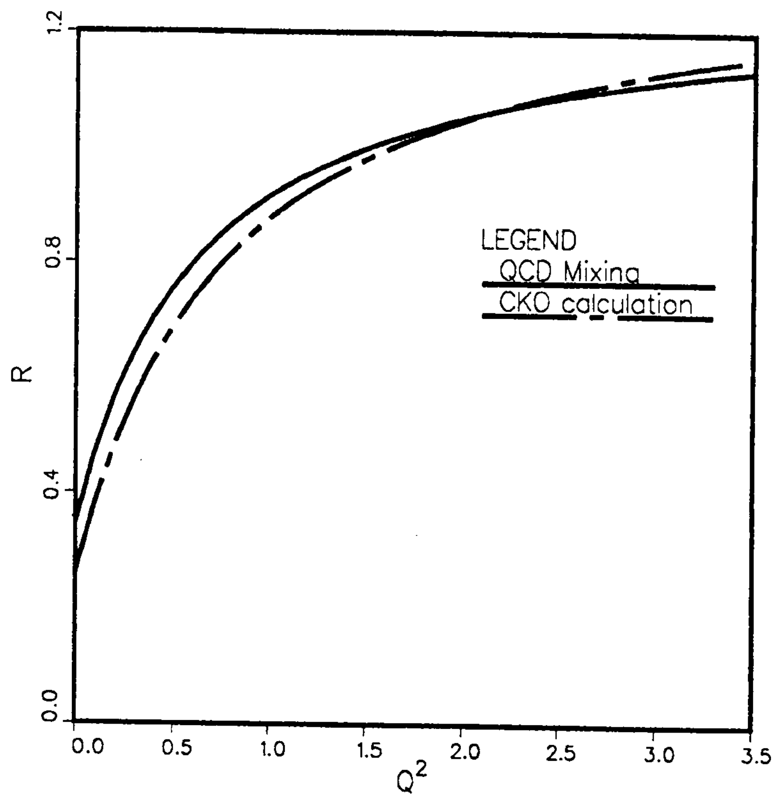

Fig. 7. The ratio $R = |A^p_{\frac{1}{2}}(D_{13})/A^p_{\frac{1}{2}}(S_{11})|$. The solid line represents the result of the QCD-mixing and the dot–dash line is the result of the nonrelativistic calculation (Copley, Karl and Obryk 1969)

CHAPTER 7

Conclusions

We have shown that relativistic corrections in the binding potential play a crucial rule in describing the baryon spectrum, and theoretical consistency requires that the calculation of electromagnetic transition amplitudes be developed to $O(v^2/c^2)$ too. In Chapter 4 we saw that relativistic corrections in the binding potential and in the electromagnetic interaction are related by gauge covariant transformation. Under the longwavelength approximation the binding potential need not play an explicit role in the electromagnetic interaction if Eq. 4-25 is used.

We have applied this $H_{em(rel)}$ to calculate electromagnetic transition amplitudes between baryons whose wavefunctions include QCD mixings inspired by Isgur and Karl's QCD potential model. We find that the successes of the NRCQM are preserved and some, though not all, of its problems are removed. A significant advance over previous work is that both spectroscopy and transitions are treated in a unified way *with a single set of parameters*; previous works have used different values for the oscillator strength in spectroscopy and electromagnetic transitions, and as such have not produced a unified QCD model of baryons. The results presented here also show that the QCD mixing effect has changed the radial behavior of baryon wavefunctions dramatically; thus an *ad hoc* form factor in the nonrelativistic calculation is no longer needed. This calculation also confirms the dramatic change of the helicity asymmetry predicted in the nonrelativistic quark model.

It is very important to establish the configuration mixing effects in the data which are directly related to the mixings in the wavefunction. This could give us insight into the quark–quark interaction in the nonperturbative region. The resonances $P_{33}(1232)$ and $D_{15}(1700)$ should provide an important test in this regard, because of the constraints and the selection rules among their helicity amplitudes under the H_{em} of Eq. 4-24. Electroproduction may provide additional useful information about the mixing effects too, because the contributions from higher shells to the wavefunction become increasingly important as q^2 increases. The electroproduction data for the resonance $S_{11}(1535)$ suggest that there should be significant contributions from the higher shells.

Despite the successes of Eq. 2-77, there are still many problems unanswered in this model such as the role of the spin–orbit interaction in spectroscopy. In the wavefunction mixing there is also the question of how results are modified when one relaxes Isgur and Karl's restriction of a single harmonic oscillator shell. As noted in the text, when

$$\frac{q^2}{2M} > \frac{N\alpha^2}{M_q} \tag{7-1}$$

mixings involving shells with different value of N may become increasingly important. Therefore a continuing effort should be made in the relativized model of

Capstick and Isgur, in which the calculations are not restricted to a single harmonic oscillator shell. Furthermore, if hybrid baryons exist below 2 GeV there should be a mixing between the hybrid and conventional baryons, and gluon degrees of freedom will play an explicit role in both the hadron spectrum and transition processes. Such effects have not yet been incorporated in the theory presented here.

In summary, when H_{em} is developed consistently to $O(v^2/c^2)$ the quark model with QCD mixing effects at this same order is successful in describing simultaneously the spectrum and electromagnetic transition processes. However, there are many unanswered questions, in particular concerning the extension to $q^2 \neq 0$. Future experiments at CEBAF will probe this region and provide more information and challenges to the potential quark model.

BIBLIOGRAPHY

Bibliography

Abdullah, T. and Close, F. E. (1972). Phys. Rev. **D5**, 2332.

Barnes, T. and Close, F.E. (1983). Phys. Lett. **B128**, 277.

Bjorken, J.D. and Drell, S.D. (1964). Relativistic Quantum Mechanics (McGraw-Hill Inc.).

Bjorken, J.D. (1966). Phys. Rev. **148**, 1466.

Bloom, E.D. and Gilman, F.J. (1970). Phys. Rev. Lett. **25**, 1140.

Brodsky, S.J. and Primack, J. (1969). Ann Phys. (N.Y.) **52**, 315.

Burkert, V. (1988). Report No. CEBAF-FR-88-012.

Capstick, S. and Isgur, N. (1986). Phys. Rev. **D34**, 2809.

Carlson, C. (1986). Phys. Rev. **D34**, 2704.

Close, F.E. (1979). Introduction To Quarks and Partons (Academic Press, New York).

Close, F.E. (1989). Nucl. Phys. **A497**, 109c.

Close, F.E. and Copley, L.A. (1970). Nucl. Phys. **B19**, 477.

Close, F.E. and Gillman, F.J. (1972). Phys. Lett. **B38**, 514.

Close, F.E. and Osborn, H. (1970). Phys. Rev. **D2**, 2127.

Close, F.E. and Li, Zhenping. (1990). Phys. Rev. **D42**, 2194.

Copley, L.A. Karl, G. and Obryk, E.(1969). Nucl. Phys. **B13**, 303.

De Rujula, A. Georgi, H. and Glashow, S.L. (1975). Phys. Rev. **D12**, 147.

Drell, S.D. and Hearn, A.C. (1966). Phys. Rev. Lett. **162**, 1520.

Feynmen, P. Kisslinger, M. and Ravndal, F. (1971). Phys. Rev. **D3**, 2706

Foster, F. and Hughes, G. (1982). Z. Phys. **C14**, 123.

Gavela, M.B. *et al.* (1981). Phys. Rev. **D21**, 182.

Gell-Mann, M. (1964). Phys. Lett. **8** 214.

Gerasimov, S.B. (1965). J. Nucl. Phys. (USSR) **2**, 598.

Isgur, N. and Karl, G. (1978). Phys. Rev. **D18**, 4187.

Isgur, N. and Karl, G. (1979). Phys. Rev. **D19**, 2194.

Isgur, N. Karl, G. and Koniuk, R. (1978). Phys. Rev. Lett. **41**, 1269.

Isgur, N. and Paton, J. (1983). Phys. Lett. **B124**, 247.

Itzykson, C. and Zuber, J–B. (1980). Quantum Field Theory (McGraw–Hill Inc.) p537.

Karl, G. And Obryk, E. (1968). Nucl. Phys. **B8**, 609.

Koniuk, R. and Isgur, N. (1980). Phys. Rev. **D21**, 1888.

Kubota, T. and Ohta, K. (1976). Phys. Lett. **B65**, 374.

Le. Yaouanc, A. *et al* (1988). Hadron Transition In The Quark Model (Gordon Breach, New York).

Li, Zhenping and Close, F.E. (1990). Phys. Rev. **D42**, 2207.

Licht, A. and Pagnamenta, A. (1972). Phys. Rev. **D2**, 1150.

McClary, R. and Byers,N. (1983). Phys. Rev. **D28**, 1692.

Moorhouse, R.G. (1966). Phys. Rev. Lett. **16**, 772.

Ohta, K. (1979). Phys. Rev. Lett. **43**, 1201.

Yost, G.P. *et al.* (1988). Phys. Lett. **B204**, 1.

Zweig, G. (1964). Cern Report 8182/TH.401 (Unpublished)

VITA

Zhenping Li was born March 13, 1959 in Jilin City, Jilin Province, People's Republic of China. He graduated in July of 1977 from Second High School in Jilin City. In the winter of 1978, he entered Jilin University, where he received Bachelor of Science Degree in 1982. In the winter of 1985, he started his graduate career as a Graduate Assistant in the Department of Physics and Astronomy at The University of Tennessee.